GENERATION AND ST
DYNAMIC WALK USIN
LEG LOA

CHRIS

THE UNIVERSITY

GENERATION AND STABILIZATION OF QUADRUPEDAL DYNAMIC WALK USING PHASE MODULATIONS BASED ON LEG LOADING INFORMATION

CHRISTOPHER MAUFROY

2003

GENERATION AND STABILIZATION OF QUADRUPEDAL DYNAMIC WALK USING PHASE MODULATIONS BASED ON LEG LOADING INFORMATION

CHRISTOPHE MAUFROY

THE UNIVERSITY OF ELECTRO-COMMUNICATIONS

MARCH 2009

GENERATION AND STABILIZATION OF QUADRUPEDAL DYNAMIC WALK USING PHASE MODULATIONS BASED ON LEG LOADING INFORMATION

CHRISTOPHE MAUFROY

Graduate School of Information Systems

The University of Electro-Communications

A thesis submitted for the degree of
DOCTOR OF PHILOSOPHY

MARCH 2009

GENERATION AND STABILIZATION OF QUADRUPEDAL DYNAMIC WALK USING PHASE MODULATIONS BASED ON LEG LOADING INFORMATION

APPROVED BY SUPERVISORY COMMITTEE:

CHAIRMAN: PROF. KUNIKATSU TAKASE

MEMBERS: PROF. KENJI TANAKA

PROF. HIROYOSHI MORITA

PROF. HIDEKI KOIKE

PROF. SHUNICHI TANO

脚負荷情報に基づく脚相調整を用いた四脚動歩行の生成と安定化

クリストフ　モフロァ

概要

この論文では、脚負荷情報に基づく脚相調整が、運動における周期運動と姿勢制御に大きな役割を果たすことを示す。特に、脚負荷情報を用いる支持脚相から遊脚相への遷移の制御がどのような役割なのかを明示する。このメカニズムは、二次元歩行における交互の脚協調と四脚動歩行における左右交互の脚協調の発生の一因を担っている。その結果、運動は両方の場合に独立した脚制御器で達成することができた。四脚動歩行における運動の安定性に関して前後脚の脚制御器につながる脚協調メカニズムを加えなければならないという結果が得られた。このメカニズムと脚相調整を加えた制御システムは、脚の周期運動を調節することで様々な外乱に対する胴体ロール運動の安定化につながった。よって、姿勢制御と周期運動制御の基礎的な統合が単純な制御システムで実現されたといえる。

GENERATION AND STABILIZATION OF QUADRUPEDAL DYNAMIC WALK USING PHASE MODULATIONS BASED ON LEG LOADING INFORMATION

CHRISTOPHE MAUFROY

ABSTRACT

Regarding the issue of legged locomotion stabilization, it can be pointed out that, at low speeds, since gravity is dominant, posture control using sensory information such as ground reaction force or vestibular information is predominant. On the other hand, at high speeds, since the influence of the inertial forces is dominant, rhythmic motion control to construct a limit cycle becomes primordial. Consequently, legged locomotion controllers should integrate both posture control and rhythmic motion control to be able to cover the whole range of locomotion speeds.

This thesis considers the use of sensory information related to leg loading (i.e. the load supported by the leg) in a CPG type controller to generate stable quadrupedal dynamic walk. Leg loading information is used at the individual leg level to regulate the transitions between the stance and the swing phases. Accordingly, the CPG activity is adjusted of via phase modulations, i.e. modulations of the relative durations of the stance and swing phases of the stepping motion in each leg. This study concentrates on the role of the regulation of stance-to-swing transition using leg loading information. Using dynamics simulations, it investigates the contribution of this mechanism to rhythmic motion control and posture control, in the range from low- to medium-speed walking.

This issue is investigated in the case of two-dimensional stepping motions and three-dimensional quadrupedal dynamic walk. In both cases, a sensor-dependent CPG is used, where phase transitions in each leg controller is controlled using leg loading information. Swing-to-stance and stance-to-swing transitions are respectively triggered when the touchdown event is detected and when leg loading becomes smaller than a given threshold.

Generation of two-dimensional stepping motions is achieved with musculoskeletal models faithful to the cat anatomy. For the hind legs, a preexistent model is used, while an original model of the forelegs is developed. A neural leg controller architecture, able to induce stepping motions of a leg at various speeds, is proposed. Using a pair of leg controllers, stepping patterns at constant speed are generated with the hind legs model and the forelegs model separately, by replacing the not-actuated pair of legs by a wheeled support. As a result of the phase modulations based on leg loading information, stable alternate stepping coordination of the legs emerges, even when the two leg controllers are independent. Next, the issue of speed modulation is considered with the hind legs model. The leg coordination maintains in the whole range of speeds considered

and adaptations of walking patterns according to the speed are characterized. Striking similarities with the adaptations taking place during real cat locomotion are found, reinforcing the hypothesis that, in animals, stance-to-swing transition is mainly regulated using sensory signals related to leg unloading.

In order to facilitate the study of the action of the phase modulations in the three-dimensional case, a traditional robotic approach, combining trajectory generation and local PD control, is used instead of a muscular model to generate the motor patterns. Using four independent controllers, stable quadrupedal dynamic walk is generated in a broad range of cyclic periods and speeds. Phase modulations using leg loading information contribute to the emergence of left-right alternate stepping coordination of the legs. The phase difference between ipsilateral legs is adjusted by setting appropriately two categories of the leg controllers parameters: the vertical coordinate of nominal touch-down position of the feet and the PD control gains of the ankle and knee joints. The stability of the walking patterns is assessed by subjecting the model to lateral perturbations. In most of the application timings, the phase modulations adjust the rhythmic motion of the legs to stabilize the body rolling motion against the disturbance. However, when the perturbation results in a sufficient decrease of the rolling motion amplitude on one side, the foreleg on the other side cannot swing and the leg coordination is severely disturbed. Hence, a leg coordination mechanism, promoting stance-to-swing transition in the foreleg when the ipsilateral hind leg is swinging, is added to the previous architecture to improve the performances. With the additional coordination mechanism, the control system realizes good performances against the lateral perturbations for all the timings of applications. Moreover, it is able to tackle terrain irregularities (such as steps and slopes) while stabilizing the posture. Hence, basic integration of posture control and rhythmic motion control is demonstrated with a simple and distributed control architecture grounded on phase modulations using leg loading information.

Contents

1 Introduction **1**
- 1.1 Overview . . . 1
- 1.2 Background . . . 2
  - 1.2.1 Biological concepts of legged locomotion control . . . 2
  - 1.2.2 Legged locomotion control methods . . . 3
- 1.3 Motivation . . . 4
  - 1.3.1 Limitations of former researches . . . 4
  - 1.3.2 Object of this thesis . . . 5
- 1.4 Related studies . . . 6
  - 1.4.1 Phase modulations . . . 6
  - 1.4.2 Musculoskeletal models and neural controllers . . . 7
- 1.5 Thesis Organization . . . 10

2 Considerations on the control system architecture **11**
- 2.1 Overview . . . 11
- 2.2 Generalities about legged locomotion . . . 11
  - 2.2.1 Locomotion phases . . . 11
  - 2.2.2 Walking pattern characteristics . . . 12
  - 2.2.3 Leg controller structure . . . 13
  - 2.2.4 Interleg coordination and phase modulations . . . 13
  - 2.2.5 Central Pattern Generator . . . 14
- 2.3 Control system architecture: choices and motivations . . . 14
  - 2.3.1 CPG model: oscillatory or sensor-dependent . . . 14
  - 2.3.2 Phase transition conditions and phases modulations based on leg loading information . . . 15
  - 2.3.3 Common principles . . . 16

3 Generation of two dimensional alternate stepping **17**
- 3.1 Overview . . . 17
- 3.2 List of symbols and notations . . . 17
- 3.3 Musculoskeletal models . . . 19
  - 3.3.1 Skeletal systems . . . 19
  - 3.3.2 Muscular systems . . . 21
  - 3.3.3 Inputs and outputs . . . 22
- 3.4 Leg controller organization . . . 24
  - 3.4.1 Overview and inspiration . . . 24
  - 3.4.2 Neural Phase Generator (NPG) . . . 25

3.4.2.1 Neuronal structure . . . 25
3.4.2.2 Sensory information used for the regulation of the phase transitions . . . 28
3.4.3 Motor Output Shaping Stage (MOSS) . . . 29
3.4.3.1 Implementation of a synergy . . . 29
3.4.3.2 Four synergies . . . 30
3.4.4 Propulsive Force Control Module (PFCM) . . . 32
3.4.4.1 Action of the PFCM . . . 32
3.4.5 Implementation of the PFCM for the hind legs . . . 32
3.4.6 Implementation of the common principles . . . 33
3.5 Generation of alternate stepping at constant speed . . . 34
3.5.1 Setup: models and parameters . . . 34
3.5.2 Initial conditions and start up . . . 34
3.5.3 Emergence of alternate stepping . . . 35
3.5.4 Contribution of the phase modulations based on leg loading information to the emergence of stable alternative stepping . . . 35
3.6 Modulation of the stepping pattern . . . 40
3.6.1 Setup: model and parameters . . . 40
3.6.2 Adjustment of the walking speed . . . 40
3.6.3 Resultant adaptations of the walking patterns . . . 41
3.6.4 Adaptations as a result of the interaction between the adjustment by the PFCM and the phase modulations . . . 45
3.7 Discussion . . . 45
3.7.1 Parameter tuning . . . 45
3.8 Summary . . . 46

4 Generation of stable quadrupedal dynamic walk 47
4.1 Overview . . . 47
4.2 List of symbols and notations . . . 48
4.3 Simulation Model . . . 49
4.4 Leg Controller . . . 51
4.4.1 Overview . . . 51
4.4.2 Foot trajectory generation . . . 51
4.4.2.1 Swing . . . 52
4.4.2.2 Stance . . . 52
4.4.3 Sensory feedback and transition conditions . . . 53
4.4.4 Leg Motion Control . . . 54
4.4.5 Implementation of the common principles . . . 54
4.5 Generation of dynamic walk using independent leg controllers . . . 55
4.5.1 Considerations about gaits . . . 55
4.5.2 Mechanisms of leg loading transfer during the locomotion . . . 56
4.5.3 Emergence of left-right alternate stepping . . . 56
4.5.4 Conditions of emergence of the walk gait . . . 59
4.5.4.1 Influence of the AEP vertical coordinate offset Δy_{AEP} . . . 60
4.5.4.2 Influence of the PD control gains of the knee and ankle joints . . . 63
4.5.4.3 Realization of the walk gait . . . 64

4.6 Modulations of the walking pattern . . . 66
4.6.1 Modulation of the walking cyclic period . . . 66
4.6.2 Modulation of the walking speed . . . 69
4.7 Summary . . . 73

5 Contribution of the phases modulations to the stability 75
5.1 Overview . . . 75
5.2 Evaluation of the stability with independent leg controllers . . . 75
5.2.1 Method . . . 75
5.2.2 Stabilization action of the phase modulations in the frontal plane . 76
5.2.3 Contribution of the stance phase termination condition to the stability . . . 77
5.2.4 Stability of the walking pattern . . . 80
5.2.4.1 Perturbations that accelerate the lateral transfer of leg loading . . . 80
5.2.4.2 Perturbations that slow down the lateral transfer of leg loading . . . 83
5.3 Ascending coordination mechanism . . . 85
5.4 Influence of the cyclic period and the speed on the stability . . . 88
5.5 Performances on uneven terrains . . . 90
5.5.1 Elevated steps . . . 91
5.5.2 Slopes . . . 91
5.6 Discussion . . . 92
5.6.1 Ascending coordination mechanism . . . 92
5.6.2 Comparison with Tekken . . . 93
5.7 Summary . . . 94

6 Conclusions 97
6.1 Conclusions . . . 97
6.2 Future work . . . 99

A Musculoskeletal Models 101
A.1 Skeletal systems . . . 101
A.2 Muscular systems . . . 102
A.2.1 Muscle model . . . 102
A.2.2 Parameters of the fore and hind legs muscular systems . . . 104

B Neural leg controller: implementation details 107
B.1 Neuronal models . . . 107
B.1.1 Interneurons (I) . . . 107
B.1.2 Sensory neurons (SN) . . . 108
B.1.3 Motor neurons (MN) . . . 108
B.1.4 Variable gain neurons (VG) . . . 108
B.1.5 Tonic input neurons (TI) . . . 109
B.1.6 Initiation and termination units (ITU) . . . 109
B.2 NPG . . . 110
B.2.1 Biological groundings of the NPG structure . . . 110
B.2.2 NPG Parameters . . . 110

B.3 MOSS . . . 112
B.3.1 Synergy implementation . . . 112
B.3.2 Muscles activated during each synergy . . . 113
B.3.2.1 Liftoff . . . 113
B.3.2.2 Swing . . . 114
B.3.2.3 Touchdown . . . 114
B.3.2.4 Stance . . . 114
B.3.3 MOSS parameters . . . 115
B.3.3.1 Activation conditions . . . 115
B.3.3.2 Muscular activations . . . 116
B.4 PFCM . . . 118

C Trajectory generation **121**
C.1 Swing phase trajectory . . . 121
C.2 Stance phase trajectory . . . 122
C.3 Inverse kinematic model . . . 125

D Quadrupedal walk: initial conditions and transient phase **127**

E Simulation environment **129**
E.1 Control levels . . . 129
E.2 Ground reaction forces . . . 129

Bibliography **131**

Acknowledgements **137**

Author Biography **139**

List of Publications Related to the Thesis **141**

List of Figures

2.1 Principal subdivisions of the walking cycle into phases 12

3.1 Musculoskeletal models 20
3.2 Muscular models of the fore and hind legs 23
3.3 Overview of the Leg Controller 25
3.4 Structure of the NPG 26
3.5 Pattern of activity of the synergies during one stepping cycle 31
3.6 Muscles activated in each synergy 31
3.7 Models used for the generation of stepping motion at constant speed . . . 35
3.8 Steady stepping motions of the hind legs. 36
3.9 Steady stepping motions of the forelegs. 37
3.10 Influence of the extensor phase termination condition on the leg coordination 39
3.11 Changes of walking speed related to the level of the control input Ψ . . . 40
3.12 Relationship between the control input Ψ and the walking speed. 41
3.13 Stepping patterns (stick diagrams and muscular activation levels) 42
3.14 Swing and stance periods 43
3.15 Cyclic period and duty ratio 43
3.16 AEP and PEP 44

4.1 Simplified quadrupedal model 50
4.2 Stance and swing trajectories 53
4.3 Phase differences between the stepping motions of the legs in the pace, the trot and the walk gaits (the left hind leg is taken as the reference). . . 55
4.4 Contribution of the phase modulations to the emergence of left-right alternate stepping 58
4.5 Entrainment between the stepping of the legs, the rolling motion of the body and the lateral transfer of leg loading. 58
4.6 Illustration of the influence of Δy_{AEP} on γ 61
4.7 Influence of Δy_{AEP} on the walking pattern 62
4.8 Influence of the PD control gains of the knee and ankle joints 64
4.9 Walking pattern with $T_{tot} = 0.40$ sec 65
4.10 Modulation of the walking cyclic period and increase of the rolling motion. 67
4.11 Adjustments required to keep a walk gait when adjusting the walking cyclic period 68
4.12 Adaptations of the walking pattern characteristics when the speed is modulated 70
4.13 Instability occurring for small values of $\hat{\beta}$ 71
4.14 Adjustments required when adjusting the walking speed 71

4.15 Modulation of the walking speed 72

5.1 Lateral perturbation 76
5.2 Stabilizing action of the phase modulations 77
5.3 Resistance ability against lateral perturbations depending on the stance to swing transition condition 79
5.4 Performances against lateral perturbations with and without phase modulations 80
5.5 Timings of the application of the perturbations and influence on the body rolling motion 81
5.6 Modulation of the duty ratios (perturbation of 15 N at FR) 81
5.7 Modulation of the stance period of the supporting legs (perturbation of 15 N at FR) 82
5.8 Modulation of the duty ratios (perturbation of 2 N at HL) 83
5.9 Modulation of the stance period of the supporting legs (perturbation of 3 N at HL) 84
5.10 Ascending coordination mechanism in action and recovery from a perturbation 87
5.11 Influence of the cyclic period and the speed on the stability 89
5.12 Types of uneven terrain 90
5.13 Proposal for the mechanisms coordinating stepping in the fore and hind legs of walking cats 92
5.14 Comparison between the proposed control system and the one used in Tekken. 93

A.1 Skeletal models 101
A.2 Definition of the joint angles and representation of the muscular systems for the fore and hind legs 106

B.1 Synergy structure 113
B.2 Detailed view of the structure of the sensory feedback pathways (stance synergy) 113

C.1 ν_x and ν_y functions. 124
C.2 Parameters of the inverse kinematics model 125

D.1 Transient phase: supporting periods and leg controller phases 128
D.2 Transient phase: cyclic periods, phase differences and body rolling motion amplitude 128

List of Tables

3.1 List of the symbols and notations 18

4.1 List of the symbols and notations 48
4.2 Dimensions and masses of the simplified quadrupedal model bodies 50
4.3 Values of the parameters used to generate the walking pattern of Figure 4.9 60

5.1 Values of the parameters in Equations 5.2, 5.3 and 5.4. 86
5.2 Performances on uneven terrain 91

A.1 Dimensions and masses of the skeletal models bodies 102
A.2 Parameter values for functions F_L, F_V and F_P of the muscle model. . . . 103
A.3 Values of the parameters of the hind legs muscular system 105
A.4 Values of the parameters of the forelegs muscular system 105

B.1 Values of the NPG interneurons parameters 111
B.2 Values of the NPG sensory neurons parameters 111
B.3 Values of the synaptic weights of the connections between the NPG neurons 111
B.4 Synergy initiation and termination conditions 116
B.5 Synaptic weights of the connections from the TI neuron to the IM neurons in each synergy 116
B.6 Parameters of the sensory feedback pathways 117
B.7 Synaptic weights $w_{TI\_IM_m}$ of the connections from the TI neuron to the IM neurons in each synergy 118
B.8 Synaptic weights $w_{TI\_VG_{s\_m}}$ of the connections from the TI neuron to the VG neurons of the sensory feedback pathways 118
B.9 Parameters of Equations B.1, B.2 and B.4 for the PFCM interneurons. . . 119
B.10 Synaptic weights $w_{IN_j\_IM_m}$ and $w_{IN_j\_VG_{s\_m}}$ of the connections from the PFCM interneurons IN_j to the IM and VG neurons in the MOSS 119

Chapter 1

Introduction

1.1 Overview

Robotics is devoted to the study and the development of machines that can replace humans in the execution of various tasks, most of the time either fastidious, boring, hard or dangerous. Robots must then be endowed with the abilities required to fulfill those tasks and one of the most primitive of them is mobility. Accordingly, much attention has been devoted since the very beginning of robotics to locomotion and the last decades have seen the development of many mobile robots with applications in the field of operations in hostile environment (including space, underwater, nuclear, rescue, military and so on) or execution of service missions (like nursing care, medical assistance, agriculture and so on) for example. In many cases, the robot must move across irregular or unstable terrains to fulfill its mission. In that situation, the limitations of the traditional wheeled and tracked vehicles become clearly apparent, to the extent that, according to Raibert (1995)(47), only half of the world's land mass is actually accessible to them. This constitutes one of the main reasons to study legged locomotion, as legged robots are expected, like humans or animals on foot, to be able to reach a much larger fraction.

At the same time, another benefit that can be found in studying legged locomotion is to investigate precisely how these models, animals and humans, are able to adapt and achieve such a high degree of mobility in virtually any kind of terrain. This question is far from being solved as these abilities are the result of intricate interactions between extremely complex mechanical and control systems, hence complicating the analysis. In this context, studies on robots and/or computational simulation models represent an alternative, synthetic approach that can be used to test hypothesis that would have been extremely difficult or impossible to consider using the analytic approach on the biological systems.

In conclusion, the study of legged locomotion presents the double benefit of potentially resulting in improvements of the robots performances on one hand, and, on the other, of deepening our knowledge about ourselves, as humans.

1.2 Background

1.2.1 Biological concepts of legged locomotion control

Legged animals are characterized by their great mobility. They are able to adjust their speed in a large range, going from low-speed walking to high-speed running, according to their ongoing behavior (rest, hunt, escape, etc) and to their environment. Moreover they show marvelous adaptation abilities which allow them to successfully travel even across very irregular terrains. However, trying to understand what gives them such abilities is far from being easy. From the standpoint of one individual, the body and the nervous system are biological systems of an extreme complexity and in close interaction with each other, which makes the analysis rather hard. In addition, legged animals present a great variety in size and anatomical organization so that, even if knowledge about locomotion is gained for a particular species, it is not trivial to discover the underlying common fundamental principles.

Despite these difficulties, the biological study of motion has progressed and it has become generally accepted that the locomotion of animals is mainly generated at the spinal cord level by neural circuits called *Central Pattern Generators* or CPG (Grillner 1981(25)). The CPG designates the set of nervous mechanisms that produces the motor patterns for a specific behavior (here the locomotion) under open loop conditions, i.e. in a feed-forward manner, in the absence of sensory-feedback. The traditional view is that the CPG is usually made of various controllers that actuate the individual locomotor organs (in the case of legged locomotion, the legs) and interact with each other to reach a common rhythm and maintain definite phase relations between them. As the activity of the CPG is essentially feed-forward, it needs to be adjusted to generate motion adapted to the environment. On one hand, the activity of the CPG is modulated by local control loops based on proprioceptive sensory feedback coming from the locomotor organs. Other adjustment signals are coming the upper neural structures of the brain, i.e. the cerebrum, cerebellum and brain stem (Cohen and Boothe 1999(11)) based amongst others on exteroceptive sensory information (vision, vestibular information, ground reaction force, etc). To summarize, it appears that the locomotion generation process in animals involves many different entities at different level and results from their harmonious interactions. However, their relative importance and contribution in each situation is still far from being completely understood.

As regards the influence of the size, Alexander (Alexander 1984(2) & 2003(3)) showed that mammals of different sizes tend to move in dynamically similar fashion whenever their Froude (Fr) numbers are equal:

$$\mathrm{Fr} = \frac{v^2}{g \cdot h} \tag{1.1}$$

where v is the locomotion speed, g the gravity acceleration, and h is the height of the hip joint from the ground. For example, transitions from walking to running, or from gait to another, occur for similar values of Fr in very different species. Hence, Fr can be used to characterized the dynamical phenomena that take place a certain locomotion speed and it was pointed out by Fukuoka et al. (2003)(21) that:

- at low Fr (low speed), since gravity is dominant, *posture control* using sensory information such as ground reaction force information and/or vestibular information is predominant to generate stable locomotion.
- at high Fr (high speed), since the influence of the inertial forces[1] is dominant, *rhythmic motion control* to construct a limit cycle becomes more important.

1.2.2 Legged locomotion control methods

According to this view, legged locomotion control methods that have been proposed until now can be classified into ZMP-based control and limit-cycle-based control.

ZMP-based control was shown to be effective for *controlling posture* and *low-speed walking.* The ZMP is the point with respect to which the moment of all the ground reaction forces is zero (Vukobratović and Borovac 2004(61)). It can be seen as the extension of the vertical projection of the center of gravity on the ground, including inertial forces and so on. In ZMP-based control, the central concept is to maintain the stability by keeping the ZMP inside the polygon defined by the supporting feet. The trajectory of the ZMP is generated to meet that condition and the trajectories of all the articulations are then computed accordingly. *ZMP-based control* was used to control posture and generate low-speed walking with biped (Takanishi et al. 1990(56); Hirai et al. 1998(27)) and quadrupeds (Yoneda et al. 1994(65)). However, it is not good for locomotion at medium- or high-speed from the standpoint of energy consumption, since a body with a large mass needs to be accelerated and decelerated by the actuators in every step cycle.

In contrast, motion generated by *limit-cycle-based control* (Miura and Shimoyama 1984(39)) has usually a superior energy efficiency because the natural dynamics of the system is taking into account to a greater extent than in the ZMP-based control methods. This

[1] in particular the centrifugal force during the circular motion of the body around the points of contact with the ground

kind of control is effective to generate *middle- and high-speed locomotion*. However, when increasing the walking cyclic period, the stability of the motion decreases and there is a practical limit of the cyclic period over which stable dynamic walking cannot be realized with such type control (Kimura et al. 1990(31)). In the medium-speed range, the most popular approach is to use an artificial neural system model, based on the biological knowledge about the CPG, to build the limit-cycle. In most of the cases, the CPG is modeled by a set of oscillators (each of them driving the motion of one joint or one leg) interacting with each others via a network of couplings. The phase of these oscillators is modulated by sensory feedback. Using such an approach, dynamic walking was generated in simulation (Taga et al. 1991(53); Taga 1995(55); Miyakoshi et al. 1998(40); Ijspeert 2001(28)) and real robots (Kimura et al. 1999(34); Ilg et al. 1999(30); Tsujita et al. 2001(60); Lewis et al. 2003(37); Ijspeert et al. 2007(29)). On the other hand, when considering high-speed running, Full and Koditschek (1999)(22) pointed out that, since kinetic energy is dominant, self-stabilization by a mechanism with a spring and a damper is more important than the adjustments by the neural system. Such approach resulted for example in the realization of high-speed mobility with quadruped (Buehler et al. 1998(9)) and hexapod (Saranli et al. 2001(50)) robots with appropriate mechanical compliance of the legs.

1.3 Motivation

Although good performances have been generated with the previously mentioned approaches, each of them was particularly adapted to a certain range of locomotion speed. Hence, no control method has been proposed yet that can, like the nervous system of animals, integrates posture and rhythmic motion controls in order to generate stable and efficient locomotion in the broad range of speeds going from low-speed walking to high-speed running. This constitutes one of the most interesting and challenging issues in legged locomotion. The research presented in this thesis represents a contribution, although modest, toward this goal.

1.3.1 Limitations of former researches

As regards the integration of posture and rhythmic motion control, the study of dynamic walking presents the benefit compared to other gaits that it is used by animals in the range going from low to medium value of Fr so that both kind of controls are important. In former studies (Fukuoka et al. 2003(21); Kimura et al. 1999(34), 2007(35)), dynamic walk was realized with a mammal-like quadrupedal robot "Tekken" using a control system based on a CPG model to generate the rhythmic motion. Their CPG model was made of network of four oscillators, each of them responsible for the actuation of one leg. The activity of each oscillator was modulated using hip joint position feedback.

The following features were added to this basic architecture:

- modulation of the activity of the CPG using feedback of vestibular information
- various feedback mechanisms, called "responses" and "reflexes", each aimed to tackle particular sources of instability

Using this approach, Tekken was able to adaptively walk on various types of terrains with medium degrees of irregularity. Hence, posture control could be achieve to a certain extend with Tekken.

However, this approach has several drawbacks. The first one is the complexity of the control architecture, which makes it hard to estimate the relative contributions of the basic CPG architecture and the additional mechanisms in the generation of the adaptive locomotion. For that reason, it is also difficult to extend this architecture any further or apply it to other robots. Moreover, Tekken was not able to realize stable low speed walking with long cyclic period.

1.3.2 Object of this thesis

The incapacity of Tekken to walk with a long cyclic period was estimated to be related to the lack of sensory feedback of the load supported by the legs (or leg loading) to the CPG (Kimura, personal communication). This idea is in agreement with the results of studies (Deliagina et al. 2002(14) for example) pointing out that feedback mechanisms based on this kind of sensory information are vital for postural control in four-legged mammals. Moreover, it has been recently demonstrated in simulation studies that the control of the stance-to-swing transition using sensory signal related to leg unloading is crucial for leg coordination during walking (Ekeberg and Pearson 2005(17)).

Grounded on these motivations, this thesis considers the use of leg loading information in a CPG controller and aims at generating stable quadrupedal dynamic walk. The leg-loading-information-based adjustments of the CPG activity are carried out in the form of phase modulations[2], which consist in the modulation of the respective durations of the stance and swing phases of the stepping motion of the legs during the walking cycle. More specifically, the stress is put on the role of the regulation of the stance to swing transition by the leg loading information. The contribution of this mechanism to the interleg coordination and stabilization of the posture against perturbations during locomotion in the range from low- to medium-speed is investigated using dynamics simulations. Moreover, this thesis aims at assessing the performances of this approach in order to provide a reference when considering additional control mechanisms in the future.

[2]see Section 2.2.4 for detailed explanations

1.4 Related studies

1.4.1 Phase modulations

The implementation in simulation or on real robots of various types of sensory-based phase modulations in CPG controllers have been reported. However, to the author's best knowledge, only the last two studies presented in this section considered phase modulations based on leg loading information.

In his simulation of a bipedal neuro-musculo-skeletal model, Taga (1995)(54)&(55) developed a CPG controller based on a neural rhythm generator made of seven neural oscillators (NO) proposed by Matsuoka (1987)(38). The phasic activity of each NO was modulated using inertial body segments angles, as well as the angle representing the position of the center of gravity of the model relative to its center of pressure. Outputs generated by the NOs were used to actuate the musculoskeletal model. Using this approach, he simulated two-dimensional adaptive walk.

The same neural oscillator model was applied to the locomotion of a quadrupedal robot on irregular terrain (Fukuoka 2003(21); Kimura 2007 (35)). The CPG was made of four NOs, each driving the pitching motion of one leg. The rhythmic activity of each NO was entrained using feedback of the hip joint angle of the leg under its control. The CPG activity was also modulated using a set of "responses", including one based on the feedback of the body roll angle.

Tsujita et al. (2001)(60) proposed a control system able to generate various quadrupedal gaits. The stepping motion of each leg was controlled by a non-linear oscillator and the gait pattern was set by adjusting the couplings between the oscillators, via a matrix of nominal phase references. Moreover, information provided by the touch sensors at the tip of the legs was used to modulate the swing phase duration by resetting the phase of the corresponding oscillator when a swinging leg touched the ground. Using this approach, adaptive gait pattern control was achieved in simulation and on a real robot.

A similar architecture, made of a network of non-linear oscillators with phase resetting at touchdown, was used in Aoi and Tsuchiya (2005)(4) to control the locomotion of a biped robot. The phase resetting mechanism was reported to enhance to stability of the locomotion against perturbations.

Using a musculoskeletal model of the hind legs of the cat, Ekeberg and Pearson (2005)(17) investigated the respective importance of hip extension and leg unloading signals for stance termination. They found that modulation of the stance phase duration using leg loading information plays an essential role in the emergence and stabilization of stable alternate stepping. The forelegs were modeled as rigid bodies supporting the model at the front, while sliding on the ground. As a result, the motion of the model was

constrained to the sagittal plane, so that their study was limited to two-dimensional stepping.

Finally, Righetti and Ijspeert (2008)(48) proposed recently a generic network of coupled oscillators able to generate different quadrupedal gaits (walk, trot, bound and pace). For each oscillator, the phase transitions between stance and swing phases are regulated using leg loading information. Although they used a phase modulations mechanism similar to the one investigated in this thesis, in their architecture, the generation of the gait as well as its stabilization is mostly considered at the level of the oscillators interactions, by setting properly the couplings between the leg oscillators. The phase modulations were said to "couple" the mechanical system with the CPG but no specific consideration was given to their role regarding the issues of rhythmic motion generation and postural control.

1.4.2 Musculoskeletal models and neural controllers

As regards neural controller of invertebrates, Kimura et al. (1993)(32) and (1994)(33) proposed a self-organizing model of walking patterns of insects. Their CPG controller was composed of three ganglia (one for each thoracic segment) and the neural network of each of them was made of non-linear oscillators. At the intrasegmental level, feedback of the position of the leg was used for the the generation of the muscular activation level patterns for a single leg. Leg coordination was insured by inhibitory intersegmental pathways, preventing adjacent legs to swing simultaneously, and excitatory and inhibitory afferent pathways based on the feedback of the force developed by the muscles of each leg. Due to this latter mechanism, the legs tended to share the load as efficiently as possible, contributing to optimize the energy transduction of the effector organs and consequently the global energy efficiency.

Espenschied et al. (1996)(20) implemented on a hexapod robot the gait pattern generator proposed by Cruse (1990)(12) referring to a stick insect. They also employed the swaying, stepping, elevator and searching reflexes observed by Pearson et al. (1984)(44) in a stick insect, and realized statically stable autonomous walking on rough terrain. A stepping pattern generator was associated to each leg and generated alternative swing and stance motions based on local kinematics information. The gait was generated in a decentralized fashion, through the interactions between the stepping pattern generators via a network of influences, linking only adjacent legs. These interactions also allowed for autonomous adjustments of the phase differences between legs when the leg motion was changed by reflexes.

As a computational simulation of a neural controller of vertebrates, Wadden and Ekeberg (1998)(62) designed an original neural controller for the actuation of a single leg, made of two links and four muscle-like actuators. Their controller was based on the Neural Phase

Generators approach that they originally proposed. The motion of the leg during one cycle was decomposed in four phases: liftoff, swing, touchdown and stance. During each phase, appropriate muscular activation levels were output and fast feedback pathways were activated. A single control input, modeling the input from the upper neural control centers, was regulating the muscular activation levels output during each phase as well as the transition between the NPG phases. This neuro-mechanical system was able to generate stepping motions in a large velocity range according to the level of the control input. As the model had only one leg, the issue of leg coordination was not investigated and the position of the hip was constrained to be over a fixed minimal height to prevent the leg to fall during the swing phase.

Tomita and Yano (2003)(59) generated bipedal stepping motions in two-dimensions, using a musculoskeletal model where each leg was actuated by four muscles based on Hill's model. This model was actuated by a CPG controller in which the muscle activity patterns generation and muscle tone adjustment were carried out separately, as in the locomotion generation system of animals. Muscle activity patterns were generated in two steps: a network of oscillators (entrained by local kinematic sensory inputs) generated phasic information, which was later translated into muscle activity patterns by a layer of four non-spiking neurons for each leg. Based on these patterns and the muscle tone level, the activation level of each muscle was computed, using additional energy optimization constraints. The activity of the CPG and the muscle tone level were modulated by an entity modeling the brainstem centers, whose outputs were computed on the basis of the desired velocity and balance constraints. The walking patterns generated using this approach were resistant to various mechanical perturbations.

A morphologically realistic musculoskeletal model of the cat hind legs, made of three links and six musculotendon actuators, was used in simulation by Yakovenko et al. (2004)(64) to evaluate the contribution of stretch reflexes to locomotion control. The influence of IF - THEN rules (using conditions on the sensory information to trigger transitions between the swing and stance phases) was also evaluated. To that purpose, the muscular activation patterns used for the swing and the stance phases were derived from a large base of biological data and fixed once for all. As a consequence, the underlying process of pattern generation and adaptation to the walking speed was not investigated.

Ekeberg and Pearson (2005)(17) developed a biologically-faithful simulation model of the hind legs of a cat. Each leg was made of three links actuated by a set of seven muscles whose activation patterns were generated by a leg controller made of a state-machine. Four states were implemented (liftoff, swing, touchdown and stance) and a set of fixed muscular activation levels, as well as a set of sensory feedback pathways, were associated to each state. Stepping motions resistant to various perturbations were generated. However, the speed of walking on flat ground was constant and no attention

was paid on how the muscular activation patterns should be modified to change the walking speed.

Aiming at the elucidation of quadrupedal/bipedal locomotion generation by the neuro-musculo-skeletal system in the Japanese monkey, Ogihara et al. (2006)(41) developed a whole-body musculoskeletal model based on anatomical data obtained from computed tomography and dissection. Based on kinematics data of the locomotion on a treadmill, they reconstructed the whole-body kinematics of the animal during quadrupedal and bipedal gaits, using the musculoskeletal model and a model-based matching technique. They also simulated the forward dynamics of the quadrupedal locomotion by coupling the model with a CPG controller made of a set of non-linear oscillators (one oscillator was associated to each limb and to the trunk segment). The oscillator phase was considered to encode the orientation and length of the limb axis, provided by the measured kinematics data. The joint torques were then obtained by inverse kinematics and local PD feedback control law.

1.5 Thesis Organization

This thesis is divided in the following manner:

Chapter 2 gives some generalities about leg locomotion and introduces a few concepts that are used across this thesis. Choices related to the architecture of the control system are presented and motivated. This leads to the definition of common principles on which are based the controllers developed in the following chapters

Chapter 3 reports the development of a neural controller able to induce two-dimensional adaptive alternate stepping at various walking speed using a musculoskeletal model faithful to the anatomy of the cat. The contribution of the control of the transition from stance to swing using leg loading sensory information to the emergence of the alternate coordination is explained. Adaptations taking place in my simulation when increasing the speed are compared with biological data and a conclusion concerning the role played by leg loading information in the regulation of the stance to swing transition in animals is drawn.

Chapter 4 presents a simplified controller used for generating stable quadrupedal dynamic walk. It explains the role of phase modulations based on leg loading information in the establishment of left-right alternate coordination of the legs. Conditions for the emergence of a walk gait using independent leg controllers are presented and modulations of the cyclic period and the speed are considered.

Chapter 5 investigates the stability of the walking patterns generated in the previous chapter. Stabilization provided by the phase modulations is evaluated and an original coordination mechanism is introduced to improve the performances against a perturbation type to which the system with the independent controllers only is quite sensitive. Performances on rough terrain are also assessed.

Chapter 6 summarizes the important findings of this thesis and enumerates possible directions for future research.

Chapter 2

Considerations on the control system architecture

2.1 Overview

This chapter regroups a series of considerations regarding the control system architecture. In the following chapters, two very different control architectures will be used for the generation of two-dimensional alternate stepping and three-dimensional quadrupedal dynamic walk. However, they both implements the common principles chosen and motivated in this chapter.

Section 2.2 gives a few generalities about legged locomotion and terms that will be employed in this thesis. Considerations about the controller architecture and motivations of the choices leading to the establishment of the common principles are given in Section 2.3.

2.2 Generalities about legged locomotion

2.2.1 Locomotion phases

In walking animals, the step cycle is made off of two principal parts, the *swing* (or transfer) phase and the *stance* (or support) phase. The swing phase starts when the leg reaches the *posterior extreme position*, or PEP, in relation to the body (Figure 2.1(a), A_1 & B). In this phase, the leg is lifted above the ground and moves forward in relation to the body until it reaches the *anterior extreme position*, or AEP (Figure 2.1(a), A_2 & B). In this position, the foot touches the ground, ending the swing phase, and the stance phase begins. In the stance phase, the leg moves backward in relation to the body until it reaches again the PEP and the cycle is over. During this phase, the leg is

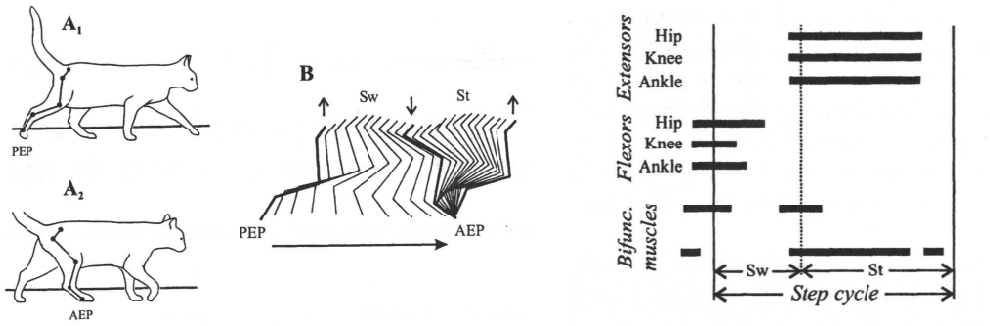

(a) A_1: PEP, A_2: AEP, B: stance and swing phases (from Smith et al. (1988)(52))

(b) Phases of activity of the main muscle groups controlling the cat hip, knee and ankle joints in the step cycle (from Orlovsky et al.(43))

FIGURE 2.1: Principal subdivisions of the walking cycle into phases (left: stance and swing phases, right: flexor and extensor phases)

loaded by a part of the body weight, and also generates a propulsive force to move the animal forward. The events of getting in touch with the ground at the beginning of the stance phase and leaving it at the end are respectively called the *touchdown* (or TD) and *liftoff* (LO).

On the other hand, when considering the pattern of activity of the muscles (or electromyographic (EMG) patterns) during the locomotion, Figure 2.1(b) shows that all the extensor muscles have very similar patterns of activity and are activated with more or less the same timing in the step cycle. Similar observations hold for the activity of the flexor muscles, although their pattern of activity are more diverse. This leads to another subdivision of the step cycle, based on muscular activities, into two phases: the *flexor* phase and the *extensor* phase. The flexor phase starts shortly before the onset of the swing phase and the activation of the flexor muscles causes the leg to shorten and to move forward during the swing phase. Termination of this phase occurs between the middle and the end of the swing phase and the extensor phase then begins. Activity of the extensor muscles start shortly before touchdown and continues nearly until the end of the stance phase.

2.2.2 Walking pattern characteristics

Walking patterns are usually characterized by various indicators or parameters. These include:

- T_{sw}: the swing period or duration of the swing phase.
- T_{st}: the stance period or duration of the stance phase.

- T_{tot}: the cyclic period. It is the duration of one locomotion cycle and is equal to $T_{sw} + T_{st}$.
- β: the duty ratio. It is the ratio between the stance and the stepping periods (i.e. T_{st}/T_{tot}).
- L_{str}: the stride length. It is the total distance traveled by the body during the stance phase. It is equal to the distance, in the coordinate attached to the model, between the foot position when the foot touches the ground (AEP) and the foot position when it leaves the ground (PEP).

2.2.3 Leg controller structure

It is broadly admitted nowadays that the organization of the CPG for locomotion in vertebrates is distributed and modular (Burrows 1996(10); Rossignol 1996(49)) and that during locomotion each of the four legs is driven by its individual control mechanism. In this thesis, it will be referred by the term *leg controller* or LC.

Generally speaking, for each phase of the stepping cycle, must be implemented in the leg controller a control entity that is responsible for the generation of motor patterns appropriate to the ongoing state of the locomotion. Hence, the number and the implementation of these control entities depend on the decomposition of the stepping cycle chosen (for example swing-stance or flexion-extension). These entities will be referred as the *phases* of the leg controller. The structure of the leg controller is usually organized in two levels:

- the *rhythm generation* level which regulates the activity of the phases of the leg controller and implements mechanisms to control the transitions between them,
- the *motor patterns generation* level which is responsible to generate the motor patterns appropriate for each phase.

2.2.4 Interleg coordination and phase modulations

When considering the locomotion at a higher level, the controllers of the different legs have to coordinate in order to generate smooth motion and insure the stability of the body posture. One method to achieve this objective is to adjust the respective durations of the swing and the stance phases of each leg controller in order to establish a common rhythm of stepping movements, with definite phase relations between the four legs, resulting in a gait. In this thesis, these adjustments of phase durations will be referred as *phase modulations*. Phase modulations are based on two main kinds of information:

- phasic information relative to the internal state of the leg controllers. For example, direct interactions between the leg controllers, inducing phases modulations in one leg based on the phase of one or more of the other leg controllers, fall in this category.
- proprioceptive and/or exteroceptive sensory informations.

In animals, numerous phases modulations mechanisms have been reported to exist but it is quite often difficult to estimate their relative importance in the generation of locomotion.

2.2.5 Central Pattern Generator

Strictly speaking, the term "*Central Pattern Generator*" or CPG designates in biology the set of nervous mechanisms that produces the motor patterns for a specific behavior (here the locomotion) under open loop conditions, i.e. in the absence of sensory-feedback (Orlovsky et al. 1999(43)). In this thesis, it is used with a broader meaning, including the influence of the sensory feedback, and refers to the whole control system, formed by the leg controllers and all the associated phase modulations mechanisms.

2.3 Control system architecture: choices and motivations

2.3.1 CPG model: oscillatory or sensor-dependent

Based on the biological knowledge that the CPG in animals presents a intrinsic rhythmic activity that allows it to generate the motor patterns even without sensory feedback, non-linear oscillators have been broadly used as CPG models to generate rhythmic motions. This kind of CPG will be referred as *oscillatory* because the cyclic period is then essentially decided by the intrinsic frequency of the oscillators and modulated to a certain extent by the sensory-feedback.

On the other hand, Cruse (2002)(13) stated that:

- *A central rhythm generator implying a "world model" in the form of a central oscillator could even cause the behavior to deteriorate in unpredictable situations.*
- *Local rules exploiting feedback loops and the mechanical properties of the body can produce the basic rhythm and can sufficiently explain a considerable part of the coordination.*

Accordingly, a more *sensor-dependent* CPG model is expected to result in a greater adaptability to the environment. Furthermore, it is also more adapted to the goal of this thesis, as using a oscillatory CPG model would complicate the estimation of the real contribution of the phase modulations to the observed performances. For that reason, the sensor-dependent CPG model was preferred. At the LC level, this choice implies that the phase transitions are controlled by sensory feedback in such a way that:

- as long as the associated conditions are not fulfilled, phase transition does not occur,
- as soon as they are, phase transition is triggered.

At the level of the interleg coordination, phase modulations due to direct interactions between the leg controllers were used as less as possible.

Using such an architecture, rhythmic motion is generated in a self-excited way (Ono et al. 2004(42), Poulakakis et al. 2006(45)), through the interaction between the mechanical structure, the motor commands and the local feedback so that various characteristics of the walking patterns (such as the cyclic period for example) are emergent properties of the system.

2.3.2 Phase transition conditions and phases modulations based on leg loading information

The *transition from swing to stance* is triggered when the contact of the foot with the ground is detected, or equivalently when the load supported by the leg, or *leg loading*, becomes greater than zero. This mechanism was shown to improve the stability of the walking of a biped (Aoi and Tsuchiya 2005(4), 2006(5)), justifying its use in our controller. However, at the beginning of the swing phase of the leg controller, the foot is usually still in contact with the ground and the first task of the swing phase is to induce the liftoff. For that reason, another condition is added to prevent the transition to occur during the early stage of the swing phase.

On the other hand, for the *transition from stance to swing*, the basic idea is that, to maintain postural stability, the leg should not swing as long as it supports a significant part of the body weight. Accordingly, the transition is triggered only when the leg loading is smaller than a certain threshold. As previously, an additional condition is used to prevent the transition to occur during the early stage of the stance phase.

During the locomotion, the weight of the body is rhythmically transfered between the legs, allowing the unloaded ones to swing while the others are supporting the body. When the normal transfer of load between the legs is perturbed, the regulation of the phase transitions using the previous conditions will adjust the respective durations of swing

and stance phases, hence resulting in phase modulations that contribute to reestablish the normal leg coordination and posture. These are referred as the *phase modulations based on leg loading information*. Detailed explanations about their action are postponed to the next chapters.

2.3.3 Common principles

In the next chapters, two very different leg controller architectures are presented. In Chapter 3, a neural controller is developed for the actuation of a complex musculoskeletal model faithful to the anatomy of the cat in order to generate two-dimensional alternate stepping. On the other hand, in Chapter 4, a much simpler leg controller is used for the experiments in three dimensions. However, both of them implements the design specifications motivated in the previous sections:

- sensor-dependent CPG model,
- control of the transitions between the stance and the swing phase based on leg loading information.

These are referred as the *common principles*.

Chapter 3

Generation of two dimensional alternate stepping

3.1 Overview

In this chapter, a biologically-inspired approach is used to generate stepping motions with musculoskeletal models faithful to the anatomy of the cat, presented in Section 3.3. A neural controller able to actuate the musculoskeletal model of one leg in order to induce stepping motions of the model at various locomotion speeds is developed in Section 3.4. Generation of two-dimensional alternate stepping at constant speed, with the fore and the hind legs models separately, is reported in Section 3.5, and the contribution of the phase modulations based on leg loading information to the emergence and stabilization of the alternate coordination is explained. Finally, in Section 3.6, adaptive stepping at various walking speeds is realized with the hind legs model. Adaptations of the stepping patterns taking place in simulation are compared with the ones occurring in real animals and an interesting conclusion about the role of leg-loading-information-based regulation of the stance-to-swing transition in animals is drawn.

3.2 List of symbols and notations

For the sake of clarity, Table 3.1 regroups and defines the symbols and notations used in the musculoskeletal model and the neural leg controller.

TABLE 3.1: List of the symbols and notations

Indexes	
m	Muscle index, $m \in \{IP, AB, PB, VL, Gas, Sol, TA\}$ (for the hind legs) or $m \in \{BC, LD, T, B, WF\}$ (for the forelegs)
s	Musculoskeletal model sensory output index, $s \in \{x_m, v_m, f_m, fc\}$
Musculoskeletal model input and outputs	
a_m	Muscular activation level of muscle m
x_m	Normalized length of muscle m
v_m	Normalized speed of contraction of muscle m
f_m	Force developed by muscle m
f_c	Foot touch sensor signal
Neurons	
TI	Tonic input neuron
IN_j	Interneuron of the PFCM
H, Q, T, IP	Interneurons of the NPG
PF, NF	Sensory neurons of the NPG
ITU	Initiation and termination unit
SN_s	Sensory neuron transducing the sensory signal s
IM_m	Interneuron located in one of the synergy and connected to MN_m
VG_{s_m}	Variable gain neuron located in one of the synergy, receiving input from a neuron SN_s in the same synergy and connected to MN_m
MN_m	Motor neuron connected to muscle m
Synaptic weights	
$w_{TI\_IM_m}$	Weights of the connections from neuron TI of one synergy to all the IM_m neurons of the same synergy
$w_{TI\_VG_{s\_m}}$	Weights of the connections from neuron TI of one synergy to all the VG_{s_m} neurons of the same synergy
$w_{IN_j\_IM_m}$	Weights of the connections from the interneurons IN_j of the PFCM to all the IM_m neurons of a synergy
$w_{IN_j\_VG_{s\_m}}$	Weights of the connections from the interneurons IN_j of the PFCM to all the VG_{s_m} neurons of a synergy

3.3 Musculoskeletal models

When considering the design of a biologically-inspired system, one always faces the trade-off between model simplicity and biological faithfulness. On one hand, from the engineering point of view, there is the need to keep the system as simple as possible to facilitate the analysis of the system behavior and its control. On the other hand however, the system has to be complex enough to account for the behaviors observed in the incredibly complex systems that are biological creatures. This latter is especially true if the very goal of implementing the system is the investigation (and if possible the elucidation) of such behaviors.

The model of the cat hind legs proposed by Ekeberg and Pearson (2005)(17) presents the benefit to be faithful to the anatomy and physiology of the cat to a good extent, while having still an acceptable level of complexity and being rather easy to use. For that reason, a model nearly identical to theirs was used for the design of the neural leg controller (Section 3.4) and the generation of stepping motion at various speeds with the hind legs (Section 3.6). It is represented in Figure 3.1(a) and will be referred from here on as the *simplified hind legs model*. The main difference with Ekeberg and Pearson's model is the tetrapod wheeled structure, used instead of two rigid forelegs to support the front part of the body. The supporting structure allows two degrees of freedom to the trunk: translation in the forward direction (i.e. along the roll axis) and rotation around the pitch axis at the junction of the trunk and the structure.

After completion of the neural leg controller design, the mechanical structure was extended to generate stepping motions with the forelegs as well (Section 3.5). The trunk and the forelegs were added to the hind legs, resulting in the model represented in Figure 3.1(b) which will be referred from here on as the *quadrupedal model*[1]. The design of the musculoskeletal model of the forelegs was achieved on the basis of measurements on a real cat skeleton and studies about the anatomy and the physiology of the cat forelegs (Boczek-Funcke et al. 1996(7); English 1978(18)(19); Kuhtz-Buschbeck et al. 1994(36)).

Although care was taken to keep the models simple, they still involve a great number of parameters that, for the sake of clarity, are given in AppendixA.

3.3.1 Skeletal systems

In both models, the hind legs are made of three segments (thigh, shank and foot) and are connected to each others and to the trunk by three rotational joints around the pitch axis (from the most proximal to the more distal: hip, knee and ankle, see Figure 3.2).

[1]However, quadrupedal walking could not be realized using this model and alternate stepping was generated with the forelegs and the hind legs models separately, as explained in Section 3.5.1.

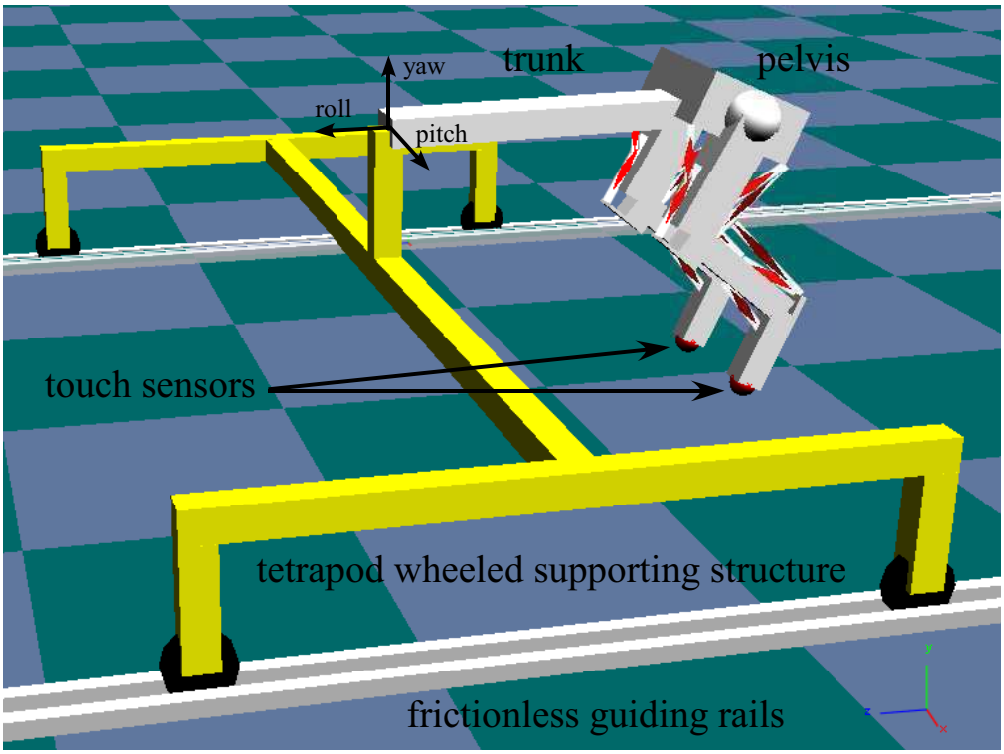

(a) Simplified hind legs model

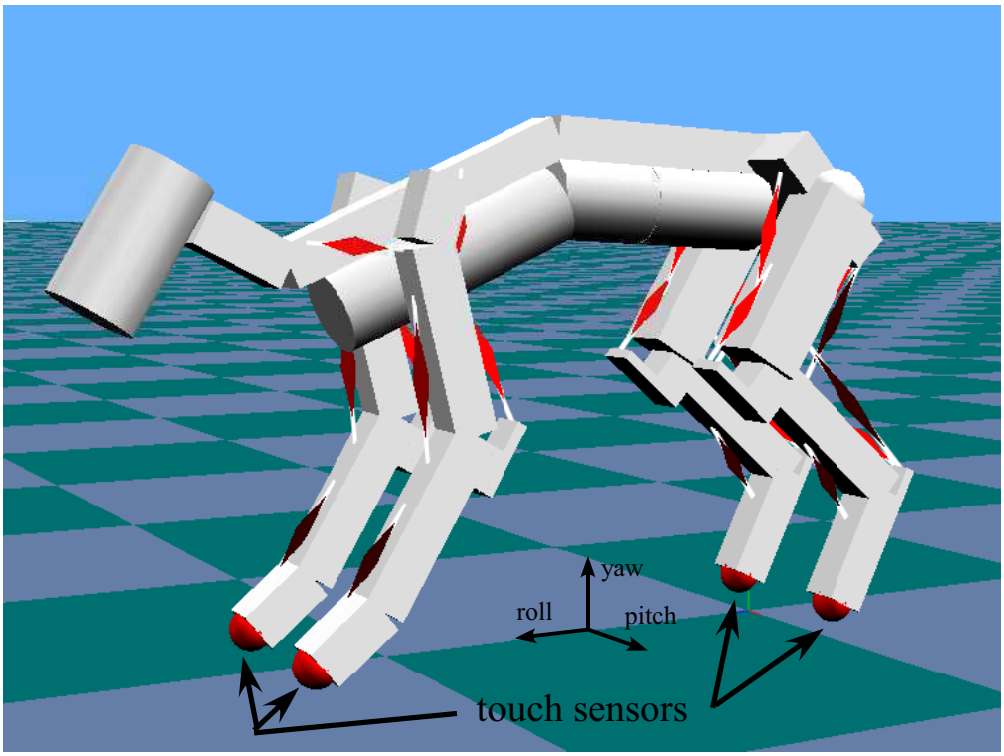

(b) Quadrupedal model

FIGURE 3.1: Musculoskeletal models

The structure of the trunk, on the other hand, differs depending on the model and reflects much more the real anatomical structure in the case of the quadrupedal model. However, in both cases, the trunk is monolithic, i.e. not articulated.

Finally, the forelegs, which are only present in the quadrupedal model, are made of four segments (scapula, humerus, radius and hand) but three rotational joints (from the most proximal to the more distal: shoulder, elbow and wrist). This is represented in Figure 3.2. To simplify the model, the scapula is fixed relatively to the trunk so that the equivalent of the hip joint in the forelegs is the shoulder joint. As a consequence, the effective length of the foreleg in the model is decreased compared to the one in real animal where the scapula contributes to the locomotion. With the same link length ratios as in the real specimen, the length of the leg was too short at the end of the stance and could not support properly the body. As a consequence, the model presented a propensity for stumbling and falling forward. For that reason, the length of the scapula link was reduced while the other links of the forelegs were elongated.

Each foot is made of a spherical touch sensor that outputs a binary signal fc (1 if the foot touches the ground and 0 if not).

3.3.2 Muscular systems

For the muscle, the model of Brown et al.(8) was used (described in details in Appendix A.2.1). Each muscle is modeled as active contractile elements (CE) in parallel with passive elastic elements (P). The force generated by the contractile elements F_P is scaled by the muscular activation level a_m and added to the fixed contribution of the passive elastic elements F_P, to give the total force output by the muscle f_m, as in the following equation (for muscle m):

$$f_m = f_m^{max} \cdot \big(a_m F_{CE}(x_m, v_m) + F_P(x_m)\big) \tag{3.1}$$

where f_m^{max} is the maximum isometric force[2] and x_m and v_m respectively the normalized length and normalized contraction speed. The muscles are considered to be directly attached to the skeleton, i.e. the tendons are not included in the model. Consequently, the torque generated by the muscles for each joint is computed using the forces of the muscles acting on the joint and the parameters describing the insertion of the muscles to the skeleton.

The muscular systems of the hind and forelegs are represented in Figure 3.2. Each hind leg is actuated by a set of seven muscles: Iliopsoas (IP: hip flexion), Anterior Biceps (AB: hip extension), Posterior Biceps and Semitendinosus (PB: hip extension and knee flexion), Vastus Lateralis (VL: knee extension), Gastrocnemius (Gas: knee flexion and

[2]Force output during isometric contraction, i.e. contraction during which the length of the muscle is not allowed to shorten

ankle extension), Tibialis Anterior (TA: ankle flexion) and Soleus (Sol: ankle extension). Most of the muscles are acting over a single joint (IP, AB, VL, TA and Sol) but two of them are biarticular muscles (PB and Gas).

On the other hand, the muscular system of the forelegs involves five muscles: Brachiocephalicus (BC: shoulder flexion), Latissimus Dorsi (LD: shoulder extension), Biceps (B: elbow flexion), Triceps (T: elbow extension) and Wrist Flexor (WF - wrist flexion).

3.3.3 Inputs and outputs

The muscular activation levels a_m of Equation 3.1 are generated by the motor neurons MN of the leg controller and are used to actuate the musculoskeletal model.

As regards the outputs, proprioceptive sensory information related to the state of the muscles (lengths x_m, contraction speeds v_m and generated forces f_m), as well as the touch sensor signal fc are fed back to the leg controller.

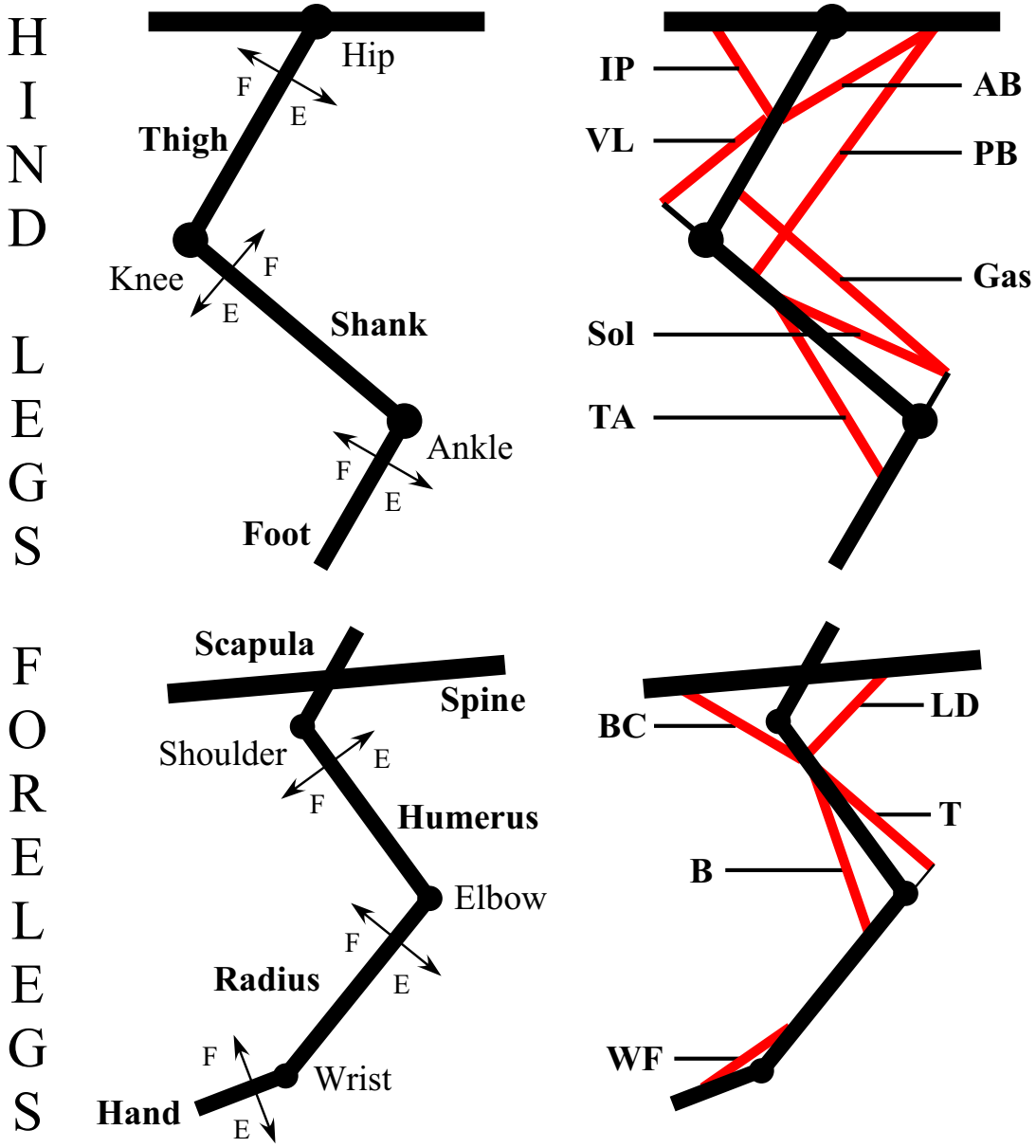

FIGURE 3.2: Muscular models of the fore and hind legs. For each joint, the directions of flexion (F) or extension (E) are indicated.

3.4 Leg controller organization

3.4.1 Overview and inspiration

Each leg is associated with one neural leg controller responsible for its actuation, i.e. for generating appropriate patterns of muscular activation levels a_m (in Equation 3.1) in order to induce stepping motion of the leg. The organization of the leg controller presented in this section is based on the Neural Phase Generators (NPG) architecture proposed by Wadden and Ekeberg (1998)(62) which was chosen for its simplicity and flexibility. Their distributed neural controller consisted of three parts: the NPG, the fast feedback pathways and an input from upper neural system. The role of the NPG in Wadden and Ekeberg (1998)(62) was to set the appropriate muscle activations and open the adequate sensory feedback pathways according to the leg phase, while being entrained by the sensory information. Their model of the NPG was an adaptation of an half-center model used for the simulation of swimming lamprey (Ekeberg 1993(16)). Since two phases were insufficient in the case of leg stepping, the number of NPG phases was set to four: liftoff, swing, touchdown and stance. Due to the simplicity of the musculoskeletal model they used, the translation of NPG activity into muscular activation levels, as well as the interaction between the controller and the tonic input from the upper neural system were straightforward and those aspects of the motor commands generation were little developed.

For these reasons, their architecture was extended in order to be used with the more complex, animal-like musculoskeletal model of Section 3.3 and to deal with additional sensory signals, in particular the leg loading sensory information. A clearer subdivision of the different parts was introduced and each of them was improved to simulate more adaptive stepping motion according to the sensory and command inputs. This resulted in a leg controller made of three parts: the Neural Phase Generator (NPG), the Motor Output Shape Stage (MOSS) and the Propulsive Force Control Module (PFCM), as represented in Figure 3.3.

As for the musculoskeletal models, the leg controller is rather complex and involves many neurons and consequently a great number of parameters to set. To clarify the presentation, details about neuronal models, the implementation of the MOSS and PFCM, as well as the settings of the parameters of the different parts the leg controller are not included in this chapter but rather given in Appendix B.

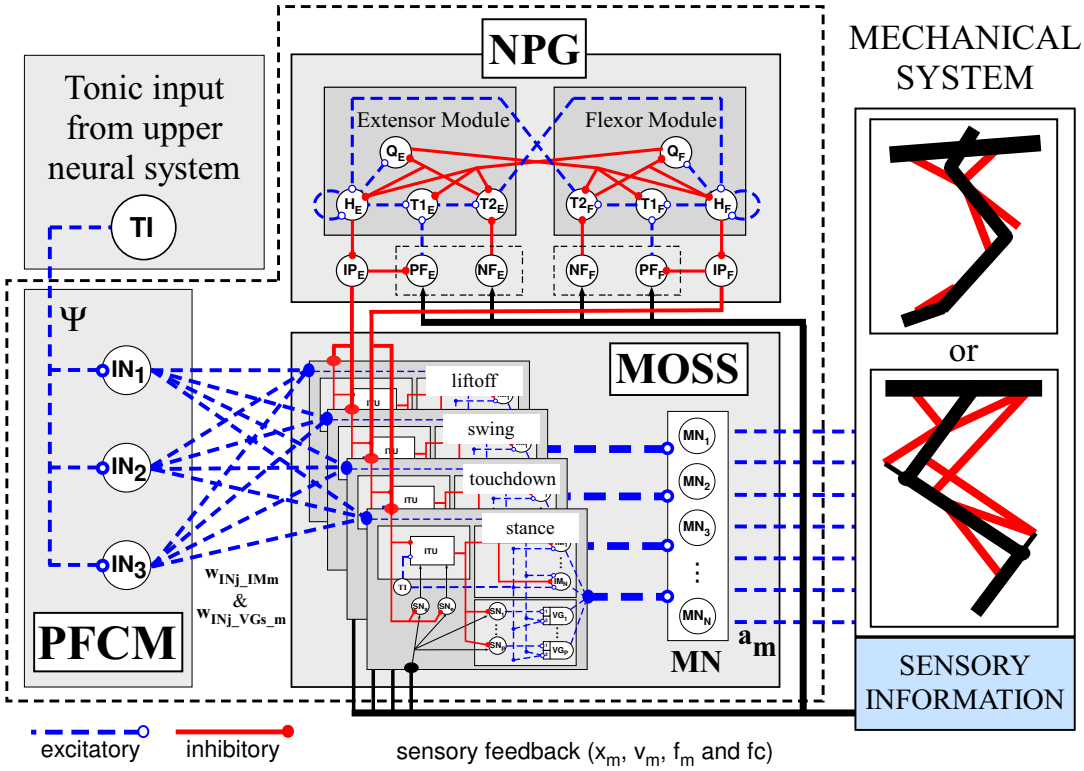

FIGURE 3.3: Overview of the Leg Controller. It is made of three parts: the Neural Phase Generator (NPG), the Motor Output Shaping Stage (MOSS) and the Propulsive Force Control Module (PFCM). The NPG is made of two modules (extensor and flexor modules), while four synergies (liftoff, swing, touchdown and stance) are implemented in the MOSS. The MOSS is under inhibitory influences from the IP neurons in the NPG and receives excitatory inputs from interneurons IN_j in the PFCM. The intensity of these excitatory inputs are adjusted by a single input Ψ modeling the tonic input[4] from the upper neural system. The MOSS is connected to the motor neurons MN that sum for each muscle the outputs generated by the synergies and output the muscular activation levels used to actuate the musculoskeletal model. Sensory information coming from the musculoskeletal model is used in the NPG to regulate the transitions between modules and in the MOSS by the sensory feedback pathways.

3.4.2 Neural Phase Generator (NPG)

First an overview of the NPG structure is given by listing the neurons constituting the NPG and explaining their role. Sensory informations used to regulate the transitions between the modules are then presented. The parameters settings for the NPG are given in Section B.2.2.

3.4.2.1 Neuronal structure

The NPG is the part of the leg controller responsible for the rhythm generation and is made of functional units called "modules", accounting for the main phases of the locomotion. It is constituted of two modules, the *flexor* and *extensor* modules, each

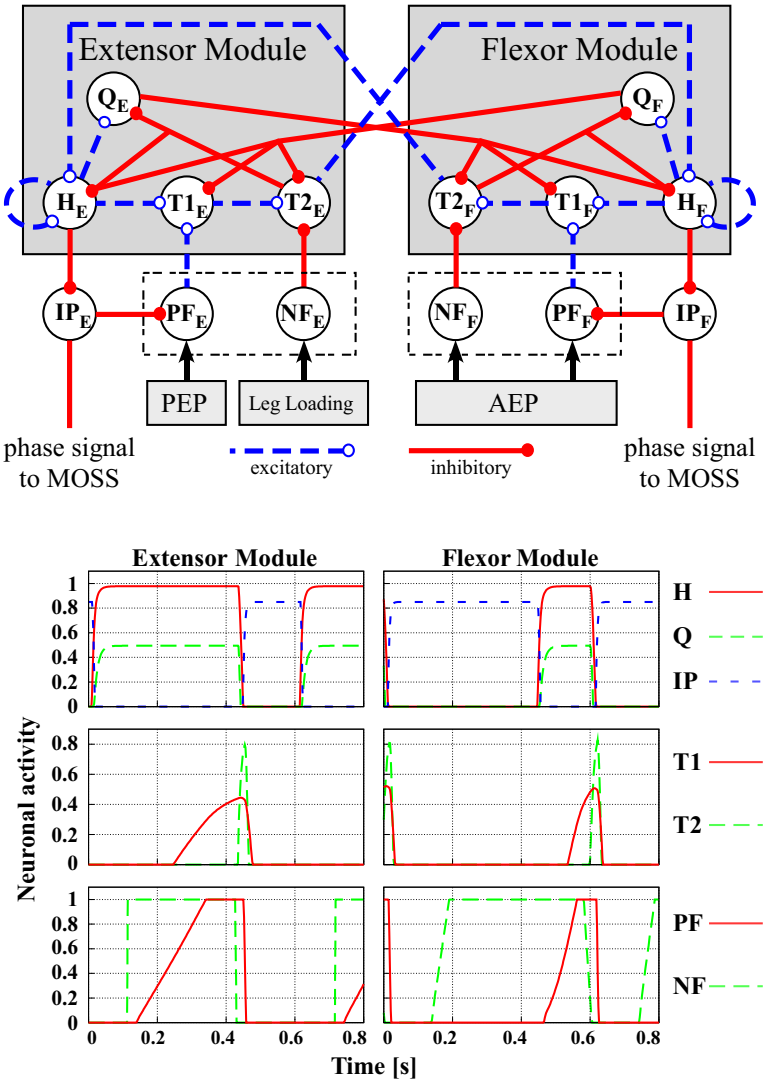

FIGURE 3.4: Internal structure of the NPG (up) and activity of its constitutive neurons during one walking cycle (down). The NPG is made of two modules, the *flexor* and the *extensor* modules, representing the two phases of the locomotor cycle. Transition of activity (represented by the activity level of H neuron) from module to the other occurs through the successive activation of the transition neurons T_1 and T_2, this later finally activating the H neuron of the next module. This process is under the control of sensory feedback, through excitatory and inhibitory influences mediated by the sensory neurons PF and NF. The corresponding neuronal activities during locomotion are represented (the locomotion speed is around 0.6 m/s).

of them accounting for the corresponding phase observed in animal locomotion (as explained in Section 2.2.1). The activity of the NPG characterizes the current phase of the locomotion of the leg. As represented in Figure 3.4, each module of the NPG is composed of seven neurons (all of them are interneurons, except PF and NF that are sensory neurons, see Appendix B.1 for details):

H **neuron** is the neuron representative for the activity of the module. It has excitatory connections with itself (self-excitation), as well as with the Q and T_1 neurons. On the other hand, it inhibits the IP neuron.

Q **neuron** ensures that only one module is active at the time by inhibiting the H and T neurons of the other modules.

T **neurons** are responsible for the transition to the next module. Two transition neurons are implemented[5]: a slow T_1 neuron which receives excitatory inputs from both the H neuron and the sensory feedback pathways (through the PF neuron) and a fast T_2 neuron, which is under inhibitory sensory influence (through the NF neuron). T_1 excites T_2 neuron which then promotes transition by exciting the H neuron of the next module, while reducing its inhibition by inhibiting the Q neuron of its own module. T_2 also inhibits the H neuron of its own module, in order to reduce the simultaneous activation of the two H neurons (hence reducing the simultaneous activation of the synergies at the MOSS level). This structure allows to set the time constant τ of T_1 in order to achieve long duration of module activity without slowing down the transition when inhibitory sensory input acting on T_2 disappears.

IP **neuron** is the complementary neuron of H: it is active when the module is inactive. This neuron has inhibitory connections to the interneurons in the MOSS and its output is used to select the synergies that can be active during the phase of the locomotion represented by the module to which the IP neuron belongs. Accordingly, the IP neuron of the flexor phase inhibits the liftoff and the swing synergies, while the one of the extensor phase inhibits the touchdown and the stance synergies. When H becomes active, it inhibits IP, hence it activates the previously inhibited synergies. The IP neuron additionally plays a gating role of the sensory feedback that promote the transition by inhibiting the PF neuron. IP receives a constant excitatory input from a tonic neuron not represented on the figure.

PF **and** NF **neurons** are sensory neurons that relay the sensory signals to the transition neurons T_1 and T_2. PF is used for the sensory feedback which promotes the transition and NF for the sensory feedback which prevents it.

[5]In the NPG model of Wadden and Ekeberg (1998)(62), there was only one T neuron per module, receiving only excitatory sensory inputs.

Activity of these neurons for both modules during one locomotor cycle is represented on Figure 3.4. Alternative activation of H, Q and IP can be observed, as well as the activation of T_1 and T_2 induced by the sensory feedback relayed by PF and NF.

Using this NPG structure, the regulation of the transition of activity from one module to another depends on two factors:

- the intrinsic properties of the neurons of the neural pathway involved in the transition ($H \rightarrow T_1 \rightarrow T_2$), as well as the synaptic weights of the connections between them;
- the excitatory and inhibitory influences to the T neurons based on sensory feedback and mediated respectively by the neurons PF and NF

The relative contributions of these two components can be adjusted to get either a more oscillator CPG model (when the first component is predominant) or a more sensor-dependent CPG model (when it is the second one that prevails). To comply with the common principles defined in Chapter 2, the parameters were set in order to get a *sensor-dependent* CPG. In particular, the synaptic weight of the excitatory connection from H to T_1 is set in order that the excitatory input coming from neuron H is insufficient to induce alone T_1 activity. In that case, the NPG does not naturally oscillate and the phase transitions are completely under the control of the sensory information relayed by PF and NF.

3.4.2.2 Sensory information used for the regulation of the phase transitions

The same kinds of sensory information as Ekeberg and Pearson (2005)(17) were used to regulate the transition of activity between the NPG phases.

The transition from the flexor to the extensor phase is triggered when the leg is getting close enough from the desired anterior extreme position (AEP). This is evaluated using the length of the extensor muscle of the most proximal joint of the leg (i.e. AB for the hind legs and LD for the forelegs). As the muscle length increases, $T1_F$ is progressively activated by the input coming from PF_F. On the other hand, NF_F is active as long as the muscle length is smaller than a certain threshold. When the threshold is reached, inhibition of $T2_F$ disappears and the transition occurs.

On the other hand, the transition from the extensor to the flexor phase is regulated using two conditions based on sensory information:

- the leg must be close enough to the posterior extreme position (PEP). This is evaluated using the length of the flexor muscle of the most proximal joint of the leg (i.e. IP for the hind legs and BC for the forelegs). As the muscle length increases, $T1_E$ is progressively activated by the input coming from PF_E.

- the leg must be unloaded (Leg Loading). Estimation of the leg loading is given by the muscular force developed by the most distal extensor muscle (i.e. *Sol* for the hind legs and T for the forelegs). As long as it is over a certain threshold, NF_E is activated and the transition is prevented.

3.4.3 Motor Output Shaping Stage (MOSS)

The MOSS is the part of the Leg Controller responsible for the generation of the muscle activation levels a_m. It is believed that in animals this complex task is realized by the nervous system using *muscle synergies* (Ting and McKay 2007(57)). This concept was introduced to explain how, despite the extreme complexity of the multi-articulated redundant musculoskeletal system that is the body, the nervous system is able to achieve simply repeatable and correlated multi-joint coordinated movements. Muscle synergies are defined as a specific pattern of muscle coactivation, constituting building blocks with which complex muscle activation patterns can be constructed. The global amplitude of the muscular activation levels provided by each synergy is temporally modulated by the nervous system using a single neural command signal. In the leg controller presented in this chapter, this concept is implemented in a really elementary way but which turned out to be sufficient. The term *synergy* designates the entity implementing a muscle synergy.

3.4.3.1 Implementation of a synergy

For the sake of clarity, only an overview about the synergy implementation is given in this section (detailed explanations can be found in Appendix B.3.1). Each synergy is characterized by:

- activity initiation and termination conditions, either related to timing or sensory event.
- a set of muscles that are activated with a constant muscular activation level during the period of activity of the synergy. This constitutes the *feed-forward component* of the muscular activation level patterns.
- a set of sensory feedback pathways that output variable muscular activation level for certain muscles, according to sensory information. It is the *feedback component* of the muscular activation level patterns. There are two kinds of sensory feedback pathways. The first one contains the pathways using the normalized length x_m and contraction speed v_m of the muscle to generate the muscular activation level, hence mimicking feedback pathways using signals from the muscle spindles in animals. The second category involves the pathways based on the muscular force f_m output

by the muscle, mimicking feedback pathways using signals from the Golgi tendon organ in animals.

The contributions of the feed-forward and feedback components are summed by the motor neurons (MN) which output the muscular activation levels for the muscular system. Each muscle of the muscular system is associated with one MN.

3.4.3.2 Four synergies

Four synergies are implemented in the MOSS: liftoff (LO), swing (SW), touchdown (TD) and stance (ST). These synergies are the same as the ones used in Wadden and Ekeberg (1998)(62) and Ekeberg and Pearson (2005)(17). The synergies that can be active during a given NPG phase are selected by the phasic signals coming from the IP neurons of the NPG. When the flexor module of the NPG is active, the touchdown and the stance synergies are inhibited and only the liftoff and the swing can be active. On the other hand, when the extensor module of the NPG is active, only the touchdown and the stance synergies can be active.

The purpose of the *liftoff* synergy is to induce a sufficient flexion of the leg at the beginning of the flexor phase to prevent the foot to subsequently hit the ground when the leg will swing forward, or equivalently, to provide a sufficient toes clearance. Accordingly, liftoff starts right after the beginning of the flexor phase for a fixed duration.

The *swing* synergy is activated at a fixed time after the beginning of the flexor phase and is active until the transition to the extensor phase. The purpose of this synergy is to move the leg forward.

The *touchdown* synergy is activated at the beginning of the extensor phase. Its activity is terminated when the contact of the foot with the ground is detected (touchdown event in Figure 3.5). The purpose of this synergy is to bring the leg in an appropriate position for landing.

Finally, initiation of the *stance* synergy activity is sensory triggered when the foot touches the ground and thus starts when the touchdown synergy terminates. It lasts until the end of the extensor phase. The purpose of this synergy is to support the body and to propel it forward.

During one walking cycle, the synergies are activated in the following order (as represented on Figure 3.5): liftoff, swing, touchdown and stance. The muscles activated in a feed-forward way and the sensory feedback pathways implemented for each synergy are given in Figure 3.6.

The MOSS also receives excitatory inputs from the PFCM, if implemented. They contribute to the shaping of the muscle activation levels within each synergy.

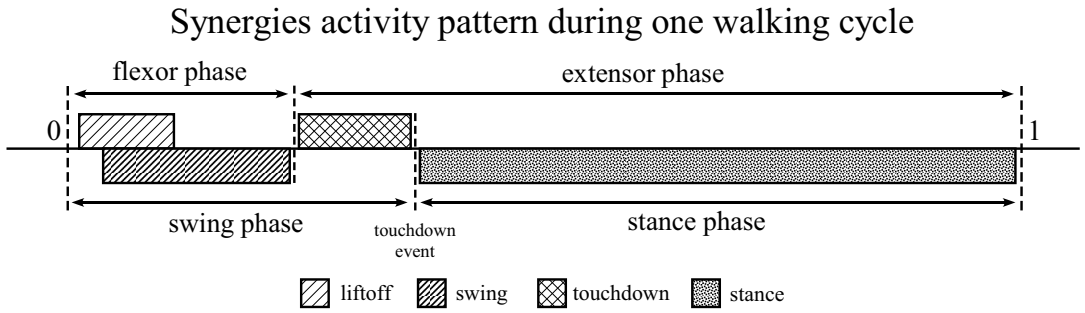

FIGURE 3.5: Pattern of activity of the synergies during one stepping cycle (parameters of the initiation and termination conditions are given in Table B.4).

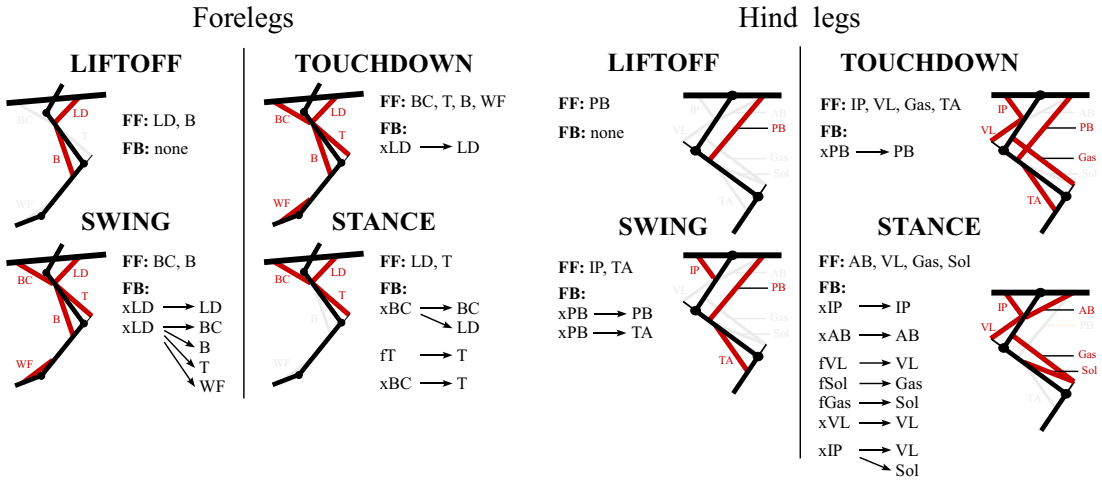

FIGURE 3.6: Muscles activated in each synergy (left: forelegs, right: hind legs). Active muscles are represented in red, while inactive muscles are in gray. FF gives the muscles activated in a feed-forward manner and FB lists the feedback pathways implemented in each synergy. For each pathway, the sensory signal used for the feedback (x_m stands for the muscular length and contraction speed, while f_m stands for the force generated by the muscle), as well as the muscle whose activation level is modified by the pathway are written respectively on the left and right sides of the arrow.

3.4.4 Propulsive Force Control Module (PFCM)

3.4.4.1 Action of the PFCM

The PFCM is the part of the leg controller that regulates the walking speed during the locomotion according to the value of the tonic input from upper neural system (Figure 3.3). This implementation is inspired by the fact that, in the cat, electrical stimulation of a small region in the midbrain, called the Mesencephalic Locomotor Region (MLR) can induce and regulate locomotion (Shik et al. 1966(51)). When the MLR stimulation is increased, a spinal cat changes its locomotion speed while changing its gait from walk to trot and even gallop. The PFCM is fulfilling a similar role as the MLR in the cat.

It was shown that the MLR stimulation is related to the propulsive force developed by the cat, i.e. the intensity of the muscle contractions. Indeed, the walking speed and the frequency of stepping are not directly controlled by the intensity of the MLR stimulation but also depend on the external conditions such as the slope and so on. This implies that, in the leg controller, the regulation of the walking speed according the tonic input by the PFCM should not be carried out by acting directly on the rhythm generation at the NPG level, to adjust the stepping frequency. This should rather be achieved through the adjustment of the propulsive force generated by the muscular system. In other words, the PFCM should interact with the MOSS to adjust the muscular activation level patterns, by scaling the intensity of the constant feed-forward muscular activations of certain muscles, as well as the gains of certain sensory feedback pathways at the MOSS level.

3.4.5 Implementation of the PFCM for the hind legs

Experiments with the PFCM were carried out only with the hind legs. It was found that speed adjustment can be carried out by modifying the values of a limited number of the MOSS parameters of the hind legs LC. These can be classified in two functional families according to the role that they play in the adjustment of the propulsion force.

The first one is the family of parameters that increases the forward trust that the leg transmits to the body when the stance synergy is active:

- the feed-forward activation of AB and VL,
- the gains of the pathways increasing the muscular activation levels of the knee and ankle muscles ($f_{VL} \rightarrow VL$, $f_{Gas} \rightarrow Sol$, $x_{IP} \rightarrow VL$ and $x_{IP} \rightarrow Sol$).

The second family contains the parameters that adjust the muscular force used to swing the leg forward, i.e. the activation of PB during the liftoff synergy and IP during

the swing synergy, as well as the feedback-induced activation of PB at the end of the swing synergy and during the touchdown synergy (pathways $x_{PB} \rightarrow PB$) which helps to regulate the landing position of the leg, and especially the knee joint angle.

Accordingly, the basic strategy to increase the propulsive force is to increase the feed-forward muscular activation levels and the feedback pathways gains of the first family to increase the forward trust and, in the same time, to increase those of the second family to increase the muscular power used to swing the leg as well. Based on these considerations, the design of the PFCM and its interface with the MOSS was carried out in order to be able to modulate the propulsive force developed by the leg by adjusting the value of the single input from upper neural system Ψ (details about the design process and the implementation are given in Appendix B.4).

3.4.6 Implementation of the common principles

The proposed leg controller implements the common principles defined in Chapter 2. As regards the control of the transitions between the stance and the swing phases based on leg loading information:

- at the NPG level, the transition from the extensor to the flexor phases is controlled using leg loading information. As the termination of the extensor phase ends the stance synergy and the initiation of the flexor phase causes the leg to swing, the transition from stance to swing is indeed controlled using leg loading information. To prevent the transition to happen in the early stage of the stance phase, sensory information about the proximity of the PEP is used as well.
- at the MOSS level, the transition from the touchdown synergy to the stance synergy occurs when the foot touches the ground, hence the transition from swing to stance is triggered using ground contact information. To prevent the transition to happen in the early stage of the swing phase, the touchdown synergy is activated only when the extensor phase becomes active. This requires first the termination of the flexor phase activity, which occurs only when the leg is close enough from the AEP.

Regarding the CPG model issue, parameters of the NPG were set in such a way that that the transitions of activity from one module to the other depend only on sensory information, hence resulting in a sensor-dependent CPG model (see Section 3.4.2.1).

3.5 Generation of alternate stepping at constant speed

This section presents the results of the experiments aiming at generating stepping motion at constant speed with the musculoskeletal models, using the leg controller architecture presented in the previous section. The case of the constant speed is first considered because the structure of the LC can then be simplified to the NPG and the MOSS, as the PFCM is no longer needed. Realization of stable alternate stepping with the hind legs and the forelegs models separately, using the simplified structure of the leg controller, is reported.

3.5.1 Setup: models and parameters

Using the quadrupedal model as a basis, two models were generated: one for the experiments with the hind legs alone and the other for the experiments with the forelegs alone. The pair of legs not used during the experiments (the forelegs for the experiments with the hind legs and vice versa) was replaced by a wheeled supporting structure, as represented in Figure 3.7. As the supporting structure used in the simplified hind legs model of Figure 3.1(a), it allowed two degrees of freedom to the trunk (translation along the roll axis and rotation around the pitch axis). The height of the supporting structure was adjusted in both models so that the front and back ends of the body were approximatively at the same height in both simulations.

In both simulation models, the musculosketal model of each leg is actuated using the muscular activation level patterns output by the simplified LC (with only the NPG and the MOSS implemented). The leg controllers are *independent*, i.e. no explicit interaction mechanism or coupling was implemented between them to insure any kind of coordination.

As regards the settings of the leg controller parameters, the same values of the NPG parameters could be used for the fore and hind legs. Moreover, they were found independent of the locomotion speed considered. They are summarized in Table B.1, B.2 & B.3. On the other hand, the MOSS parameters depend on the model (because the muscular systems are different) and on the speed. Parameters values adjusted to the desired locomotion speed, i.e. $0.6ms^{-1}$, are given in Table B.5 & B.6.

3.5.2 Initial conditions and start up

At start-up, all the joints are in the position represented in Figure 3.7 (it corresponds to the neutral values of the joints for the hind legs, while for the forelegs, the shoulder and the elbow joints starts respectively in a more flexed and more extended positions than the neutral ones). The two LCs are set to the extensor phase. To break the static

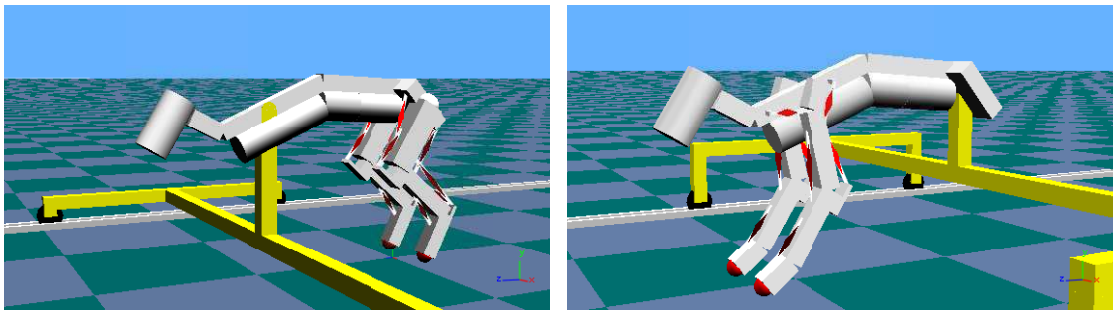

FIGURE 3.7: Models used for the generation of stepping motion at constant speed.

standing, the first step must be evoked manually at the beginning of the simulation by setting the LC of one leg to the flexor phase. This is done by applying a short excitatory stimulus on H_F while inhibiting Q_E. After the first step, no more external stimulus is provided and the LCs are acting autonomously.

3.5.3 Emergence of alternate stepping

Starting from rest ($v = 0\ ms^{-1}$), the speed progressively increases and then stabilizes around the desired speed ($v = 0.6\ ms^{-1}$) for both the models (the transitory state only lasts a few steps after the initiation of the stepping). Although the two leg controllers are independent, i.e. there is no direct connection between them, the activity of the leg controllers organizes. As a result, a steady walking motion emerges in which the stepping of the right and the left legs alternates with a phase difference of half a period. This walking motion is referred as *alternate stepping*. Steady alternate stepping of the hind legs and the forelegs are respectively represented in Figure 3.8 and Figure 3.9. The emergence of alternate stepping does not result from the setting of the NPG parameters but is rather a consequence of the phase modulations using leg loading information, as explained in the next section.

3.5.4 Contribution of the phase modulations based on leg loading information to the emergence of stable alternative stepping

As emphasized in the previous section, alternate stepping occurs without any explicit interaction between the leg controllers. Hence, the coordination of the legs is an emergent property of the system, induced by the *indirect* interaction between the LCs via the environment (i.e. the ground). This indirect interaction is mediated by the feedback of leg loading information. Indeed, when the swinging leg touches the ground, the touchdown synergy is terminated while the stance synergy becomes active. As a result, this leg starts to move backward and support the body so that the weight of the body is progressively transfered from the contralateral leg to the new supporting leg. When

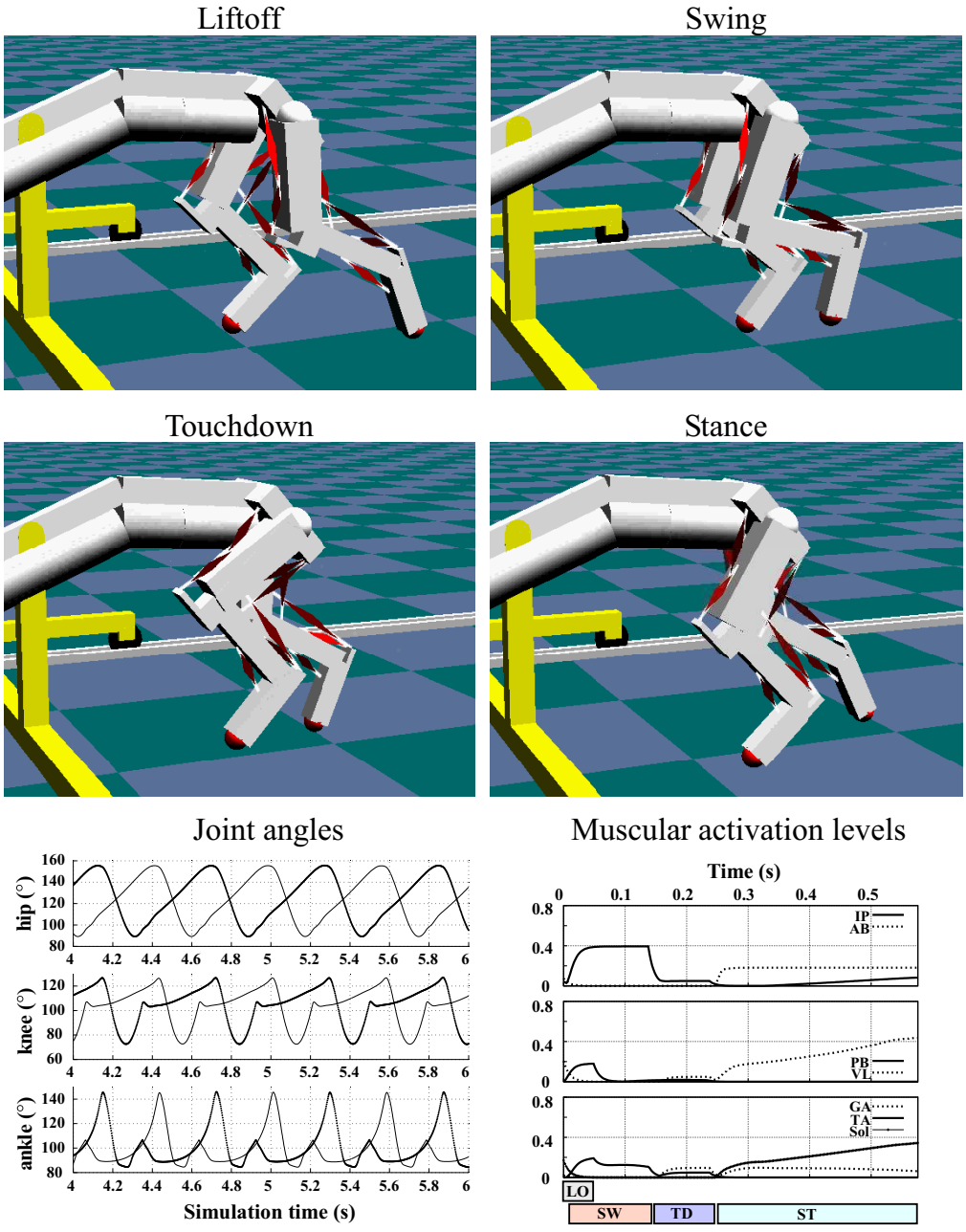

FIGURE 3.8: Steady stepping motions of the hind legs.

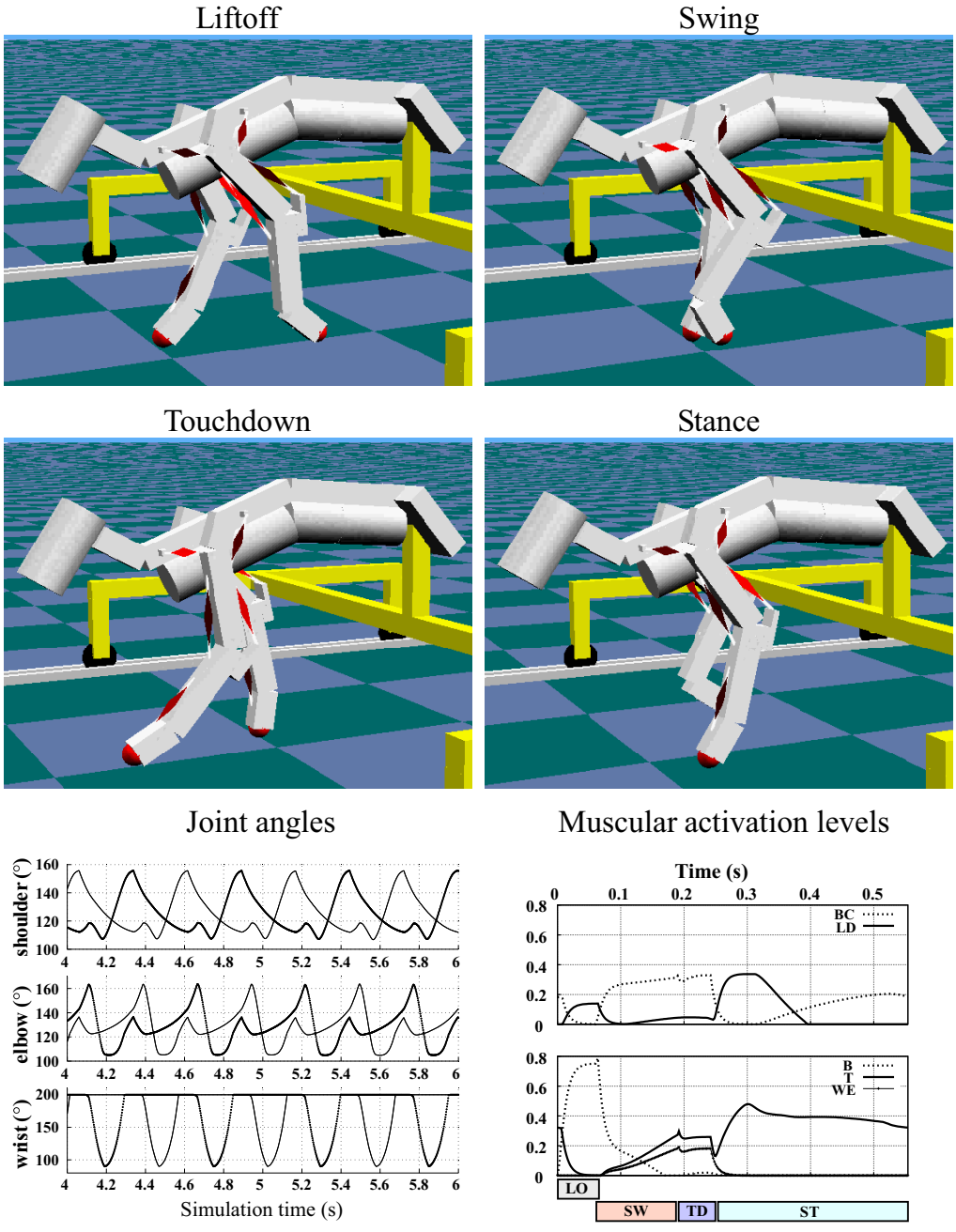

FIGURE 3.9: Steady stepping motions of the forelegs.

the load supported by the contralateral leg becomes smaller than the threshold allowing the transition, the extensor phase of the contralateral legs is terminated and it starts to swing. This process is repeated symmetrically and alternate stepping emerges.

When considering the role of modulation of the timing of the stance phase termination using the leg loading information in the stability of the alternate stepping and the half a period out of phase coordination, Ekeberg and Pearson (2005)(17) developed the following argument. In order to maintain a stable alternate coordination, any delay or advance in the stepping of one leg should be compensated by a corresponding delay or advance in the stepping of the other leg. Such adaptation takes place when using modulation of the stance phase duration based on the leg loading information as any delay of the touchdown of one leg causes a delay of the transfer of load from the supporting leg to the leg that just touched the ground. As a result, the supporting leg stays loaded longer and the termination of the stance, as well as the onset of the swing are delayed. Using the same argument, advance of the touchdown of one leg will cause an advance of the transition from stance to swing of the contralateral leg. Hence, in both cases, a modulation of the stance phase duration occurs in reaction to the perturbation of the touchdown timing of the other leg in order to maintain the half a period out of phase coordination.

The stabilizing action of the modulation of stance phase duration was directly investigated with the hind legs model. This was achieved using a condition based on the hip position instead of the condition on leg loading to control the transition of activity from the extensor to the flexor phase at the NPG level. Accordingly, the length x_{IP} of the hip flexor muscle IP was used as the input of neuron NF_E in Figure 3.4 instead of the force f_{Sol} generated by the ankle extensor Sol. The parameters of NF_E were set as the one of NF_F (see Table B.2), except for the offset value s_{off} (see Equation B.5). s_{off} corresponds basically to the value of x_{IP} over which NF_E is activated and the transition from the the extensor phase to the flexor phase is triggered. The experiments were carried out the following way:

- The model started from the rest position and, for the first five seconds, the condition based on leg loading was used to bring the model to the steady state.
- From the fifth to the tenth second, the condition controlling the transition of activity from the extensor to the flexor phase was switched to the condition based on hip position.
- After the tenth second, the conditions were switched back to the original state.

For all the values of s_{off} investigated, switching to the condition based on the hip position disturbed the normal leg coordination (as represented in Figure 3.10 for $s_{off} = 1.0$). On the other hand, switching back to the condition based on leg loading brought

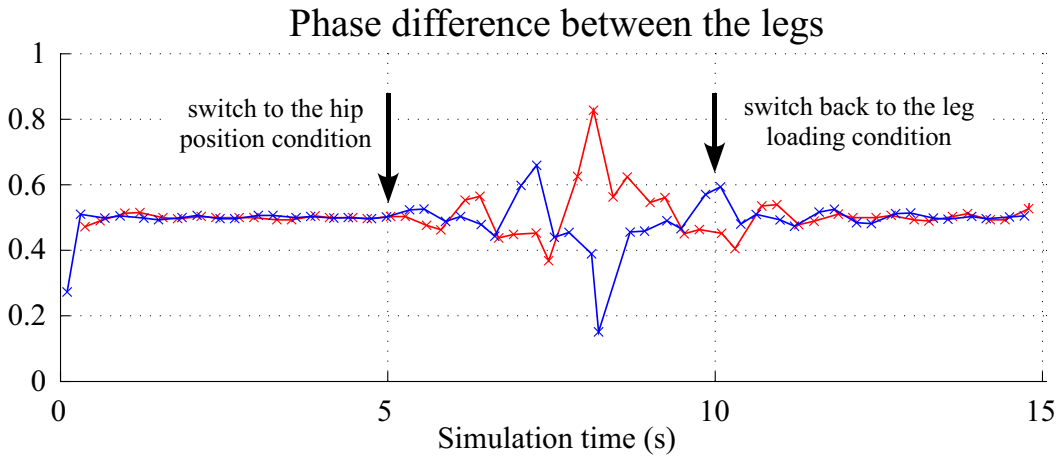

FIGURE 3.10: Influence of the extensor phase termination condition on the leg coordination. This latter is characterized by the phase difference between the legs ($0 \sim 1$), measured at touchdown and liftoff. When condition based on the hip position is used (s_{off} of NF_E is set 1.0.), leg coordination is disrupted (although the model does not fall). When the condition based on leg load is switched back, it restores the normal half a period phase difference between the legs.

back the phase difference between the legs to 0.5, hence it restored the coordination. This clearly shows that the modulation of stance phase duration using leg loading information contributes to the emergence and stabilization of the alternate stepping motion.

Another demonstration of the stabilization action of the phase modulations is that alternate stepping emerged and stabilized even starting from the rest position, which is quite far from the steady state. As reported in Section 3.5.3, the stabilization of the speed and the establishment of the phase difference between the legs are realized in a few steps.

3.6 Modulation of the stepping pattern

This section reports the generation of alternate stepping at various locomotion speeds with the simplified hind legs model. The PFCM was added to the leg controller architecture to modulate the muscular activation levels output by the MOSS, resulting in adjustments of the speed and the stepping motions. When comparing the variations according to the speed of the main locomotion characteristics (cyclic period, duty ratio and stride length) in the simulated stepping motions with the data on real cat walking, similar tendencies were found.

3.6.1 Setup: model and parameters

The simulations presented in this section were realized with the simplified hind legs model (Figure 3.1(a)). As regards the parameters of the leg controllers, their values for the NPG do not change compared to Section 3.5, while those of the MOSS are different due to the addition of the PFCM. The settings for these two latter parts of the LC are given in Appendix B.4.

3.6.2 Adjustment of the walking speed

Stable alternate stepping could be generated in a broad range of speed. The PFCM allowed for speed adjustment by simply modifying the value of the control input Ψ of the two LCs. Value of Ψ ranging from 0.05 to 0.45 evoked walking speed ranging from approximatively 0.15 to 0.80 m/s on flat ground, as represented in Figure 3.11. The relation between Ψ and the resulting average walking speed is shown in Figure 3.12.

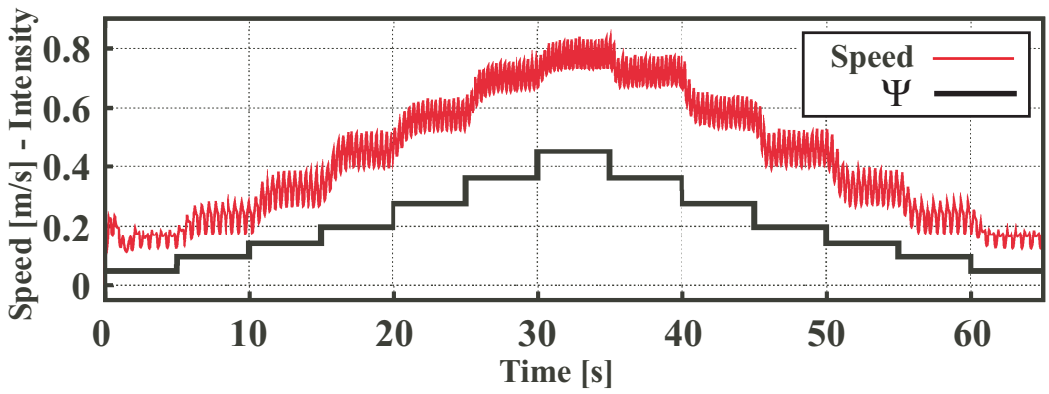

FIGURE 3.11: Changes of walking speed related to the level of the control input Ψ. Increasing or decreasing Ψ resulted respectively in an increase or decrease of speed (in the range going from 0.15 to 0.80 m/s). High frequency oscillations of the speed are due to its variation during a single step.

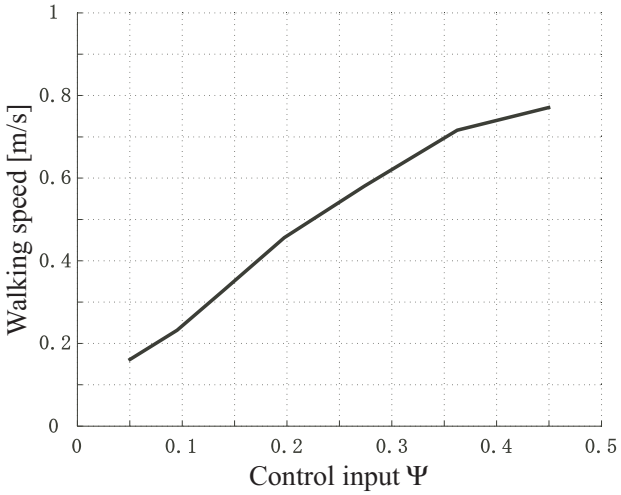

FIGURE 3.12: Relationship between the control input Ψ and the walking speed.

3.6.3 Resultant adaptations of the walking patterns

Modulation of the walking speed was accompanied with adaptations of the stepping patterns, as illustrated in Figure 3.13 which represents the stick diagrams of the stepping patterns at low and medium speeds, as well as the corresponding muscular activation levels a_m generated by the LC during one cyclic period. These adaptations were investigated by analysis of the behavior of the following indicators: T_{sw}, T_{st}, T_{tot}, β and L_{str}.

The variations of stance and swing periods obtained in simulation expressed the following global tendencies (represented in Figure 3.14):

- T_{sw} was more or less constant with respect to the speed.
- As the speed increases, T_{st} progressively decreased.

As a consequence, the cyclic period and the duty ratio (respectively upper and lower parts of Figure 3.15) both decreased as the speed increased.

The horizontal positions of the AEP (upper curves) and the PEP (lower curves) relative to the hip joint position are represented in Figure 3.16. As the speed increases, the PEP progressively shifted backwards while the AEP was more or less invariant. Consequently, the stride length (the difference between the AEP and PEP curves) also increased with the speed.

The variations of these indicators with the speed was compared with those measured during cat walking in the same range of speed (Halbertsma 1983(26)), also represented on the figures. Quite interestingly, similar tendencies were observed for all of them, some of them even presenting a really good match with their biological counterparts.

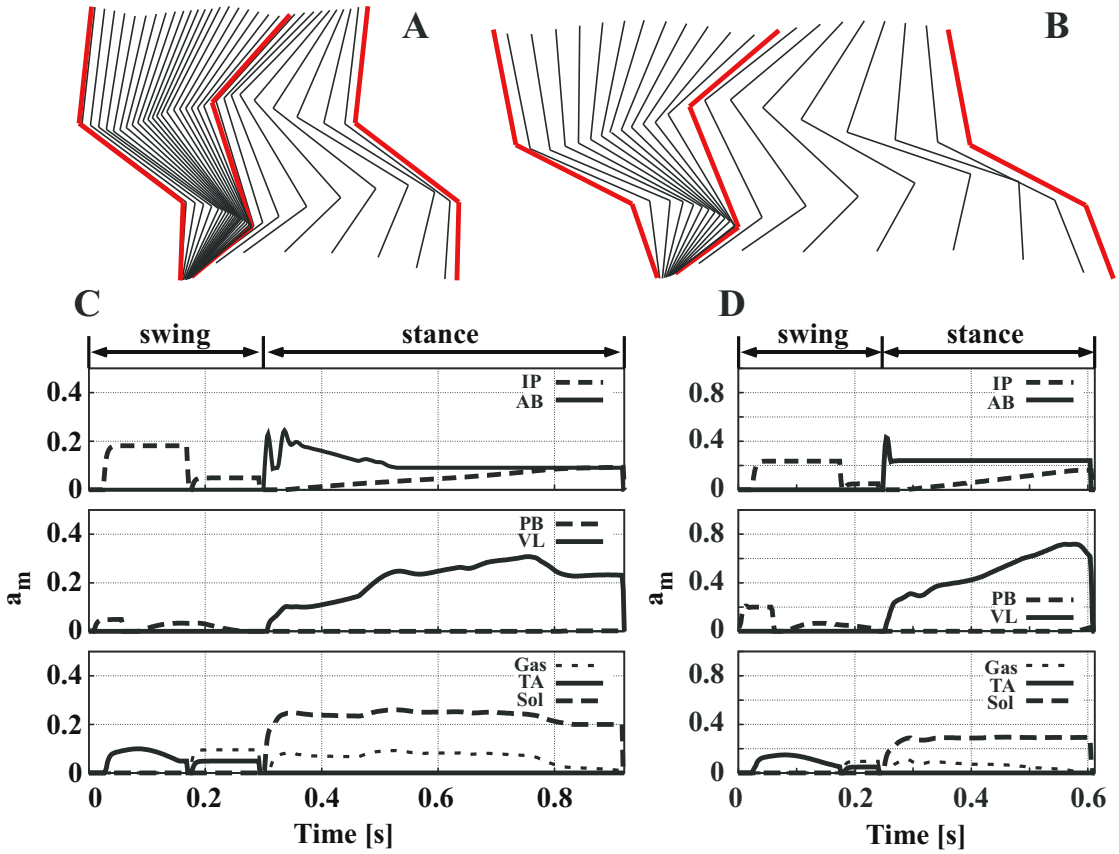

FIGURE 3.13: *Up:* stick diagrams of one stepping cycle (A: walking speed $\approx$ 0.2 m/s, B: walking speed $\approx$ 0.6 m/s) - *Down:* muscular activation levels a_m during one stepping cycle for the same speeds. In this figure, "swing" and "stance" refer respectively to the swing and the stance phases and should not be confused with the synergy names.

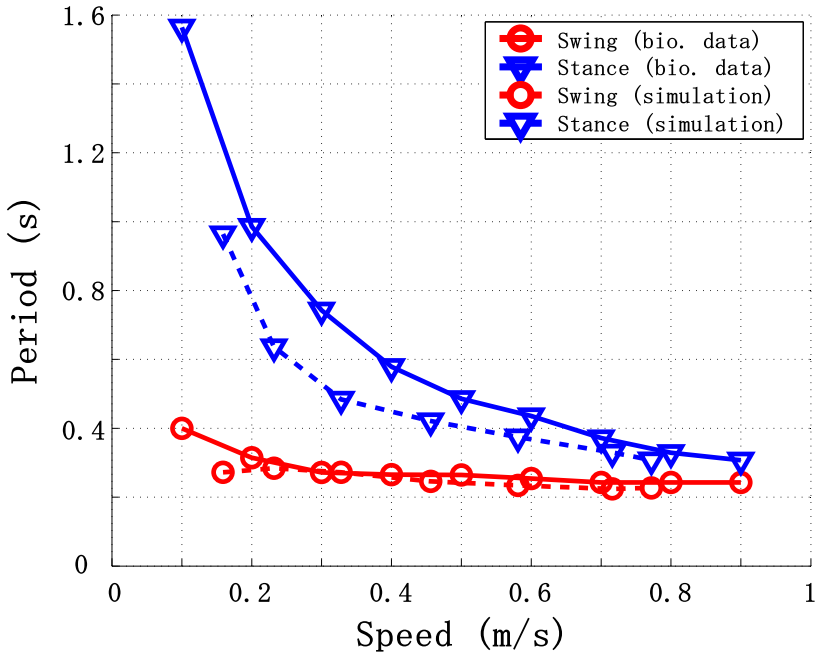

FIGURE 3.14: Swing and stance periods as functions of the walking speed in the cat and in our simulations. In both cases, the swing phase is approximatively constant, while the stance phase decreases with the speed.

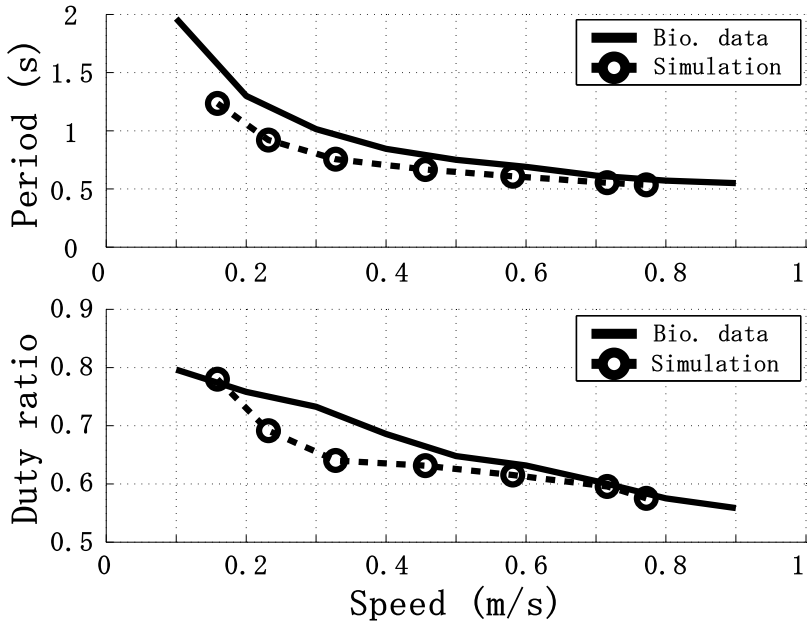

FIGURE 3.15: Cyclic period and duty ratio as functions of the walking speed. The main tendency, i.e. the progressive decrease when the speed increases, observed in real animals is also present in our simulation results.

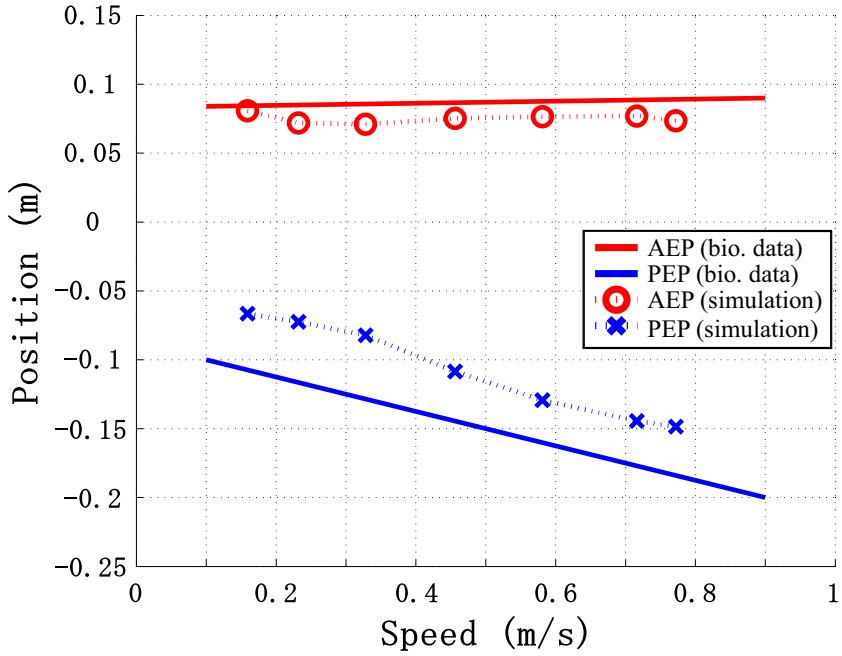

FIGURE 3.16: AEP and PEP as functions of the walking speed. The positions are relative to the hip articulation, positive values expressing a more rostral position and negative values a more caudal position. In real animals, the AEP is approximatively constant, while the PEP shifts progressively backwards when the speed increases. This was also the case in our simulations.

3.6.4 Adaptations as a result of the interaction between the adjustment by the PFCM and the phase modulations

As mentioned in Section 3.4.4, the mechanism used in the LC to adjust the walking speed is based on the adjustment of the propulsive force. This function is achieved by the PFCM, which modulates the muscular activation levels output by the MOSS according the value of the single control input Ψ. Hence, increasing Ψ has theoretically no influence on the rhythm generation at the NPG level, i.e. it does not set directly the respective durations of the swing and stance phases, nor the cyclic period, just as the MLR in real animal cannot control directly the stepping frequency (Shik et al. 1966(51)). However, considering the results of the previous section, it appears that the PFCM adjustments actually induced various adaptations of the stepping patterns, in particular a shortening of the cyclic period with the speed. The only explanation is that the adjustment of the propulsive force has an indirect influence on the rhythm generation, mediated by the sensory feedback to the NPG. According to Figure 3.14, the swing phase duration is more or less constant with the speed and the shortening of the cyclic period is mainly due to the shortening of the stance phase. As the stance phase duration is modulated on the basis of leg loading information, it can be concluded that the observed adaptations are the result of the interaction between the phase modulations and the adjustment of the propulsive force.

As regards the similarities of the adaptations taking place with the simulated model and during the locomotion of the cat, an additional conclusion can be drawn. The experiments suggest that, like in the case of the simulated model, the adaptations observed in the real animal are due to phasic modulations based on leg loading information. Hence it brings one more argument in favor of the hypothesis formulated in Ekeberg et Pearson (2005)(17) that the sensory information related to leg loading is critical to regulate the transition from stance to swing in animals.

3.7 Discussion

3.7.1 Parameter tuning

When working with a neural controller, a lot of parameters have to be tuned. Since the NPG is only dealing with phasic information about the locomotion, the number of parameters involved in the neural circuit is relatively small. Moreover, as the neuronal models and neural circuit were similar to those used in Wadden and Ekeberg (1998)(62), the value of the interneuron parameters were adapted from their work. The rest of the parameters could easily be tuned manually by trial and error.

On the other hand, the tuning of the parameters of the MOSS and the PFCM was much more complicated. The main reason is that the interaction between the MOSS and the musculoskeletal model is rather complex and depends on its dynamical properties. The shape and intensity of muscle activation patterns at that level become important so that the number of parameters needed to specify them properly is big. An additional source of complexity is that the muscular system is redundant due to the presence of the biarticular muscles in the case of the hind legs. Previous studies using similar musculoskeletal models and EMG patterns recorded during the locomotion of real animals were really useful as they provided me with very valuable insights. However, they usually concerned only a limited range of speeds and/or were difficult to adapt to my model. Consequently, finding appropriate values for the parameters involved a lot of tuning by trial and errors and turned out to be very time consuming.

3.8 Summary

In this chapter, a musculoskeletal model of the cat forelegs was developed and added to an existing model of the hind legs, resulting in a quadrupedal musculoskeletal model of the cat. Based on the common principles defined in Chapter 2, a sensor-dependent neural controller relying on leg loading information and able to actuate the musculoskeletal model of a single leg to induce stepping motion at various speeds was developed.

Next, using two independent leg controllers, stable two-dimensional alternate stepping patterns were realized with hind legs and forelegs models separately. The contribution of the control of the stance phase termination based on leg loading information to the emergence and the stabilization of the leg coordination was explained. Even though this result was already reported by Ekeberg and Pearson (2005)(17), it was shown in this chapter that its validity can be extended to a completely different musculoskeletal structure (i.e. the forelegs) and to a broad range of walking speeds (as demonstrated with the hind legs model).

Finally, adaptations taking place in the simulations as the speed increases were compared to the ones that occur during the locomotion of the real animal and striking similarities were found. This constitutes an additional argument in favor of the hypothesis that the sensory information related to leg loading plays an essential role in the regulation of the transition from stance to swing in animals as well.

Chapter 4

Generation of stable quadrupedal dynamic walk

4.1 Overview

Attempts were made to extend the neural controller presented in Chapter 3 to generate three-dimensional quadrupedal walking patterns with the quadrupedal musculoskeletal model. However, these attempts failed and the reasons of the failure could not be precisely established. In particular, the complexity of the neural controller prevented to analyze whether the problem was due to an intrinsic limitation of the phase modulations mechanism, acting at the rhythm generation level in the NPG, or was simply related to the wrong setting of the numerous parameters, used at the motor patterns generation level in the MOSS. As explained in Section 3.7.1, the great number of parameters involved in the motor patterns generation process was required by the complex biologically-faithful musculoskeletal model. As this latter was not essential for the investigation of the main point of the thesis, i.e. the contribution of the phase modulations to the generation of stable quadrupedal dynamic walk, it was removed from the simulation model. Instead, a much simpler approach, combining foot trajectory generation and local PD control, was used for the generation of the motor patterns. This resulted in a great simplification of the leg controller structure that allowed to study the role of the phase modulations based on leg loading information in the generation and stabilization of the walk gait in the three-dimensional case.

Section 4.3 presents the simplified simulation model. The structure of the leg controller is given in Section 4.4 and its compliance to the common principles defined in Chapter 2 is verified. Section 4.5 explains how phase modulations based on leg loading information contribute to the emergence of harmonious left-right alternate stepping. Additional conditions for the emergence of the walk gait are investigated as well. Finally, Section 4.6

describes how the walking patterns can be easily modulated by changing a small number of the controller parameters.

4.2 List of symbols and notations

For the sake of clarity, Table 4.1 regroups and defines the symbols and notations used in Chapter 4 and Chapter 5. As regards the leg index i, HL, FL, HR and FR stands respectively for left hind leg, left foreleg, right hind leg and right foreleg. $*$ can be used as a wild card to replace one of the two characters (for example, $F*$ refers to both forelegs, while $*R$ refers to both right legs). For the leg controller parameters, if needed, a hat symbol $\hat{}$ will be placed on top of a parameter to represents its nominal value. On the other hand, the bar symbol $\bar{}$ will represents its effective value, i.e. the value observed during the simulation.

TABLE 4.1: List of the symbols and notations

Indexes	
i	Leg index
j	Joint index
k	Walking cycle index
n	Body roll angle extremum index
Simulation model	
f_n	Normal reaction force measured by the foot force sensor
θ_j	Joint angle
θ_{roll}	Body roll angle
Θ_n	Extremum of the body roll angle
Θ	Body rolling motion amplitude
Leg controller	
T_{sw}	Swing phase duration
T_{st}	Stance phase duration
T_{tot}	Walking cyclic period
β	Duty ratio
ϕ	Oscillator phase
ω	Oscillator angular frequency
L_{str}	Stride length
H	Body height
Δy_{AEP}	Offset of the vertical coordinate of the AEP position
χ	Force threshold of the stance-to-swing transition condition
Γ	Joint torque
K_P, K_D	PD control gains
c, c_{per}, c_{spd}	Coefficients for the adjustment of the PD control gains
Walking pattern	
γ	Phase difference from the left hind leg to the left foreleg
I_r	Regularity index

4.3 Simulation Model

The simulation model used for the experiments described in this chapter is represented in Figure 4.1. Compared to the quadrupedal model of Chapter 3, the mechanical structure is much simplified. The dimensions and masses of the trunk and the leg segments are summarized in Table 4.2.

The four legs are identical and each of them is made of three segments (thigh, shank and foot) articulated around three rotational joints around the pitch axis (hip, knee and ankle). As represented in Figure 4.1(b), θ_j represents the angle of the j^{th} joint. The legs have no joint around the roll axis so that the motion of each foot is two-dimensional and restricted to a plane parallel to the sagittal plane. At the tip of each foot is a force sensor used to measured the normal ground reaction force f_n.

The trunk is modeled as a cylindrical body, whose center of mass is slightly forward (at a position of 40% of its length from the front) to account for a similar mass repartition in animals (Tomita 1967(58)). The width of the model, i.e. the distance between the hip joints of contralateral legs, is set to 12 cm. In contrast with Chapter 3, the motion of the simulation model is not constrained and the trunk has six degrees of freedom, respectively translation along and rotation around the pitch, roll and yaw axes.

During dynamic walking, rotation of the body around its roll axis is naturally induced because a dynamic system similar to an inverted pendulum appears in the two-legged stance phases (as explained in more details in Section 4.5.3). This motion is referred as the *body rolling motion* (or simply the rolling motion) and the body roll angle is represented by θ_{roll}. In four-legged locomotion, control of the rolling motion is the main issue to insure postural stability in the frontal plane and prevent the model to fall on the side[1]. In this context, it may appear paradoxical not to provide the legs with joints around the roll axis, in order to be able to control directly the rolling motion via lateral motions of the legs. However, this is justified by the objective of this thesis, which is to evaluate the contribution to rolling motion control and posture stabilization of an indirect mechanism: the phase modulations based on leg loading information. As adding another rolling motion control mechanism would complicate this evaluation, a simulation model was defined with no joint around the roll axis.

[1]Contrary to bipeds, quadrupeds are naturally stable when the motion is considered in the sagittal plane.

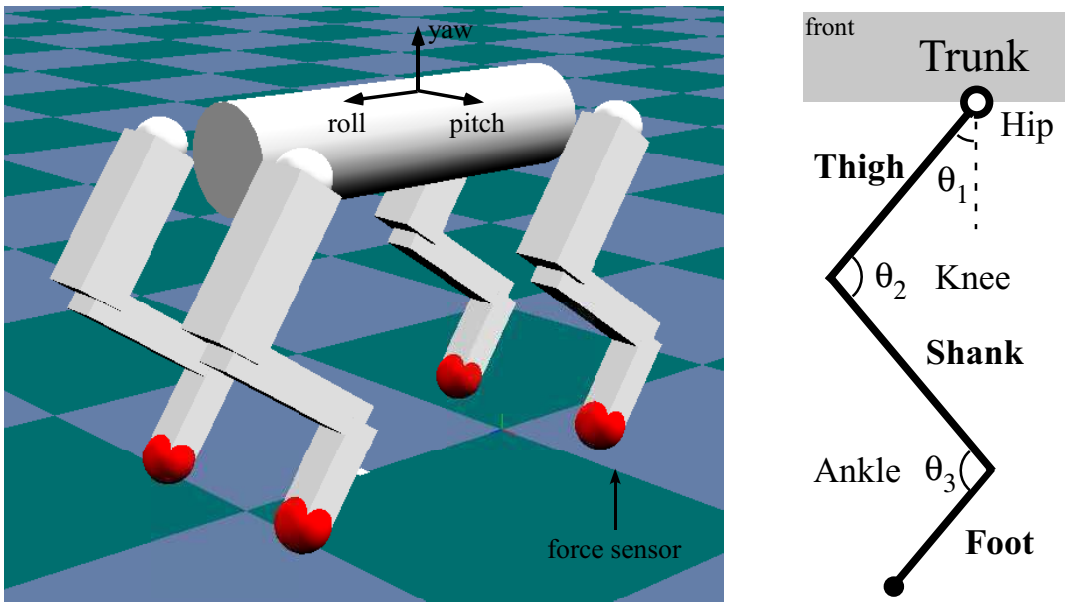

(a) (b)

FIGURE 4.1: Simplified quadrupedal model used in three-dimensional experiments

TABLE 4.2: Dimensions and masses of the bodies constituting the simplified quadrupedal model

	L (cm)	l (cm)	h (cm)	mass (g)
thigh	9	3	3	202.5
shank	10	2	2	100
foot	6	2	2	60

	H (cm)	r (cm)	mass (g)
trunk	23	3	3000

	R (cm)	mass (g)
force sensor	1.5	50

4.4 Leg Controller

4.4.1 Overview

Each leg is actuated by one leg controller. Each LC has two phases, *swing* (sw) and *stance* (st), activated alternatively and the transfer of activity between them is controlled using conditions based on the load supported by the leg, as measured by the force sensor.

For the sake of convenience, each LC is associated with an oscillator[2]. The phase of the oscillator ϕ^i is used for the trajectory generation, as well as to express the phase relationship between the legs. The nominal value of the oscillator angular frequency ω is given by:

$$\hat{\omega} = 2\pi(1 - \hat{\beta})/\hat{T}_{sw}, \tag{4.1}$$

where β is the duty ratio and T_{sw} the swing phase duration (see Section 2.2.2).

4.4.2 Foot trajectory generation

In order to keep the presentation of the system as clear as possible, only the outline of the trajectory generation are presented in this chapter (detailed explanations are given in Appendix C). For each leg, the trajectories of the foot during both phases, represented in Figure 4.2, are expressed in the Cartesian coordinate system fixed to the trunk and centered at the hip joint. The subscripts $*_x$ and $*_y$, used in the following sections and in Appendix C, refer to the x and y coordinates in that coordinate system.

The position of the foot where the transition from swing to stance is desired to happen is called the *anterior extreme position* (AEP), while the position where it really happens is the *touchdown position* (TD), referred respectively as $\hat{\boldsymbol{r}}_{AEP}$ and $\boldsymbol{r}_{TD}$.

Similarly, the position where the transition from stance to swing is desired to happen is the *posterior extreme position* (PEP), while the position where it really happens is called the *liftoff position* (LO), referred respectively as $\hat{\boldsymbol{r}}_{PEP}$ and $\boldsymbol{r}_{LO}$.

The nominal phases at AEP and PEP are respectively:

$$\hat{\phi}_{AEP} = 2\pi(1 - \hat{\beta}) \quad , \quad \hat{\phi}_{PEP} = 0 \tag{4.2}$$

[2]Although an oscillator is associated to each LC, the CPG model constructed by these LCs is still sensor-dependent, as explained in Section 4.4.5.

4.4.2.1 Swing

At the beginning of the swing phase, ϕ is reset to $\hat{\phi}_{PEP}$ and the phase dynamics is subsequently given by:

$$\omega = \hat{\omega} + \omega_{mod} \qquad \text{and} \qquad \dot{\phi} = \begin{cases} \omega & \text{if } 0 \leq \phi < \hat{\phi}_{AEP} \\ 0 & \text{if } \phi \geq \hat{\phi}_{AEP} \end{cases} \tag{4.3}$$

where ω_{mod} can be used to modulate the swing phase duration (it is equal to zero except when it is set by the ascending coordination mechanism, see Section 5.3). The trajectory $\boldsymbol{r}_{sw}(\phi)$ satisfies:

$$\boldsymbol{r}_{sw}(0) = \boldsymbol{r}_{LO} \qquad \boldsymbol{r}_{sw}(\hat{\phi}_{AEP}) = \hat{\boldsymbol{r}}_{AEP} \tag{4.4}$$

with:

$$\hat{r}_{AEP,x} = \hat{L}_{str}/2 \tag{4.5}$$

$$\hat{r}_{AEP,y} = \hat{H} - \Delta y_{AEP} \tag{4.6}$$

where L_{str} is the stride length (see Section 2.2.2), H the body height and Δy_{AEP} an offset of the vertical coordinate of the AEP position (as explained in Section 4.5.4.1, this parameters influences the phase difference between ipsilateral legs of the emergent walking pattern).

4.4.2.2 Stance

At the beginning of the stance phase, ϕ is reset to $\hat{\phi}_{AEP}$ and the phase dynamics is subsequently given by:

$$\omega = \hat{\omega} \qquad \text{and} \qquad \dot{\phi} = \begin{cases} \omega & \text{if } \hat{\phi}_{AEP} \leq \phi < 2\pi \\ 0 & \text{if } \phi \geq 2\pi \end{cases} \tag{4.7}$$

The trajectory $\boldsymbol{r}_{st}(\phi)$ satisfies:

$$\boldsymbol{r}_{st}(\hat{\phi}_{AEP}) = \boldsymbol{r}_{TD} \qquad \boldsymbol{r}_{st}(2\pi) = \hat{\boldsymbol{r}}_{PEP} \tag{4.8}$$

with:

$$\hat{r}_{PEP,x} = r_{TD,x} - \hat{L}_{str} \tag{4.9}$$

$$\hat{r}_{PEP,y} = \hat{H} \tag{4.10}$$

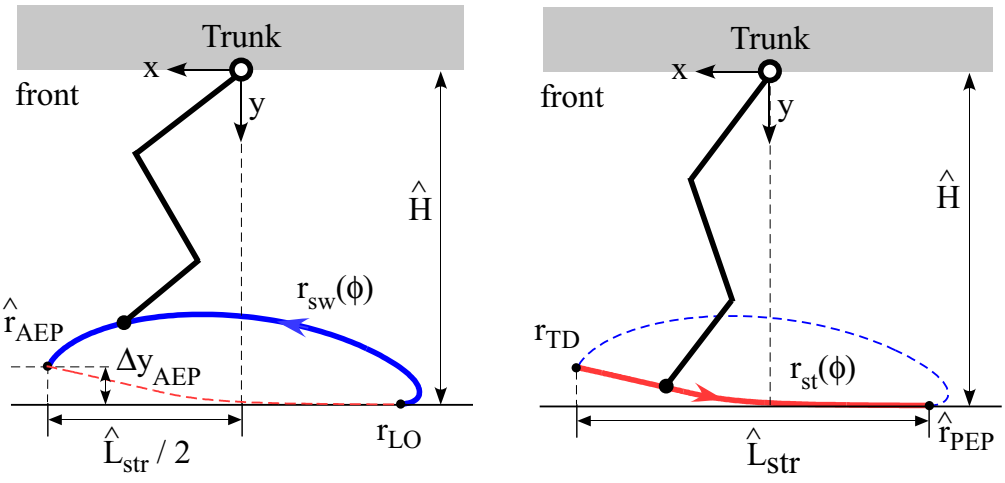

(a) (b)

FIGURE 4.2: Stance and swing trajectories

The x component of the velocity $v_{st,x}$ is constant during the stance phase but for a short initial acceleration period, and is given by:

$$v_{st,x} = -\frac{\hat{L}_{str}}{\hat{T}_{st}} = -\frac{\hat{L}_{str}(1-\hat{\beta})}{\hat{\beta}\hat{T}_{sw}} \tag{4.11}$$

where T_{st} and T_{sw} are respectively the stance and swing phases durations and β the duty ratio.

On the other hand, the profile of the y component of the velocity is computed to recover from the height difference between $\boldsymbol{r}_{TD}$ and $\hat{\boldsymbol{r}}_{PEP}$. Different profiles have been tested and they lead to similar results as long as the velocity is large at the beginning of the stance phase and decreases fast enough afterward.

4.4.3 Sensory feedback and transition conditions

Transitions between the swing and the stance phases are regulated using leg loading information, where to the load supported by the leg is evaluated by the normal ground reaction force f_n measured by the foot force sensor. Additional conditions regarding the phase ϕ are added only to prevent a transition to occur at the very beginning of a phase that just started and avoid cascading transition triggering that would otherwise happen, as the foot is still touching the ground just after the termination of the stance phase and the leg not yet fully loaded just after the touchdown.

Conditions for the *transition from swing to stance* are:

- $f_n > 0$ (i.e. the foot touches the ground)

- $\phi > \hat{\phi}_{AEP}/2$

and for the *transition from stance to swing*:

- $f_n < \chi = \hat{\chi} + \chi_{mod}$
- $\phi > (\hat{\phi}_{AEP} + \pi/2)$

where χ_{mod} can be used to modulate the force threshold (as ω_{mod} in Equation 4.3, it is equal to zero, except when it is set by the ascending coordination mechanism, see Section 5.3). In the following experiments, $\hat{\chi}$ is set to 10 N which represents slightly less than one fourth of the simulation model weight.

4.4.4 Leg Motion Control

The trajectories of the joint angles (θ) are computed using the inverse kinematics model of the leg (see Appendix C.3). The torque at joint j is generated by local PD control as follows:

$$\Gamma_j = K_{Pj}(\hat{\theta}_j - \theta_j) + K_{Dj}(\dot{\hat{\theta}}_j - \dot{\theta}_j) \tag{4.12}$$

4.4.5 Implementation of the common principles

The leg controller implements the common principles defined in Chapter 2. The transitions between swing and stance phases are triggered using leg loading information, characterized by the normal ground reaction force.

As regards the CPG model issue, although an oscillator is associated to each LC, transitions are prevented as long as the conditions are not fulfilled by setting $\dot{\phi}$ to zero when ϕ reaches the maximum value allowed for the phase (i.e. $\hat{\phi}_{AEP}$ for the swing or 2π for the stance). Similarly, when the transition occurs, the phase is reset. Consequently, the leg controller is actually sensor-dependent.

4.5 Generation of dynamic walk using independent leg controllers

4.5.1 Considerations about gaits

A gait is a locomotion pattern that can be defined by phase differences between the legs during their pitching motion. When considering normalized values comprised between 0 and 1, a phase difference of 0 (or 1) corresponds to in phase motion of the pair of legs considered, while 0.5 means that the legs are half a period out of phase. Typical symmetric gaits[3] include the pace where the ipsilateral legs are paired and move together (Figure 4.3(a)), and the trot where the diagonal legs move together (Figure 4.3(b)). The walk gait is an intermediate gait between the pace and the trot gaits (Figure 4.3(c)). Although, when trained to do so, animals can walk with a trot gait, this gait is usually used for running at high speed. In the range of low- to medium-speed locomotion, the gaits used by medium sized mammals (like the cat and the dog) are mainly the walk and, to a lesser extent, the pace.

In this thesis, the phase difference from the left hind leg to the left foreleg will be represented using the symbol γ. The value of γ for the pace and trot gaits is respectively 0 and 0.5, while for a walk gait it is around 0.25. Accordingly, locomotion patterns with γ included in the interval $[0.125, 0.375[$ will be regarded as walk gaits.

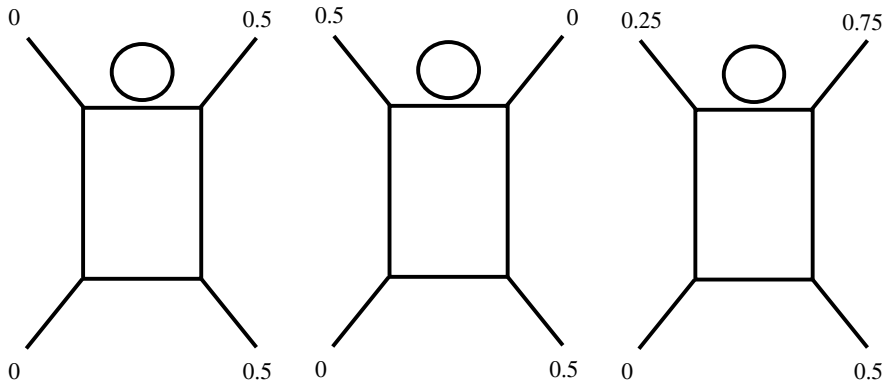

(a) Pace gait ($\gamma \simeq 0$) (b) Trot gait ($\gamma \simeq 0.5$) (c) Walk gait ($\gamma \simeq 0.25$)

FIGURE 4.3: Phase differences between the stepping motions of the legs in the pace, the trot and the walk gaits (the left hind leg is taken as the reference).

[3] A gait is *symmetric* if the motion of the legs of any right-left pair is exactly half a cycle out of phase

4.5.2 Mechanisms of leg loading transfer during the locomotion

Mainly two mechanisms are acting during the locomotion to transfer the load induced by the weight of the body between the supporting legs:

- The *lateral transfer* of leg loading is related to the lateral motion of the body (i.e. the translation along its pitch axis) with respect to the positions of the feet of the supporting legs. As explained in Section 4.3, as the legs have no joint around the roll axis, the lateral motion of the body is closely related to its rolling motion. This load transfer mechanism increases the load supported by the legs on the side toward which the body is moving, while the legs on the opposite side are unloaded. Hence, its influence on ipsilateral legs is identical.
- The *longitudinal transfer* of leg loading is related to the forward motion of the body (i.e. the translation along its roll axis) with respect to the positions of the feet of the supporting legs. This mechanism results in a transfer of leg loading from the hind to the forelegs during the stance phase. Contrary to the lateral transfer, the influence of this mechanism on ipsilateral legs is opposite in the fore and hind legs, as it unloads the hind legs while increasing the load supported by the forelegs.

4.5.3 Emergence of left-right alternate stepping

The simplest control system configuration, which corresponds to the situation where the four leg controllers are operating independently (i.e. without any direct interaction mechanism), was first investigated. Even in that case, coordinate locomotion patterns emerge and maintain in a broad range of parameters when stepping is initiated in both right legs by forcing the transition to the swing phase in the leg controllers (see Appendix D for more details on the initiation of the locomotion). The leg coordination in all the emergent patterns presents the particularity that, during the walking cycle, the legs on one side are all stepping consecutively, followed by the consecutive stepping of all the legs on the other side. It can be seen as the extension to four legs of the alternate stepping coordination described in Chapter 3. To distinguish it from this latter, it will be referred as *left-right alternate stepping*. Pace and walk gaits present such coordination, while the trot gait does not.

The mechanism of emergence of left-right alternate stepping coordination is schematically explained in Figure 4.4, when considering the motion in the frontal plane[4]. If the transition to the swing of all the legs on one side (the right side for example) is triggered

[4]This representation supposes that the stepping of ipsilateral legs is simultaneous, which is strictly speaking only true when $\gamma = 0$. However, even when $\gamma \neq 0$ (as in the case of the walk for example), as the ipsilateral legs are still stepping consecutively and their swing phases overlap, that representation still provides important clues about the behavior of the system.

at the beginning of the simulation (Figure 4.4-(c2)), the system becomes equivalent to an inverted pendulum. Due to the moment induced by the gravity, the model starts to rotate around the left feet and rolling motion of the body is generated ($\dot{\theta}_{roll} > 0$). As the motion of the legs is planar (i.e. there is no joint around the roll axis), rolling and lateral motions of the body are directly related, so that the body also starts to move laterally. After the touchdown of the swinging legs (Figure 4.4-(a)), the lateral motion of the body causes the lateral transfer of the load from the left to the right legs (Figure 4.4-(b1)). When the load supported by the left legs becomes smaller than threshold χ, swing phase is initiated in the left legs (Figure 4.4-(c1)). The same sequence of events is repeated on the other side as $\dot{\theta}_{roll}$ becomes negative (Figure 4.4-(a),(b2),(c2)) and then periodically. Hence, left-right alternate stepping coordination emerges and maintains through the entrainment between the stepping of the legs, the rolling motion and the lateral transfer of leg loading, as represented in Figure 4.5. Accordingly, modulation of the stance phase duration based on leg loading information contributes to the emergence and the regulation of left-right alternate stepping.

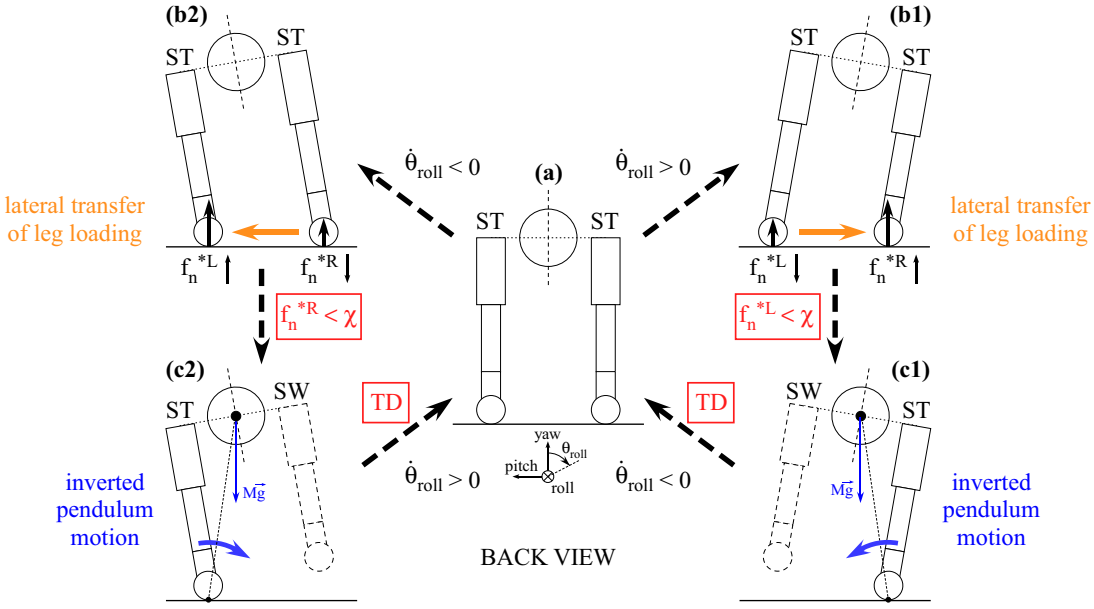

FIGURE 4.4: Contribution of the phase modulations based on leg loading information to the emergence of left-right alternate stepping.

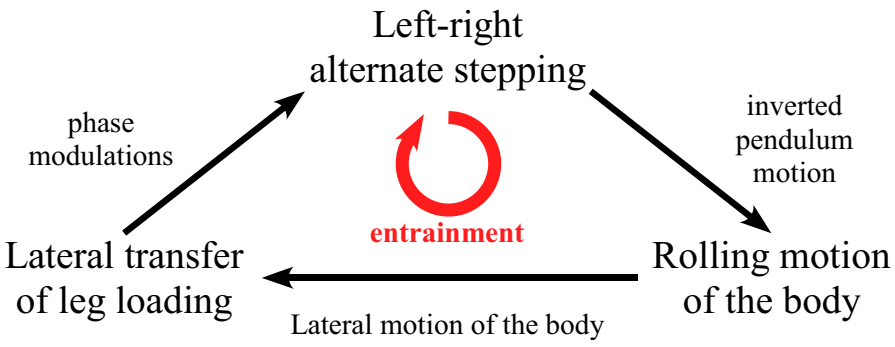

FIGURE 4.5: Entrainment between the stepping of the legs, the rolling motion of the body and the lateral transfer of leg loading.

4.5.4 Conditions of emergence of the walk gait

As left-right alternate stepping coordination is naturally provided by the phase modulations, the only condition left to satisfy in order to obtain a walk gait is to induce an appropriate value of the phase difference γ. Accordingly, the influence of the various leg controllers parameters on γ was evaluated in order to investigate if walk gait could be realized or not with independent leg controllers. As it will be explained in Section 4.6, the cyclic period and speed of the walking patterns can be modulated by adjusting the values of $\hat{T}_{sw}$ and $\hat{\beta}$ in all the leg controllers. At constant $\hat{T}_{sw}$ and $\hat{\beta}$, two sets of parameters where found to have a particular influence on the value of γ:

- the offset Δy_{AEP} of the vertical coordinate of the AEP
- the PD control gains K_P and K_D of the knee and ankle joints during the stance

Their influence is investigated in the next paragraphs (the values of the other parameters will be set as in Table 4.3).

In addition to the impact of the parameters on the gait, it is interesting to consider at the same time their influence on the amplitude and the regularity of the rolling motion. Let us consider the sequence of extremum values of the body roll angle during the locomotion $(\Theta_n)_{n\in\mathbb{N}_0}$, with Θ_n defined as follows:

$$\Theta_n = \begin{cases} \theta_{roll}(t_n) & \text{if maximum} \\ -\theta_{roll}(t_n) & \text{if minimum} \end{cases} \tag{4.13}$$

where t_n is the time at which the n^{th} extremum occurs. The regularity of the walking pattern is evaluated using an index I_r quantifying the dispersion of the values of the sequence around its mean value Θ, by using the normalized standard deviation σ_Θ:

$$\Theta = \frac{\sum_{n=n_s}^{n_f} \Theta_n}{N} \tag{4.14}$$

$$\sigma_\Theta = \frac{((\sum_{n=n_s}^{n_f} (\Theta_n - \Theta)^2)/N)^{1/2}}{\Theta} \tag{4.15}$$

$$I_r = -log(\sigma_\Theta) \tag{4.16}$$

with $N = n_f - n_s + 1$, where n_s and n_f are the indexes of first and last extrema of the body roll angle reached in the time interval considered for the evaluation of I_r. For the sake of convenience, Θ will be referred to as the *rolling motion amplitude* from here on.

TABLE 4.3: Values of the parameters used to generate the walking pattern of Figure 4.9

Parameter	Value	Parameter	Value
$\hat{T}_{sw}$ (s)	0.15	Δy_{AEP}^{H*} (m)	0
$\hat{\beta}$	0.75	Δy_{AEP}^{F*} (m)	0.01
$\hat{H}$ (m)	0.18	$\hat{L}_{str}$ (m)	0.10
K_P during stance (Nm rad^{-1})		K_P during swing (Nm rad^{-1})	
hip	40	hip	20
knee	20	knee	10
ankle	10	ankle	5
K_D during stance (Nm s rad^{-1})		K_D during swing (Nm s rad^{-1})	
hip	0.56	hip	0.40
knee	0.40	knee	0.28
ankle	0.28	ankle	0.20

4.5.4.1 Influence of the AEP vertical coordinate offset Δy_{AEP}

By introducing an offset in the vertical coordinate of the AEP of the foot, parameter Δy_{AEP} influences the timing of the touchdown (situations (c1) or (c2) to situation (a) in Figure 4.4), when the body rotates around its roll axis. For the same value of $\dot{\theta}_{roll}$ before touchdown, the increase (resp. the decrease) of Δy_{AEP} of one LC should result in the delay (resp. the advance) of the onset of the stance phase of the corresponding leg. Accordingly, the relative values of Δy_{AEP} for the fore and hind legs have an influence on γ. In particular, $\Delta y_{AEP}^{F*} > \Delta y_{AEP}^{H*}$ should result in $\gamma > 0$ as the touchdown of the hind leg happens then earlier than the one of the foreleg (as illustrated in Figure 4.6).

The experimental results, represented in Figure 4.7(a), are globally in agreement with that argument. When $\Delta y_{AEP}^{F*} < \Delta y_{AEP}^{H*}$, the phase difference γ is negative, while for Δy_{AEP}^{F*} sufficiently larger than Δy_{AEP}^{H*}, γ becomes positive and, in some cases, greater than 0.125, resulting in a walk gait. However, as Δy_{AEP} of one or both legs increases, the duration of the inverted pendulum motion phase (Figure 4.4-(c1) or (c2)) becomes longer so that the angular speed of rolling $\dot{\theta}_{roll}$ has more time to build up. As a consequence, the rolling motion amplitude Θ gets larger (Figure 4.7(b)) and there is an upper limit to the value of γ that can be realized by increasing the Δy_{AEP}. Accordingly, as long as Θ is small, increasing Δy_{AEP}^{F*} with Δy_{AEP}^{H*} constant causes the increase of γ, but, as Θ becomes larger, γ reaches its maximum value and then decreases (this is particularly clear in the case where $\Delta y_{AEP}^{H*} = 0$).

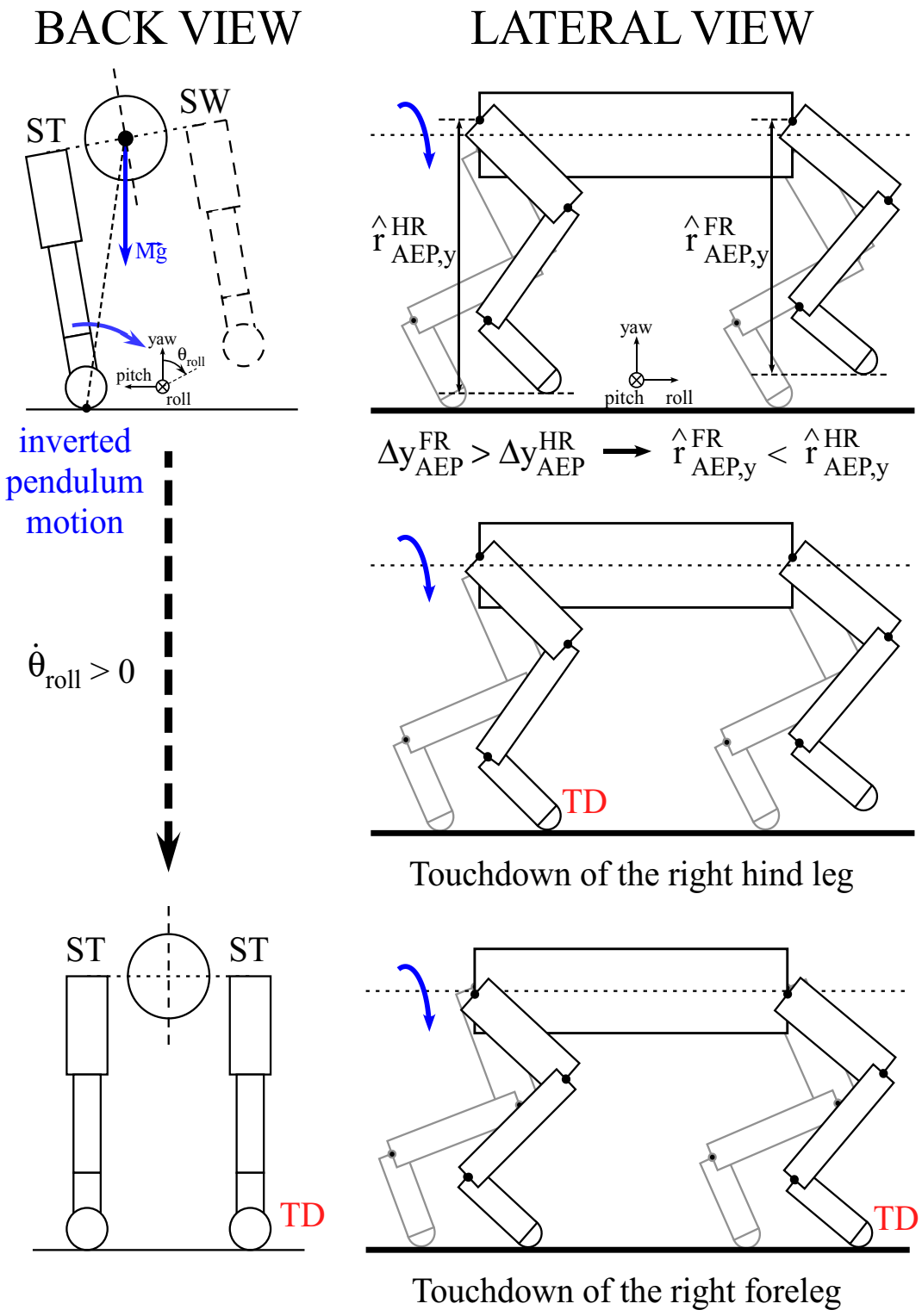

FIGURE 4.6: Illustration of the influence of Δy_{AEP} on γ. For $\Delta y^{F*}_{AEP} > \Delta y^{H*}_{AEP}$, as the body rotates around the roll axis, the touchdown of the hind leg occurs earlier than the one of the foreleg, hence resulting in $\gamma > 0$.

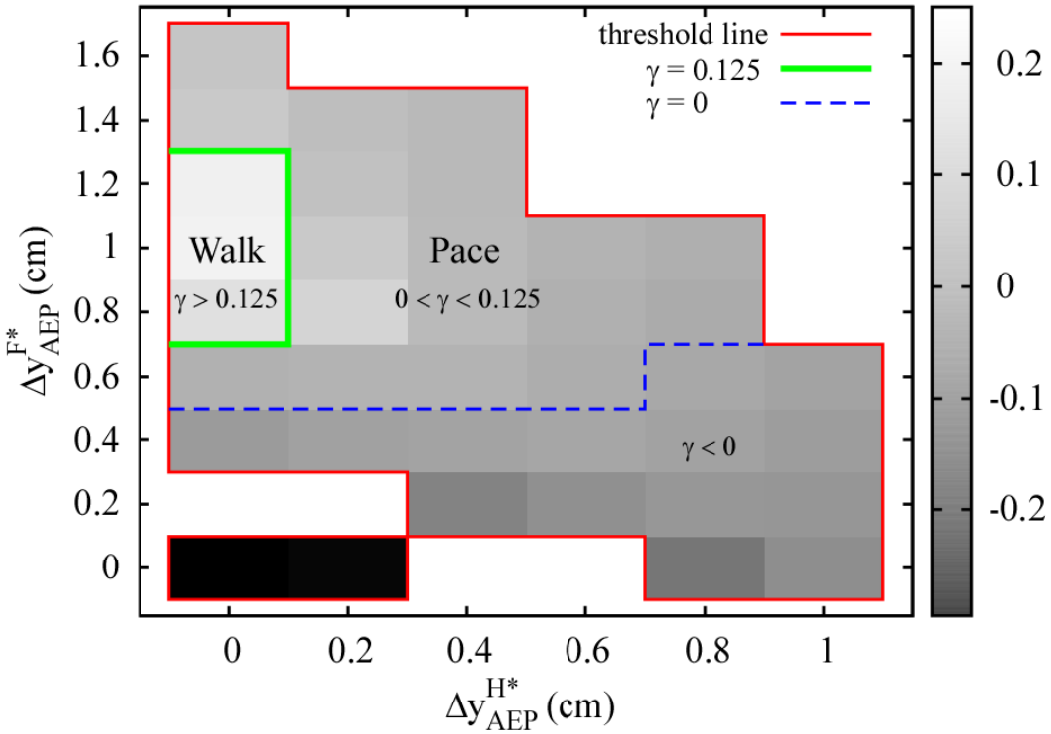

(a) Phase difference γ from the hind to the front legs

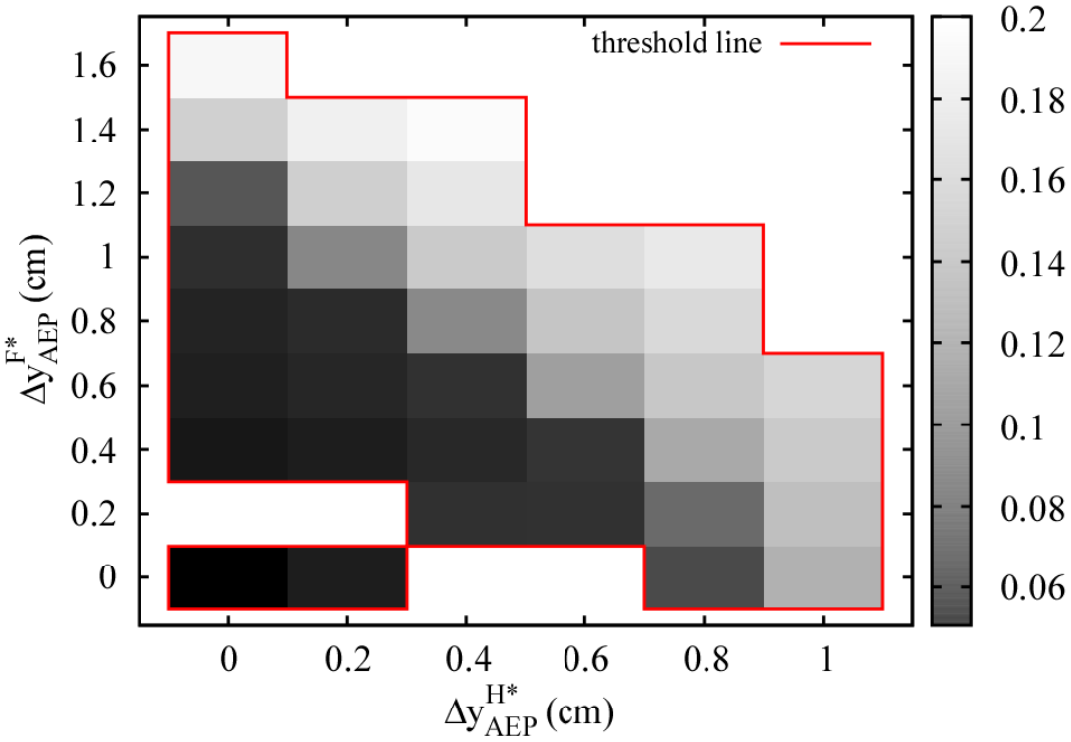

(b) Body rolling motion amplitude Θ (rad)

FIGURE 4.7: Influence of Δy_{AEP} on the walking pattern. Only walking patterns with a regularity index I_r greater than 1.8 were represented (inside the red threshold line). Under that value, the pattern was either unstable, irregular or the rolling motion amplitude was greatly asymmetric.

4.5.4.2 Influence of the PD control gains of the knee and ankle joints

As the transition from the stance phase to the swing phase is controlled using force related sensory information, it is evident that the mechanical impedance of the leg during the stance phase has an influence on the locomotion. Due to its structure, the leg length (i.e. the distance between the hip joint and the foot) is completely determined by the value of the knee and ankle joints angles, so that the mechanical impedance of the leg is mainly characterized by the PD control gains K_P and K_D (Equation 4.12) of these joints. Their influence was investigated by adjusting the coefficient c in:

$$K_{P,j} = c \cdot K_{P,j}^{ref} \quad \text{with } j = \{knee, ankle\} \tag{4.17}$$

$$K_{D,j} = \sqrt{c} \cdot K_{D,j}^{ref} \tag{4.18}$$

where the reference values $K_{P,j}^{ref}$ and $K_{D,j}^{ref}$ are the ones of Table 4.3.

Increasing the stiffness of the legs accelerates the lateral transfer of leg loading in the situation represented in Figure 4.4-(b1) (resp. (b2)), resulting in an earlier transition from stance to swing of the left (resp. right) legs. This results in:

- the shortening of the duration of the double stance phase (Figure 4.4-(a)), so that the effective duty ratios are reduced (Figures 4.8(a) and 4.8(b));
- the beginning of the inverted pendulum motion in a position with θ_{roll} closer from 0, so that the amplitude of the rolling motion generated during the swing phase of the legs increases, as represented on Figure 4.8(c).

As a consequence of the increase of the rolling motion amplitude, $\dot{theta}_{roll}$ just before the touchdown of the swinging legs also increases. The values of Δy_{AEP} being fixed, γ decreases and the gait switches to a pace for high values of c for both legs (Figure 4.8(d)).

When c of the forelegs is smaller or equal to 0.8 and c of the hind legs becomes higher than a certain value, the walking pattern becomes unstable and the model fall forward because the load supported by one of the forelegs does not become smaller than χ and the foreleg cannot swing (this is related to the decrease of the rolling motion amplitude, as it will be explained in Section 5.2.4.2).

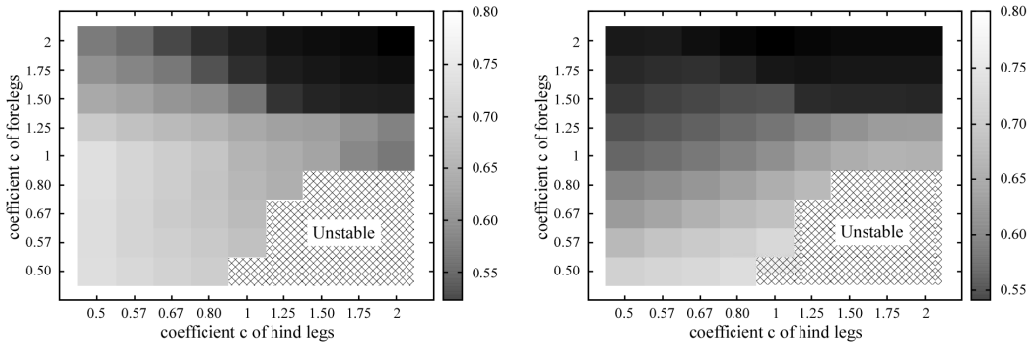

(a) Hind legs duty ratio $\bar{\beta}^{H*}$

(b) Forelegs duty ratio $\bar{\beta}^{F*}$

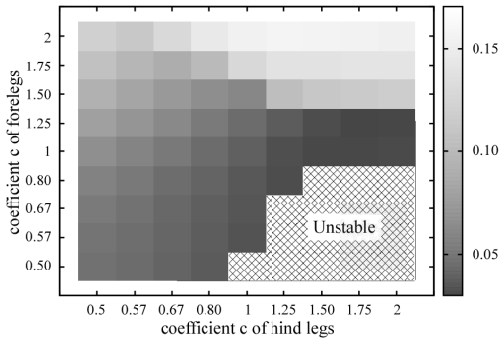

(c) Rolling motion amplitude Θ

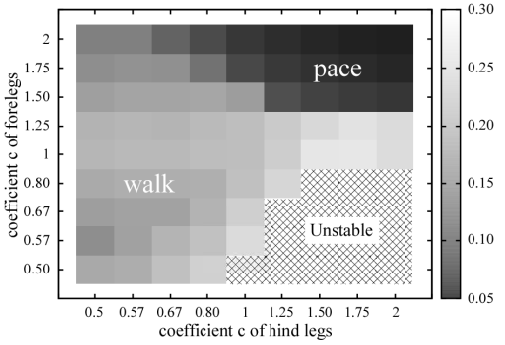

(d) Phase difference γ

FIGURE 4.8: Influence of the PD control gains of the knee and ankle joints on the effective duty ratios $\bar{\beta}$, the body rolling motion amplitude Θ and the phase difference γ (Δy_{AEP} are respectively set to 1 and 0 cm for the fore and hind legs).

4.5.4.3 Realization of the walk gait

Based on the previous considerations, parameters were set as in Table 4.3 and walk gait could be realized, as represented in Figure 4.9. The characteristics of the walking pattern are: $\bar{T}_{tot} \simeq 0.4$s, $\gamma = 0.216$, and $\bar{\beta}^{F*} = \bar{\beta}^{H*} = 0.686$. This pattern is used as the reference for the experiments described in Section 4.6, related to the modulations of the walking pattern, and in Chapter 5, related to the evaluation of the walking pattern stability, so that, except for explicit mention, the parameters in these cases are set to the values given in Table 4.3.

The transient phase, i.e. the transitory phase from rest (at the beginning of the simulation) until steady walking, is represented in Appendix D.

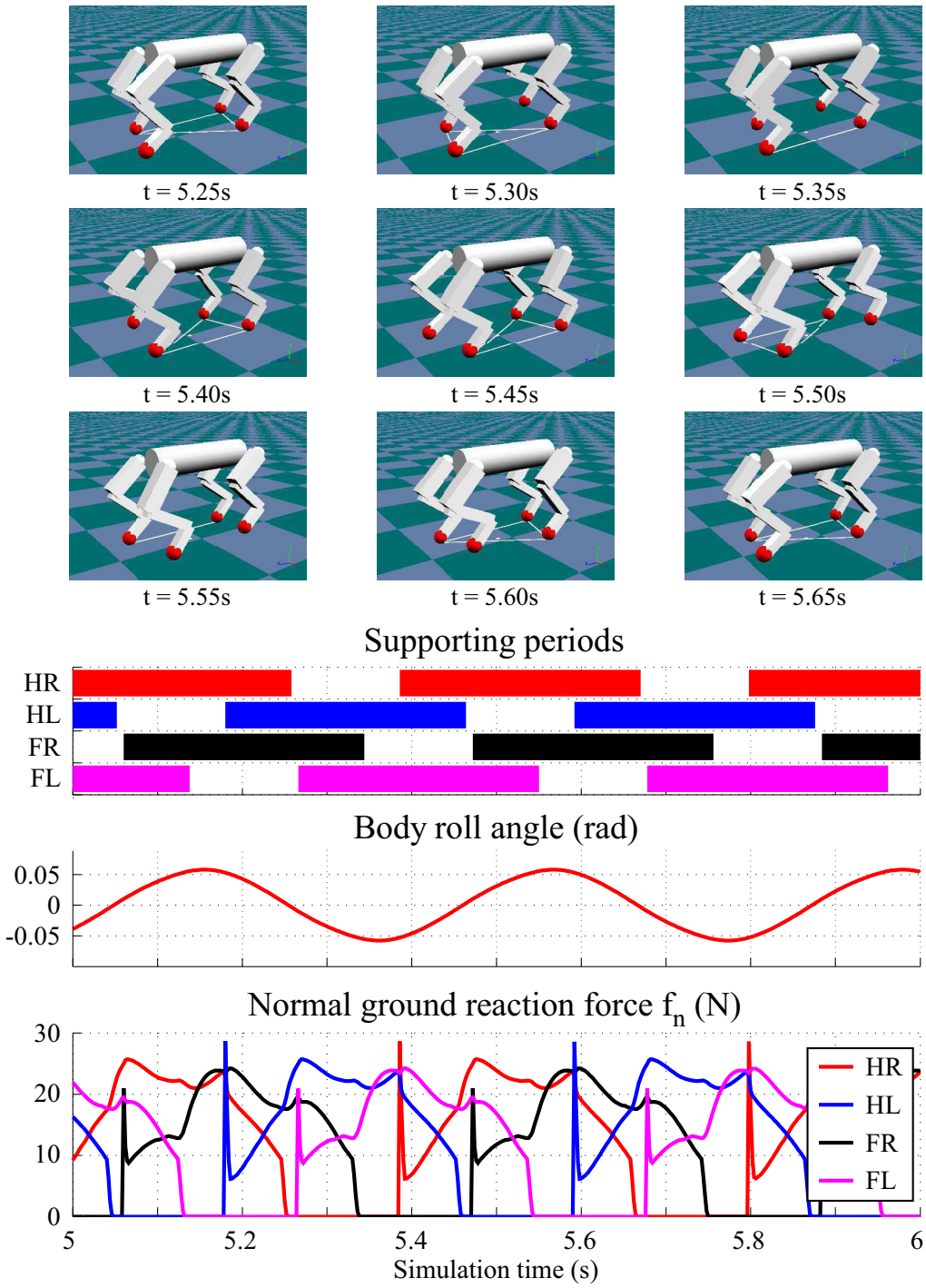

FIGURE 4.9: Walking pattern that emerges with the parameters settings given in Table 4.3. It is characterized by: $T_{tot} \simeq 0.4$s, $\gamma = 0.216$, and $\bar{\beta}^{F*} = \bar{\beta}^{H*} = 0.686$.

4.6 Modulations of the walking pattern

4.6.1 Modulation of the walking cyclic period

The cyclic period $\bar{T}_{tot}$ can be widely modulated via the variation of the nominal value of the swing phase duration $\hat{T}_{sw}$, while keeping constant the value of the nominal duty ratios $\hat{\beta}$ (Figure 4.10(a)). As the cyclic period increases, the amplitude of the rolling motion becomes larger and, in agreement with Kimura et al. (1990)(31), it was found to be more or less proportional to the square of the cyclic period (Figure 4.10(b)). This also implies that the amplitude of the angular speed of rolling $\dot{\theta}_{roll}$ increases more or less linearly with the cyclic period, resulting in a faster lateral transfer of leg loading if all the other parameters are constant. Hence, adaptations similar to the ones observed when the PD control gains were increased (Section 4.5.4.2), i.e. decrease of the effective duty ratios $\bar{\beta}$ and the phase difference γ, also occurs as the cyclic period increases. As a result, the gait progressively shifts to a pace.

To preserve the walk gait, Δy^{F*}_{AEP} and the PD control gains need to be adjusted as $\bar{T}_{tot}$ increases, as shown in Figures 4.11(a) and 4.11(b), where are represented the values of the parameters that were experimentally found suitable to realize stable walk with $\gamma \simeq 0.20$ and $\bar{\beta} \in [0.65, 0.70]$. Δy^{F*}_{AEP} must increase linearly with the cyclic period while the PD control gains must be roughly proportional to inverse of the square of the cyclic period (the adjustment of the PD control gains is carried out by multiplying the values of Table 4.3 by a coefficient c_{per} as in Equations 4.17 and 4.18). Moreover, c^{F*}_{per} needs to decrease slightly less than c^{H*}_{per} as the cyclic period increases, most likely because Δy^{F*}_{AEP} also increases and the forelegs are more bended than the hind legs during the stance phase, resulting in a reduction of the global stiffness of the leg for the same value of the gains.

With the previous adjustments, walking patterns with cyclic periods ranging from 0.30 s (for $\hat{T}_{sw} = 0.10s$) to 0.88 s (for $\hat{T}_{sw} = 0.35s$) were realized, as represented in Figure 4.10(a) (with $\hat{\beta} = 0.75$).

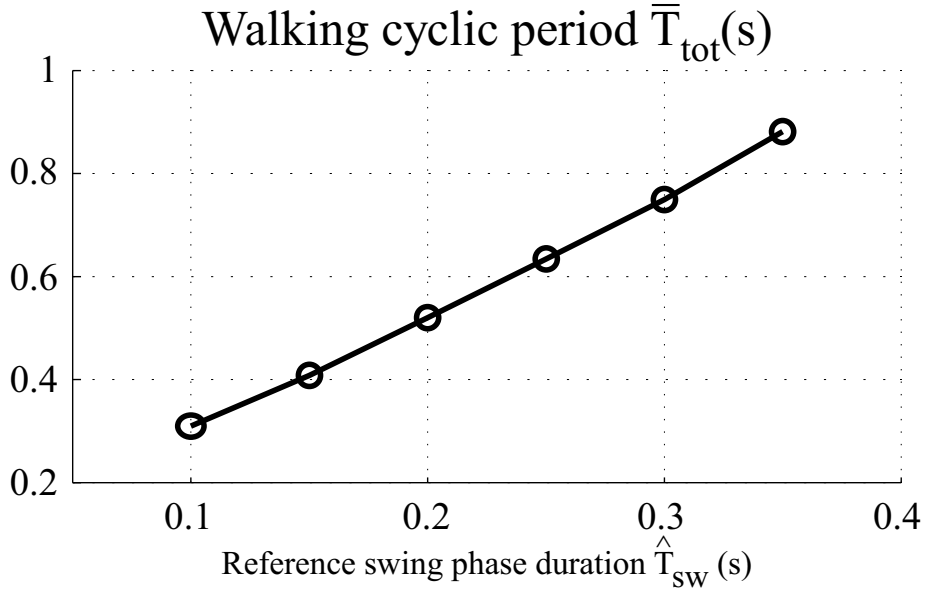

(a)

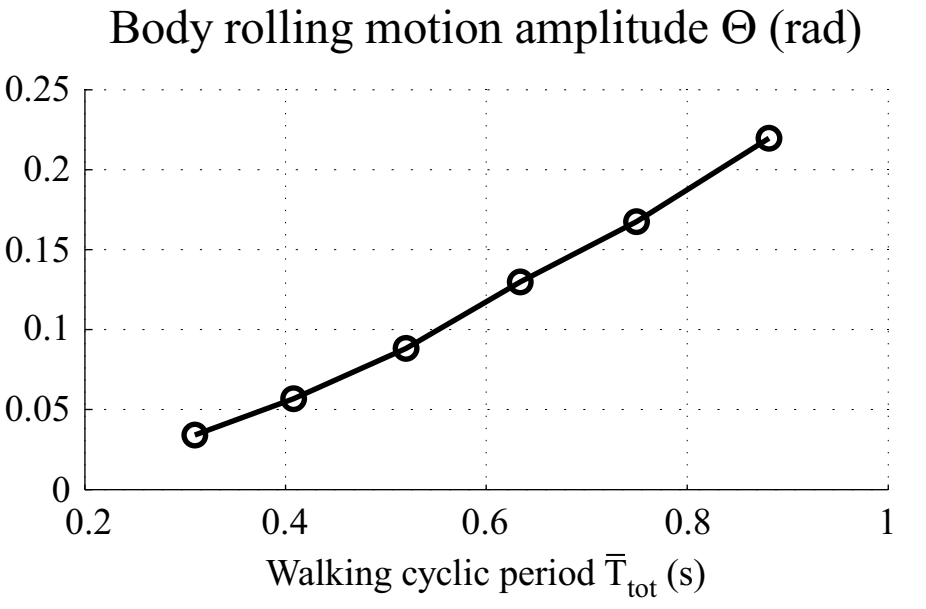

(b)

FIGURE 4.10: Modulation of the walking cyclic period and increase of the rolling motion.

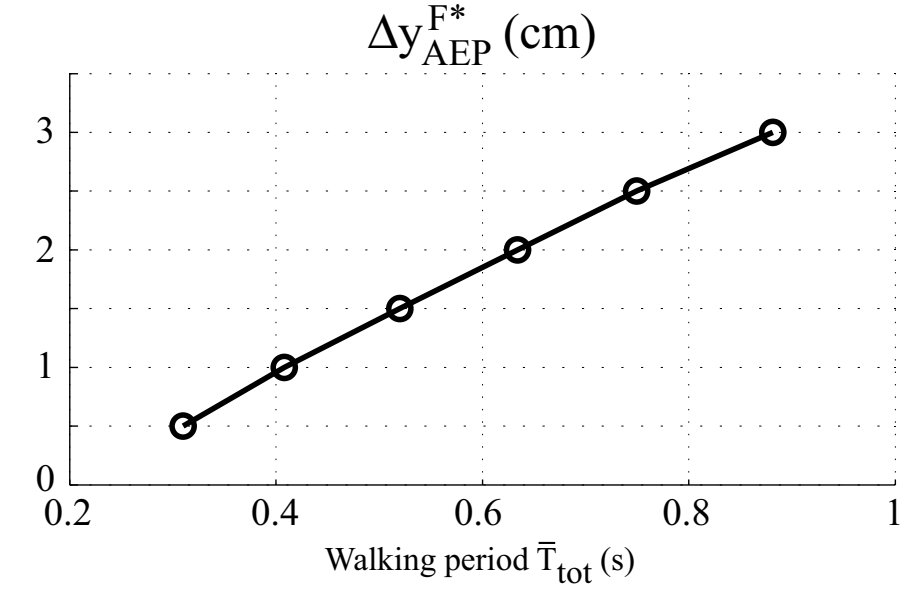

(a)

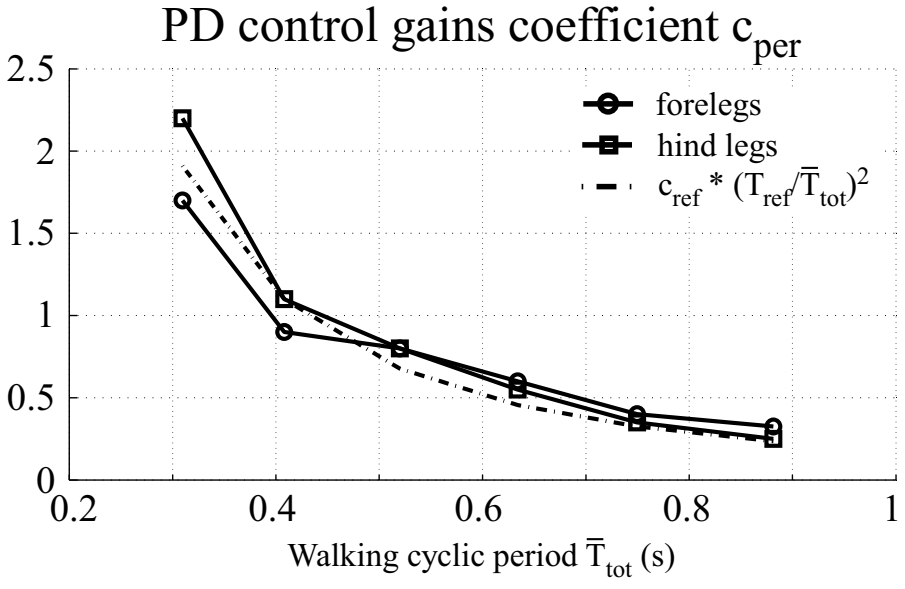

(b)

FIGURE 4.11: Adjustments required to keep a walk gait when adjusting the walking cyclic period (in (b), c_{ref} and T_{ref} are respectively equal to 1.1 and 0.408 s.).

4.6.2 Modulation of the walking speed

For a fixed value of $\hat{T}_{sw}$, the walking speed can be modulated via the variation of the nominal value of the duty ratios $\hat{\beta}$, resulting in the modification of the horizontal speed of the feet during the stance phase (see Equation 4.11). The variation of $\hat{\beta}$ has no direct influence on the duration of the stance phase because the termination of the stance phase is regulated using sensory information (Section 4.4.3), so that the increase of the speed is mainly due to the lengthening of the stride (Figure 4.12(b)). As the horizontal component of the AEP is fixed (Equation 4.5), the position of body at the end of the stance phase with respect to the positions of the feet of the supporting legs is progressively shifting forward as the speed increases. Due to the longitudinal transfer of leg loading, unloading of the hind legs occurs earlier, shortening the duration of their stance phase. As the swing phase duration is fixed, the effective duty ratios decrease (Figure 4.12(c)) and the cyclic period shortens (Figure 4.12(a)), causing the decrease of the rolling motion amplitude Θ (Figure 4.12(e)). On the other hand, the unloading of the forelegs is delayed, resulting in the increase of γ (Figure 4.12(d)) so that the gait gets closer to a trot.

The maximum realizable speed for a given value of $\hat{T}_{sw}$ is limited because there is a lower boundary of $\hat{\beta}$ under which the walking pattern becomes unstable. In such case, γ does not stabilize and grows continuously, disturbing the stepping coordination and eventually causing the model to fall (as represented in Figure 4.13). Moreover, even within the range of $\hat{\beta}$ values for which locomotion is stable, the regularity of the walking patterns decreases with the speed (Figure 4.12(f))

As for Section 4.6.1, it was found that adjustments of Δy_{AEP}^{F*} and the PD control gains are necessary. Decreasing Δy_{AEP}^{F*} and increasing the gains, as $\hat{\beta}$ is reduced, help to limit the increase of γ and to improve the regularity of the walking pattern. This is illustrated in Figure 4.14, with $\hat{T}_{sw}$ set to 0.25 s. With such adjustments, stable locomotion was achieved with $\hat{\beta} \in [0.50, 0.75]$ for all the values of $\hat{T}_{sw}$ considered in Section 4.6.1. Figure 4.15 shows the variation of the speed as a function of the nominal value of the duty ratios for three of them. Walking speed can be modulated in a broad range, from 0.08 to 0.72 m/s (or 0.33 to 3 body length/s).

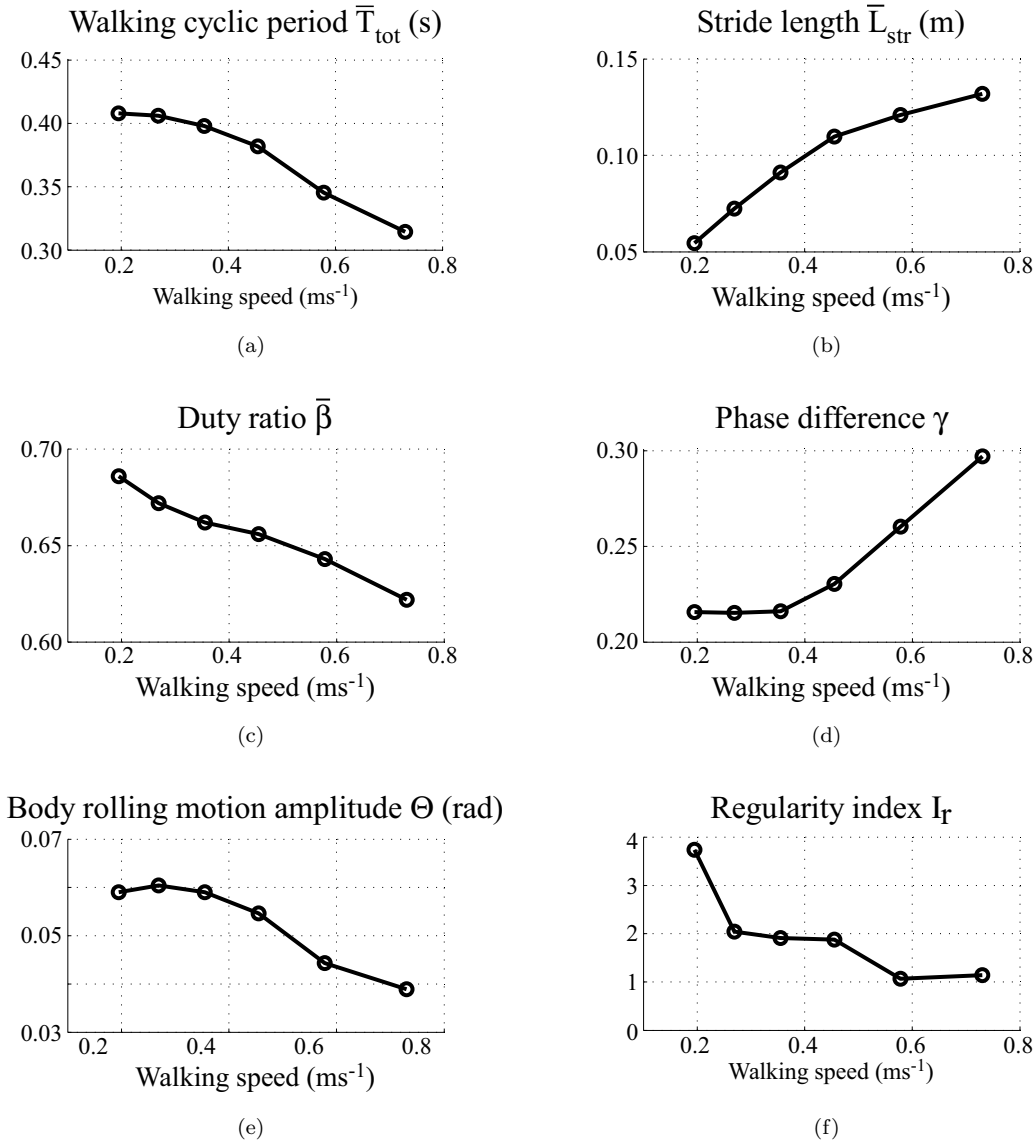

FIGURE 4.12: Adaptations of the walking pattern characteristics when the speed is modulated via the variation of the nominal value of the duty ratios $\hat{\beta}$, with $\hat{T}_{sw}$ constant. Here, the reference walking pattern of Section 4.5.4.3 is considered but similar adaptations were observed for all the walking patterns investigated.

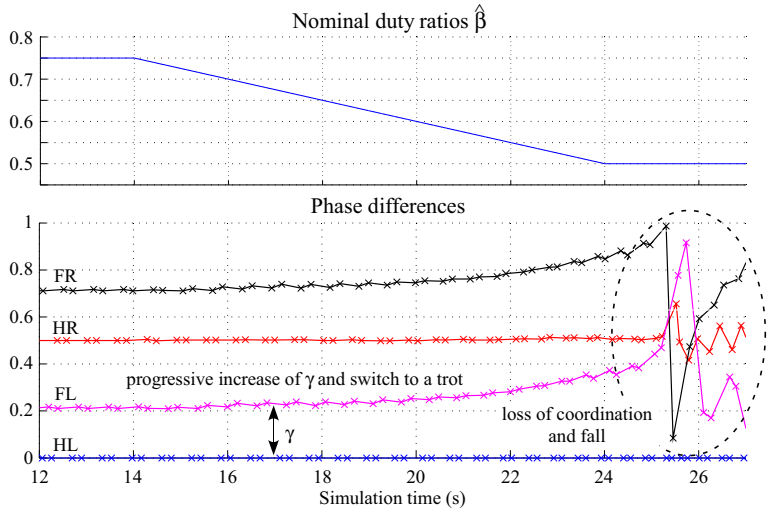

FIGURE 4.13: When decreasing $\hat{\beta}$ (hence increasing the speed), γ progressively increases. When it reaches a certain level, instead of stabilizing, γ continues to grow and the gait switches briefly to a trot ($\gamma = 0.5$) then becomes unstable. In this case, $\hat{T}_{sw}$ is set to 0.25 s. and the walking pattern becomes unstable when $\hat{\beta}$ is smaller than 0.55.

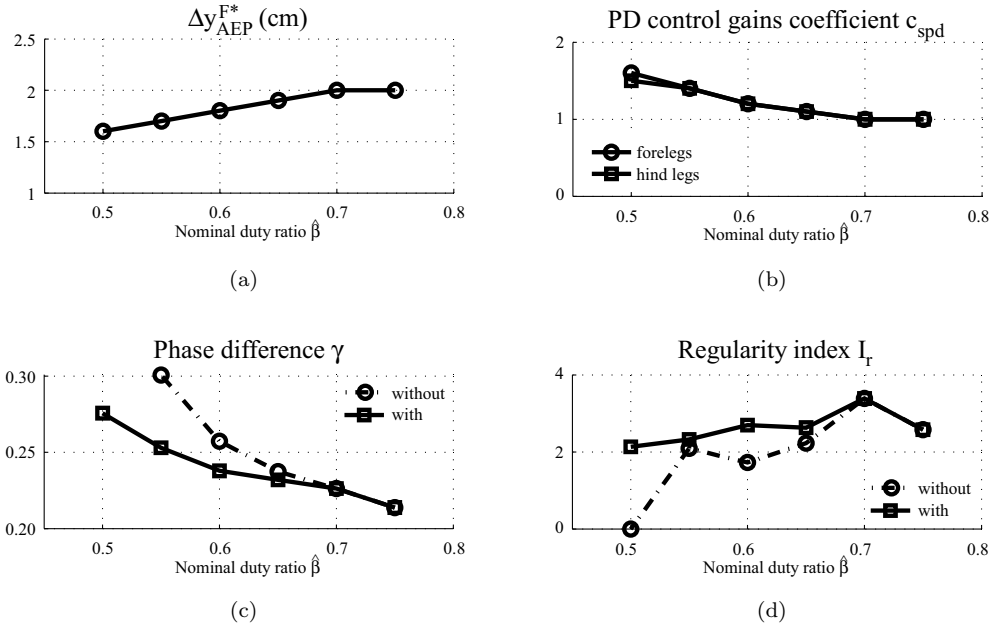

FIGURE 4.14: Adjustments of Δy_{AEP}^{F*} and the PD control gains with $\hat{\beta}$, as well as the resultant phase difference and regularity index with and without the adjustments ($T_{sw} = 0.25s$). For the PD gains, the coefficient c_{spd} must be multiplied to the coefficient c_{per} of Figure 4.11(b). Without the adjustments, the walking pattern is unstable for $\hat{\beta} = 0.50$ and I_r is set to 0. With the adjustments, the increase of γ is reduced and the regularity of the patterns is increased, so that locomotion at $\hat{\beta} = 0.50$ can be achieved.

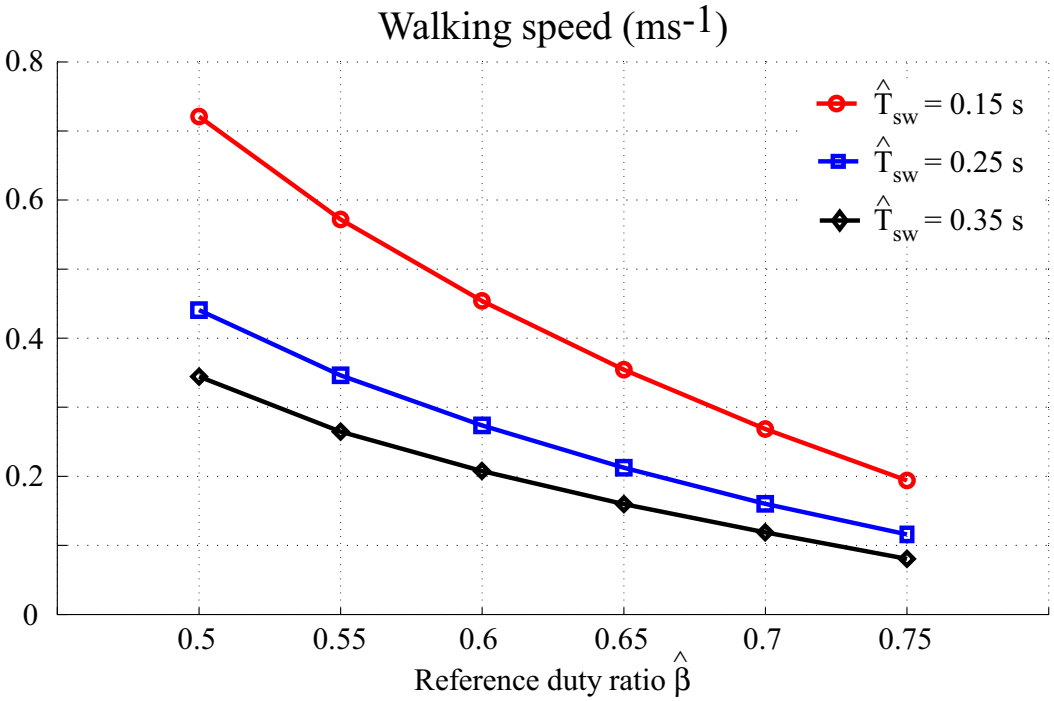

FIGURE 4.15: Modulation of the walking speed when changing the reference of the duty ratio $\hat{\beta}$ for the walking patterns with T_{sw} respectively equal to 0.15, 0.25 and 0.35 s (with the necessary adjustments of Δy_{AEP}^{F*} and the PD control gains).

4.7 Summary

In this chapter, a simple leg controller based on the common principles was developed to actuate a simplified three-dimensional quadruped model. The contribution of the control of the phase transitions using leg loading information (particularly the transition from stance to swing) to the emergence of left-right alternate stepping coordination was investigated. Using independent leg controllers, various gaits characterized by a left-right alternate coordination could be realized in a distributed way. Left-right alternate stepping coordination emerged and maintained via the entrainment between the stepping of the legs, the rolling motion and the lateral transfer of leg loading.

Two categories of parameters, the offset of the vertical coordinate of the nominal AEP and the PD control gains of the ankle and knee joints, were found to influence the emergent gait. The influence of these parameters was investigated and conditions for the emergence of a walk gait were formulated. As a result, walk gait could be generated with independent leg controllers.

Next, modulations of the walking pattern resulting in adjustments of the cyclic period and the speed were realized and parameters adjustments required to preserve the walk gait were identified. Using this approach, walking patterns with cyclic periods from 0.3 s to 0.88 s. and speed from 0.33 to 3 body length/s could be generated.

Chapter 5

Contribution of the phases modulations to the stability

5.1 Overview

In order to evaluate the stability of the walking patterns generated in Chapter 4, the model is subjected to lateral perturbation in Section 5.2. When using phase modulations, the system is resistant to perturbations increasing of the absolute value of the angular velocity of rolling, resulting in a larger extremum of the body roll angle just after the application of the perturbation. On the other hand, it is sensitive to perturbations that have the opposite influence on the rolling motion. Consequently, an additional ascending coordination mechanism, linking the hind and the forelegs, is introduced in Section 5.3 to improve the performances of the system when the absolute value of the angular velocity of rolling is decreased. The influence of the cyclic period and the speed of the walking pattern on the stability is investigated in Section 5.4. Finally, Section 5.5 reports the achievement of walking on terrains with a medium degree of irregularity.

5.2 Evaluation of the stability with independent leg controllers

5.2.1 Method

In order to investigate how the phase modulations contribute to the stability of the stepping patterns generated by the controller, the model was subjected to lateral perturbations. These consist in the temporary perturbation of the rolling motion by applying a force at the center of mass of the trunk during 0.1s. The force is directed to the left of the model (as represented in Figure 5.1) and is applied at various timings during the

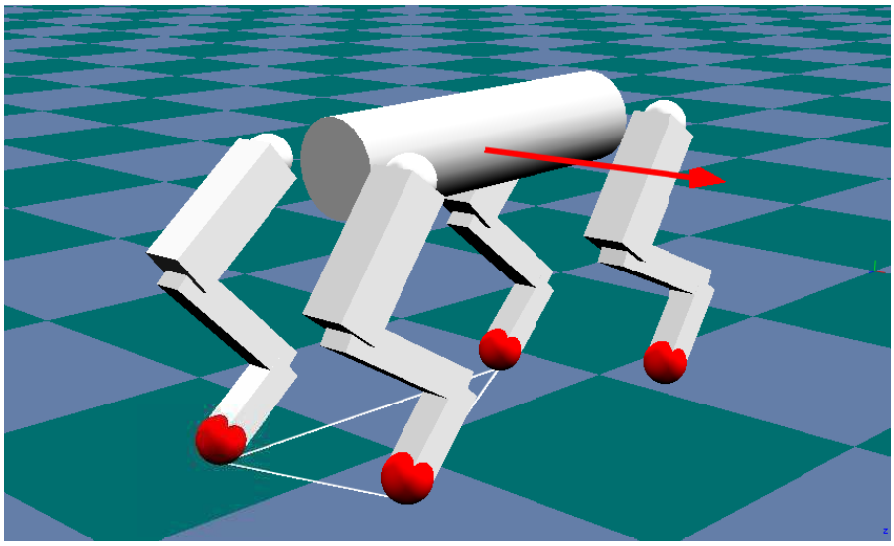

FIGURE 5.1: Lateral perturbation of the model by applying a force, directed to the left of the model, at the center of mass of the trunk. Here, the perturbation is applied at the onset of the swing phase of the left hind leg.

walking cycle. Four timings were considered: the onset of the swing phase of the left hind leg (HL), left foreleg (FL), right hind leg (HR) and right foreleg (FR) respectively. The walking pattern of Section 4.5.4.3 was used for the experiments.

5.2.2 Stabilization action of the phase modulations in the frontal plane

The way the phase modulations contribute to the stabilization of the posture in the frontal plane when the model is perturbed is schematically represented in Figure 5.2. Considering first the case where a perturbation directed to the left is applied, the rolling motion of the body becomes asymmetric so that the model is leaning toward the left side during the locomotion. In other words, the average body rolling angle over the cyclic period when the perturbation is applied becomes negative, or $< \theta_{roll} >_k < 0$, using the following definition:

$$< f >_k = \frac{\int_{ts_k}^{te_k} f(\tau) d\tau}{(te_k - ts_k)} \tag{5.1}$$

where k is the walking cycle index, while ts and te are respectively the starting and ending times of the cycle, when taking a particular event as reference (for example the onset of the swing phase of the left hind leg). The asymmetry of the rolling motion causes a similar asymmetry in the load supported by the legs so that $< f_n^{*L} >_k$ becomes greater than $< f_n^{*R} >_k$. As f_n is used to modulate the transition from the stance to the swing phase (as explained in Section 4.4.3), increase of $< f_n >_k$ (for the left legs) leads to the prolongation of the stance phase, while it is shortened if $< f_n >_k$ decreases (for the right legs). Consequently, the duty ratios of the left legs increase, while they decrease for the right legs ($\bar{\beta}_k^{*L} > \bar{\beta}_k^{*R}$), amplifying the original asymmetry of the $< f_n >_k$. This

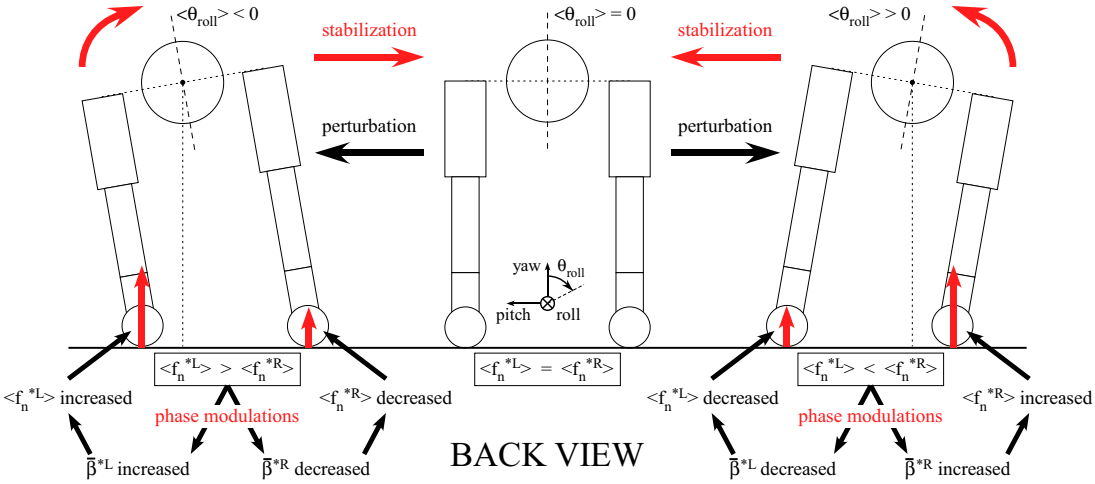

FIGURE 5.2: Stabilization and recovery from perturbation provided by the phase modulations, through the adjustment of the duty ratios (index k is omitted to simplify the figure).

is equivalent to say that the duration of inverted pendulum motion around the left legs feet (situation (c2) in Figure 4.4) becomes longer than the one around the right legs feet (situation (c1)) during the k^{th} walking cycle. Hence, via the automatic adjustment of the duty ratios, a global recovery force in the opposite direction to the original perturbation is generated. It tends to attenuate the asymmetry and bring $< \theta_{roll} >_{k+1}$ back to 0, i.e. it contributes to stabilize the posture in the frontal plane. The same arguments also hold, of course, for perturbations that cause an asymmetry of the body rolling motion in the opposite direction.

5.2.3 Contribution of the stance phase termination condition to the stability

As explained in Section 5.2.2, the adjustment of the stance phase duration via the regulation of the stance phase termination based on leg loading information is playing a great role in the stabilization of the walking pattern in the frontal plane. In order to assess the effectiveness of this mechanism, the situation where the condition $f_n < \chi$ of Section 4.4.3 is not used but is replaced instead by a condition based on the oscillator phase ($\phi > \phi_{cnd}$) was first investigated.

First, ϕ_{cnd} was set for each leg to the value ϕ_{tr} at which the transition usually occurs when using the condition based on leg loading. In that case, the walking gait still exists but is quite instable. Indeed, applying a lateral force of low intensity induced a permanent asymmetry in the rolling motion amplitude (the model leaned on the opposite side from where it was pushed, as represented in Figure 5.3(a)). The asymmetry increased

with the intensity of the perturbation and eventually resulted in the loss of interleg coordination and the disappearance of the walking gait (the model subsequently fell or the gait switched to a bound-like gait) at low level of the perturbation force (as illustrated in Figure 5.3(c)). The maximum supported intensity of the perturbation is between 3 and 6 N for all the timings (see Figure 5.4). This represents less than 30% of the intensity of the perturbation supported with the condition using leg loading, except in the case where the perturbation is applied at the onset of the swing phase in HL (the reason for this exception is given in Section 5.2.4.2). The same experience was also carried out with a walking pattern with a longer cyclic period (T_{tot} = 0.63 s instead of 0.40 s for the reference walking pattern). In that case, the walking gait did not survive to the modification of the stance phase termination condition and the model fell.

In a second time, other values of ϕ_{cnd} were considered but none of them improved the stability of the walking pattern. However, for ϕ_{cnd} greater than ϕ_{tr} (for both the fore and hind legs or for the hind legs only), the walking gait switched to a pace (the stability was not investigated in that case however).

Hence it can be concluded that modulation of the stance phase duration by the condition based on leg loading is playing a vital role for the existence and the stability of the walking gait.

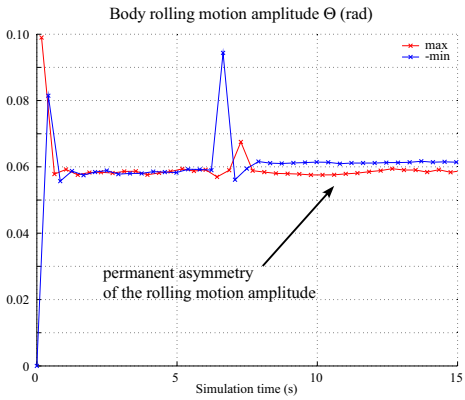

(a) Perturbation of 4 N (condition $\phi > \phi_{cnd}$): permanent asymmetry of the rolling motion amplitude is caused by the perturbation.

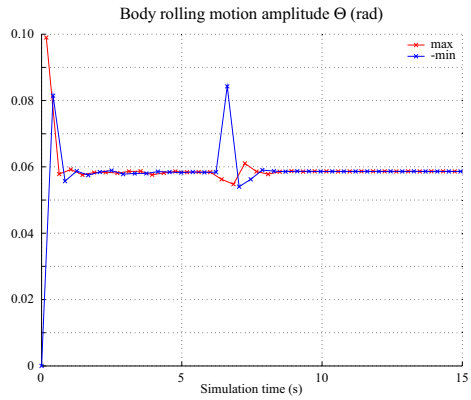

(b) Perturbation of 4 N (condition $f_n < \chi$): the perturbation is completely rejected within a few steps.

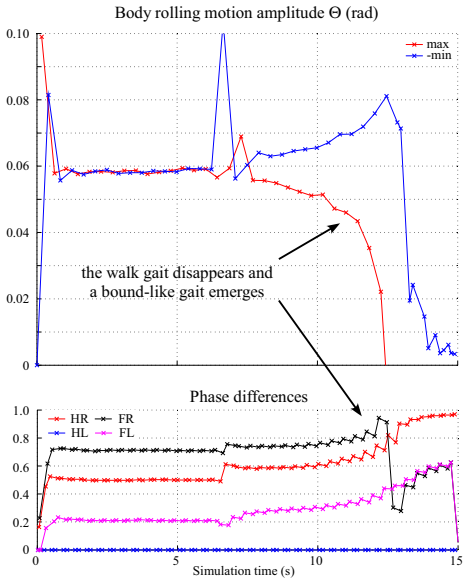

(c) Perturbation of 5 N (condition $\phi > \phi_{cnd}$): the perturbation results in the disappearance of the walk gait and the model switches to a bound-like gait.

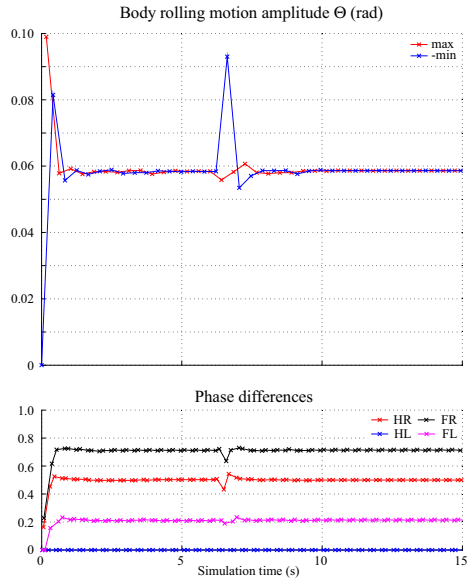

(d) Perturbation of 5 N (condition $f_n < \chi$): the perturbation is completely rejected within a few steps.

FIGURE 5.3: Resistance ability against lateral perturbations when the transition from stance to swing is controlled using the phase of the leg controller (left) or leg loading information (right). ϕ_{tr} is respectively equal to 4.42 and 4.38 for the hind and the forelegs. The perturbation is applied at the onset of the swing phase in FL.

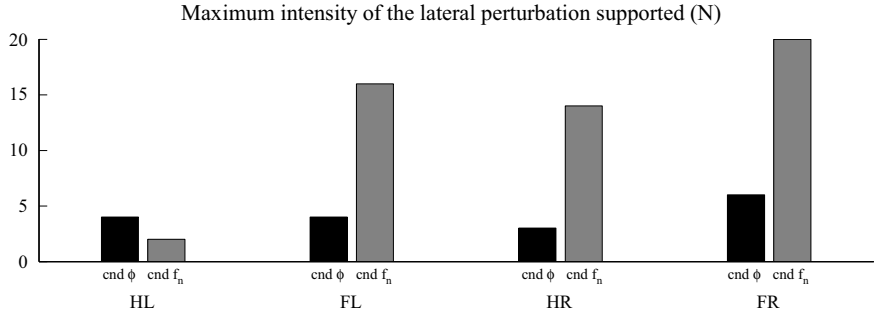

FIGURE 5.4: Maximum intensities of the lateral perturbations supported by the model for each timing of application (increasing the intensity of the perturbation over the values represented causes the walk gait to disappear or the model to fall). cnd ϕ refers to the case where the condition based on ϕ ($\phi > \phi_{cnd}$) is used, while for cnd f_n, condition based on leg loading ($f_n < \chi$) is used.

5.2.4 Stability of the walking pattern

The situation where the normal stance phase termination condition, based on leg loading information, is used was investigated next. Figure 5.4 shows that the resistance ability of the walking patterns against perturbations greatly varies according to the timing at which the perturbation is applied. When the perturbation occurs at the onset of the swing phase of either FL, HR or FR, the maximum intensity of the perturbation supported by the model before falling is relatively high, while the model seems to be particularly sensitive to perturbations at applied at HL. This situation can be explained if the influence of the perturbation on the body rolling motion and the lateral transfer of leg loading is considered.

5.2.4.1 Perturbations that accelerate the lateral transfer of leg loading

When the perturbation is applied at the onset of the swing phase of FL, HR or FR, it tends to *increase* the absolute angular velocity of rolling $\dot{\theta}_{roll}$, resulting in the augmentation of the modulus of the next extremum of the body roll angle (see Figure 5.5). This contributes to accelerate the lateral transfer of leg loading that occurs with the rolling motion during the right-left alternate stepping (as explained in Section 4.5.3). For the sake of convenience, this case will be referred from here on as a perturbation that increases the rolling motion amplitude or, equivalently, that accelerates the lateral transfer of leg loading.

Consistent with the considerations of Section 5.2.2, duty ratios are adjusted by the phase modulations to compensate the asymmetry in the rolling motion amplitude induced by the perturbation. As the perturbation is directed to the left, it induces an asymmetry of the rolling motion amplitude in the same direction (i.e. $< \theta_{roll} >$ becomes smaller than 0). This results in the increase of the left legs duty ratios while the ones of the right legs

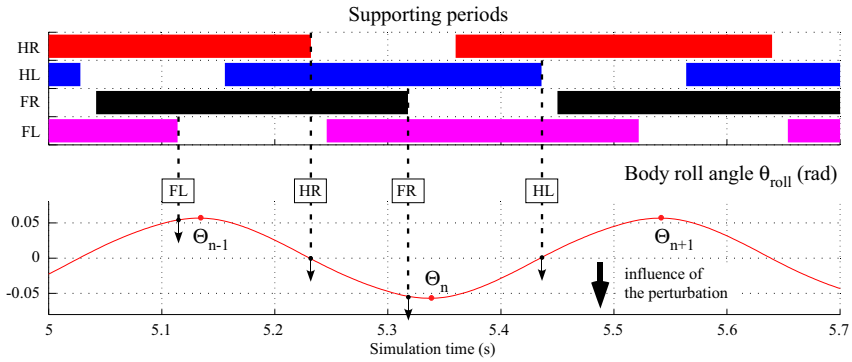

FIGURE 5.5: Timings of the application of the perturbations and influence on the body rolling motion. The arrows in the lower graph represent the influence of the perturbations on the body roll angle: as it is directed to the left, the perturbation causes a decreases of the body roll angle. In the case of HR and FR, the perturbation results in the increase of the modulus of the next extremum of the body roll angle Θ_n. The situation is basically the same for FL because the body roll angle is already too close from its maximum value Θ_{n-1} for the perturbation to have a big influence on its modulus. Hence the perturbation instead causes the increase of Θ_n modulus. On the other hand, in the case of HL, the perturbation reduces the modulus of the the next maximum of the body roll angle Θ_{n+1}.

are decreased (as represented in Figure 5.6). The details of how the phase modulations result in the adaptation of the stance and swing phases durations are represented on Figure 5.7. The limit of the resistance to the perturbation is reached when the intensity of the perturbation is strong enough to bring the projection of the center of mass beyond the line of support defined by the left fore and hind legs feet, resulting in an avoidable fall of the model on the side.

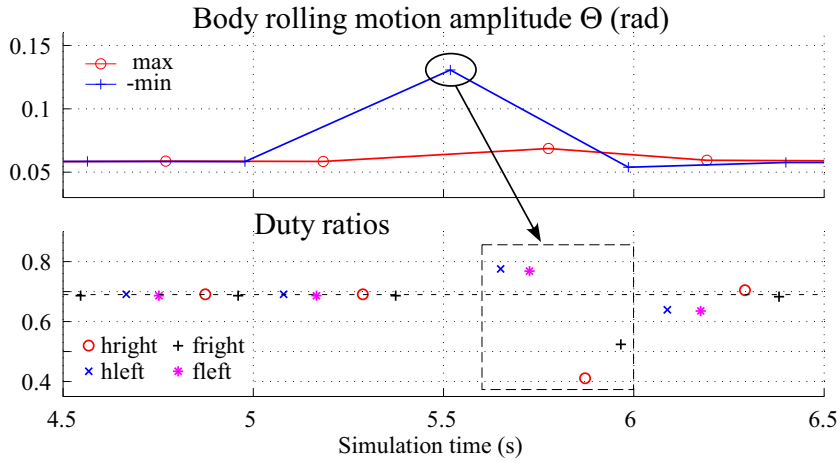

FIGURE 5.6: Modulation of the duty ratios subsequent to a perturbation of 15 N at the onset of the swing phase of the right foreleg (FR). Duty ratios of the left legs are increased while the ones of the right legs are decreased, hence leading to the recovery of the symmetry of the rolling motion amplitude Θ.

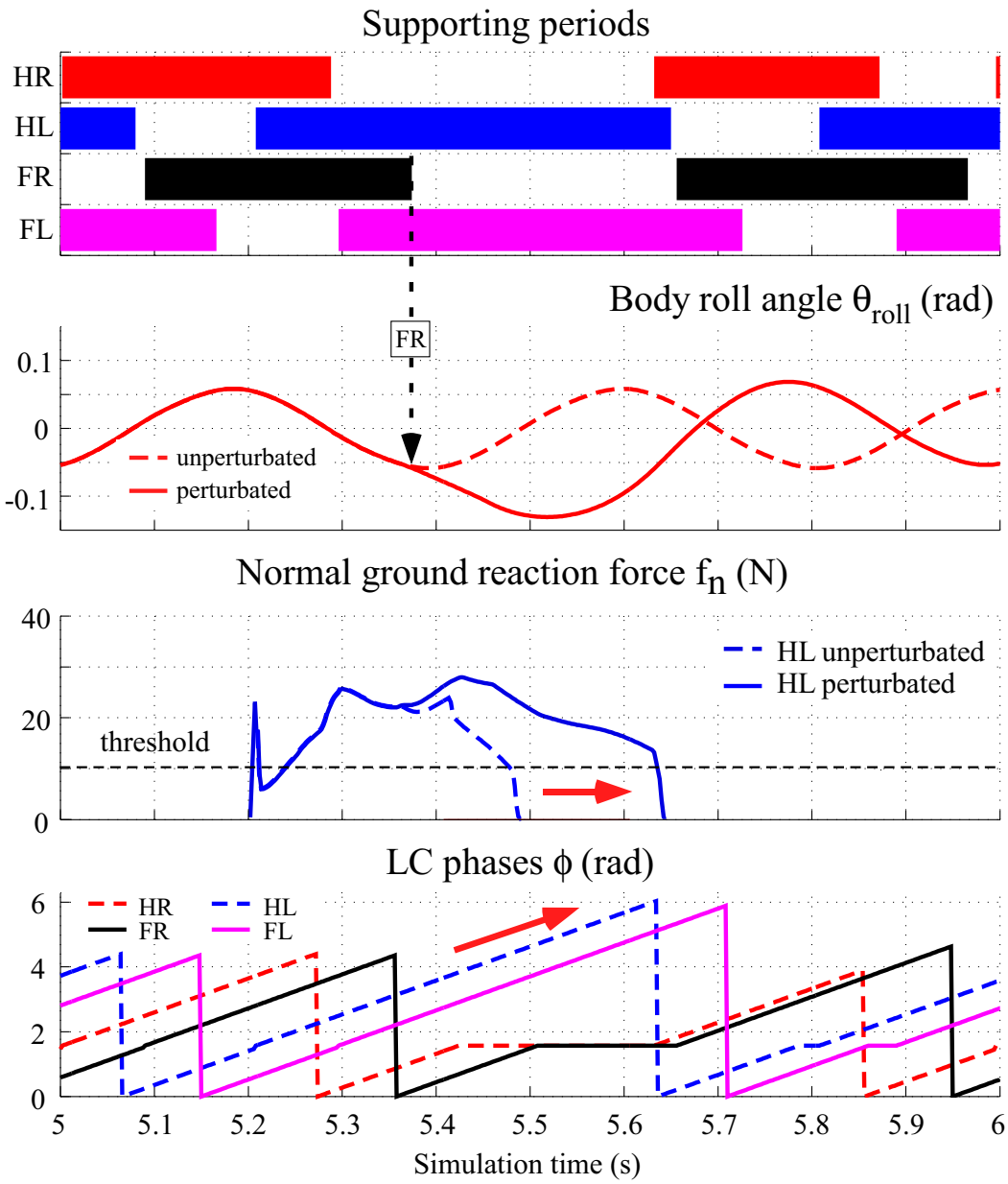

FIGURE 5.7: Modulation of the stance period of the supporting legs, subsequent to a perturbation increasing the rolling motion amplitude (the perturbation is the same as in Figure 5.6). The perturbation induces an additional load on the supporting legs (represented by HL here), so that their stance phase is extended as long as the normal reaction force f_n is bigger than the threshold χ. On the other hand, the contralateral legs, having reached the AEP, are waiting for the touchdown event. Consequently, the duration of inverted pendulum motion around the left feet (situation (c2) in Figure 4.4) is extended. This contributes to bring back θ_{roll} to zero and restore the normal posture.

5.2.4.2 Perturbations that slow down the lateral transfer of leg loading

On the other hand, when the perturbation is applied at the onset of the swing phase of HL, it tends to *decrease* the absolute angular velocity of rolling, resulting in the reduction of the modulus of the next extremum of the body roll angle (see Figure 5.5). In other words, the perturbation tends to cancel the rolling motion and causes the lateral transfer of leg loading that occurs in situation (b1) of Figure 4.4 to slow down. The main consequence is that the rate of unloading of the left foreleg (FL) is much reduced. For the sake of convenience, this case will be referred from here on as a perturbation that decreases the rolling motion amplitude or, equivalently, that slows down the lateral transfer of leg loading.

For small intensities of the perturbation, the controller can reject the perturbation by adjusting the right and left duty ratios in a similar way as for a perturbation increasing the rolling motion amplitude (Figure 5.8). However, if the intensity of the perturbation is higher than a certain level, the load supported by FL never becomes smaller than the threshold χ and the transition from stance to swing is prevented (Figure 5.9). This disturbs greatly the leg coordination, often causing the model to fall.

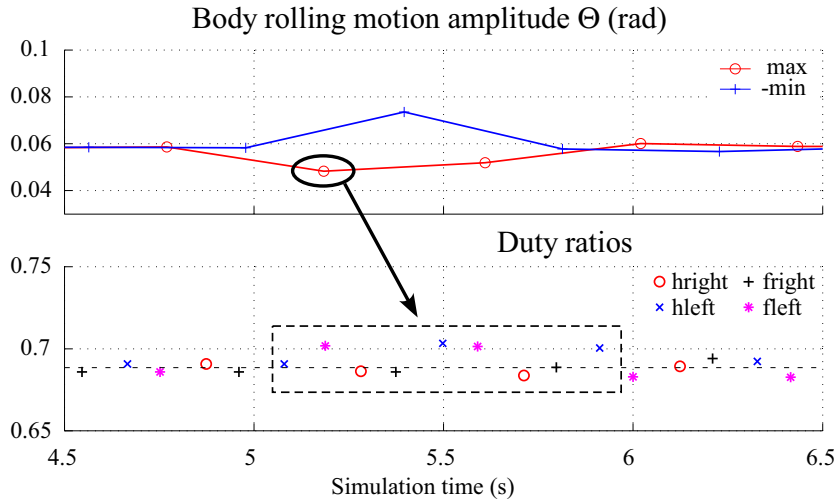

FIGURE 5.8: Modulation of the duty ratios subsequent to a perturbation of 2 N applied at the onset of the swing phase of the left hind legs (HL). The perturbation causes the decrease of the rolling motion amplitude. Duty ratios are adjusted similarly as in Figure 5.6.

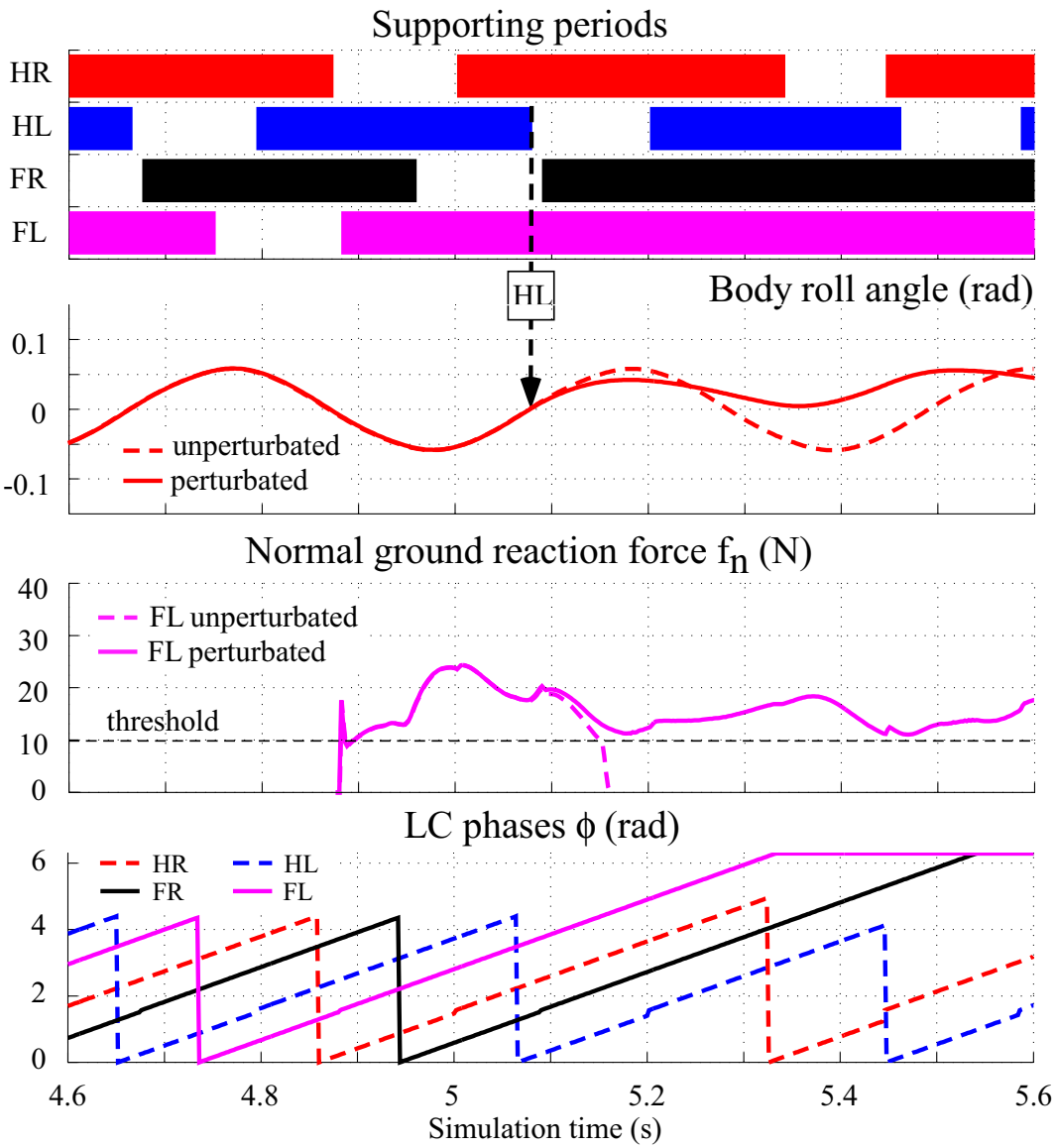

FIGURE 5.9: Modulation of the stance period of the supporting legs subsequent to a perturbation of 3 N applied at the onset of the swing phase of the left hind leg (HL). The perturbation causes the decrease of the rolling motion amplitude and slows down the lateral transfer of leg loading. As a result, f_n^{FL} never becomes smaller than the threshold and the transition from stance to swing is prevented.

5.3 Ascending coordination mechanism

Regarding the previous results, it clearly appears that an additional control mechanism is needed to help the model to recover from the perturbations that reduce the rolling motion amplitude. It should bring a solution to the main cause of failure (i.e. the transition from stance to swing of the foreleg is prevented due to abnormal loading) without sacrificing the stability. Based on the observation that, even when the rolling motion is completely canceled, the load supported by the hind leg eventually decreases due to the longitudinal transfer of leg loading, allowing it to switch to the swing phase, the following two-fold ascending coordination mechanism was implemented:

- The transition from stance to swing in a hind leg (Hx) tends to induce the same event in the ipsilateral foreleg (Fx). This is achieved by progressively increasing the force threshold of the foreleg χ^{Fx} as ϕ^{Hx} increases during the swing phase of the hind leg (Hx), as follows:

$$\chi^{Fx} = \begin{cases} \hat{\chi} & \text{if } \phi^{Hx} < \Phi_s \\ \hat{\chi} + \chi_{mod} & \text{if } \Phi_s \leq \phi^{Hx} \leq \Phi_e \\ \hat{\chi} & \text{if } \phi^{Hx} > \Phi_e \end{cases} \tag{5.2}$$

$$\chi_{mod} = \frac{\phi^{Hx} - \Phi_s}{\Phi_e - \Phi_s} \cdot \chi_{ampl} \tag{5.3}$$

  where Φ_s and Φ_e are the starting and ending thresholds, defining the interval of ϕ^{Hx} in which the modulation occurs, while χ_{ampl} is the maximum value of the modulation.

- The duration of the subsequent swing phase of the foreleg is shortened, by setting ω_{mod} of Equation 4.3:

$$\omega_{mod}^{Fx} = \lambda \cdot \frac{f_{n,LO}^{Fx} - \hat{\chi}}{\chi_{ampl}} \cdot \hat{\omega} \tag{5.4}$$

  where $f_{n,LO}^{Fx}$ is the ground reaction force measured by the force sensor of the foreleg when the transition from stance to swing occurs.

The action of this ascending coordination mechanism can be decomposed the following way:

- First, by progressively increasing the force threshold of the forelegs χ^{Fx}, Equations 5.2 and 5.3 play the functional role of detecting the disruption of the normal leg loading and unloading cycle (that leads to the incapacity for the foreleg to swing) and restarting the body rolling motion by forcing the foreleg to swing.

- Second, if the transition to swing of the foreleg is triggered by increasing the force threshold, it means that the load supported by the leg is greater than normal

or, equivalently, that the body roll angle at the initiation of the swing phase is smaller than in the normal conditions. Consequently, the subsequent swing phase duration has to be shortened to prevent the generation of an excessive rolling motion amplitude in the direction of the swinging foreleg. This is the role of the modulation of Equation 5.4, where the state of the rolling angle at the initiation of the swing phase is estimated by the load supported by the leg at the transition.

While allowing the overloaded foreleg to swing, the conjugated action of the two previous adjustments is to globally increase the duty ratio of the foreleg. Indeed, the transition to the swing phase is still delayed compared to normal, hence prolongating the stance phase (Equation 5.2 and 5.3), while the duration of the subsequent swing phase is shortened (Equation 5.4). Moreover, the increase of the duty ratio is positively related with the increase of the load supported by the foreleg (i.e. with the intensity of the perturbation). Consequently this mechanism acts in cooperation with the stabilization provided by the phase modulations. Figure 5.10 illustrates the action of the ascending coordination mechanism.

The values of the parameters of Equations 5.2, 5.3 and 5.4 are given in Table 5.1. Φ_s is set to a value slightly higher than the value of ϕ^{H*} when the transition to the swing of the foreleg happens in normal conditions. On the other hand, Φ_e is set to $\hat{\phi}_{AEP}$ to insure that, even if the phase of the hind leg is reset due to the touchdown, the mechanism can still trigger the transition to the swing phase of the foreleg, if the leg loading is less than $\hat{\chi} + \chi_{ampl}$. Appropriate values for the two other parameters were determinated experimentally

Adding this mechanism to the previous architecture leads to the improvement of the resistance to the perturbation at the onset of the swing of HL up to 25 N. The results for the other timings are not changed as, in these cases, the perturbation tends to advance the transition from stance to stance in the foreleg, hence the ascending coordination mechanism is not used. Furthermore, it also improves the performances when tackling certain types of terrain unevenness (see Section 5.5).

TABLE 5.1: Values of the parameters in Equations 5.2, 5.3 and 5.4.

Φ_s	Φ_e	χ_{ampl}	λ
$0.55 \cdot \hat{\phi}_{AEP}$	$\hat{\phi}_{AEP}$	15 N	1

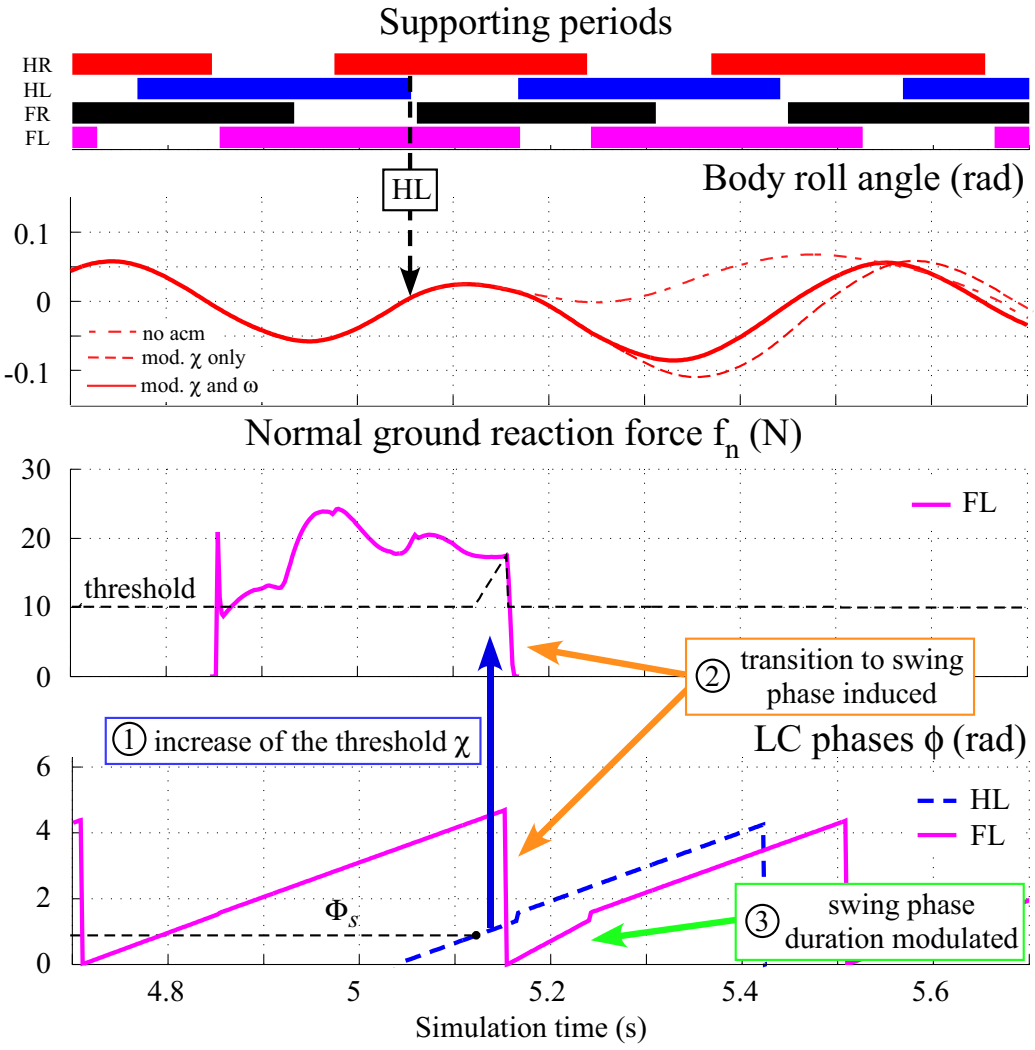

FIGURE 5.10: Ascending coordination mechanism in action and recovery from a perturbation of 7 N applied at the onset the swing phase of the left hind leg (HL). When ϕ^{HL} reaches Φ_s a bit after 5.1s, χ^{FL} starts to increase (1). When it reaches the value of load supported by FL, the transition from stance to swing is triggered (2). This restarts the rolling motion (curve "mod. χ only" compared to curve "no acm"). Subsequently, swing phase duration is shortened (3) to prevent excessive increase of the body roll angle (curve "mod. χ and ω" compared to curve "mod. χ only").

5.4 Influence of the cyclic period and the speed on the stability

The influence of the cyclic period and the speed on the stability was investigated by applying lateral perturbations to walking patterns with respectively:

- a larger of $\hat{T}_{sw}$ (this pattern is referred as (LNG) and $\hat{T}_{sw} = 0.25$ s.)
- a smaller of $\hat{\beta}$ (this pattern is referred as (FST) and $\hat{\beta} = 0.60$)

than the reference walking pattern (referred as (REF)). As represented Figure 5.11, the performances decreased in both cases but for different reasons.

Increasing the walking cyclic period results in the augmentation of the amplitude of the rolling motion, as explained in Section 4.6.1. Hence, the projection of the center of mass of the body during the locomotion gets closer to the line of support defined by the feet of the ipsilateral legs on the side toward which the body is leaning. Consequently, a lower intensity of lateral perturbation is needed to bring it over the line of support, resulting in the fall of the model on the side. Hence, the drop of performances is due to the increase of the rolling motion amplitude.

On the other hand, as the rolling motion amplitude was found to decrease with the speed (see Figure 4.12(e)), the deterioration of the performances in that case must have another reason. As explained in Section 5.2.2, stabilization of the posture in the frontal plane is insured by the automatic adjustment of the relative values of the duty ratios of the right and left legs. In other words, the stance phase durations are adjusted via the phase modulations to compensate the disturbances in the lateral transfer of leg loading resulting from the perturbation of the body rolling motion. However, as the stride length increases with the speed, the influence of the longitudinal transfer of leg loading on the unloading of the legs becomes greater (as explained in Section 4.6.2) and it increasingly interferes with the lateral transfer mechanism in the control of the stance termination of the legs. As a result, it sets a limit to the extension of the stance phase durations of the hind legs (directly) and the forelegs (via the ascending coordination mechanism). Hence, the upper bound of the range of duty ratios that can be realized gets lower and lower. This affects the postural stabilization provided by the phase modulations so that the resistance ability against perturbation consequently decreases with the speed.

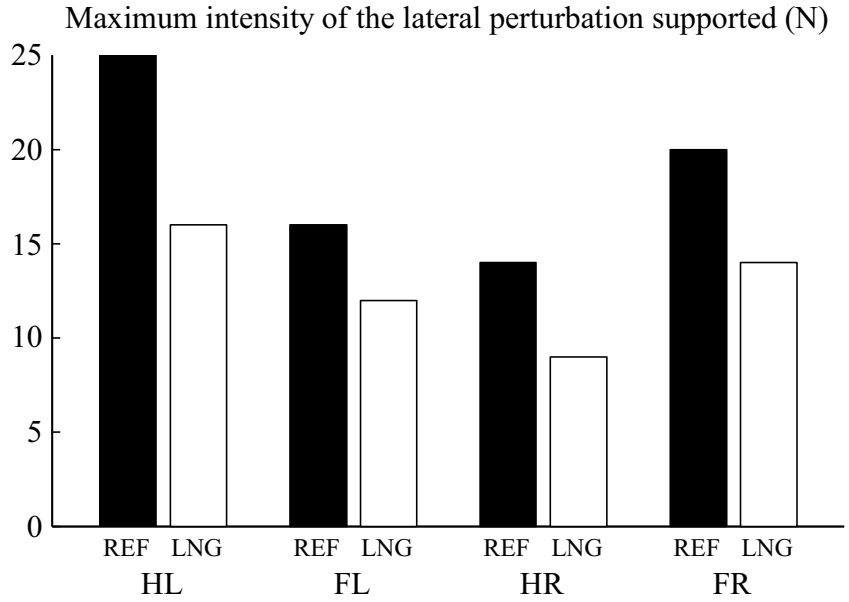

(a) Comparison of the resistance against perturbations of (REF) and (LNG) walking patterns

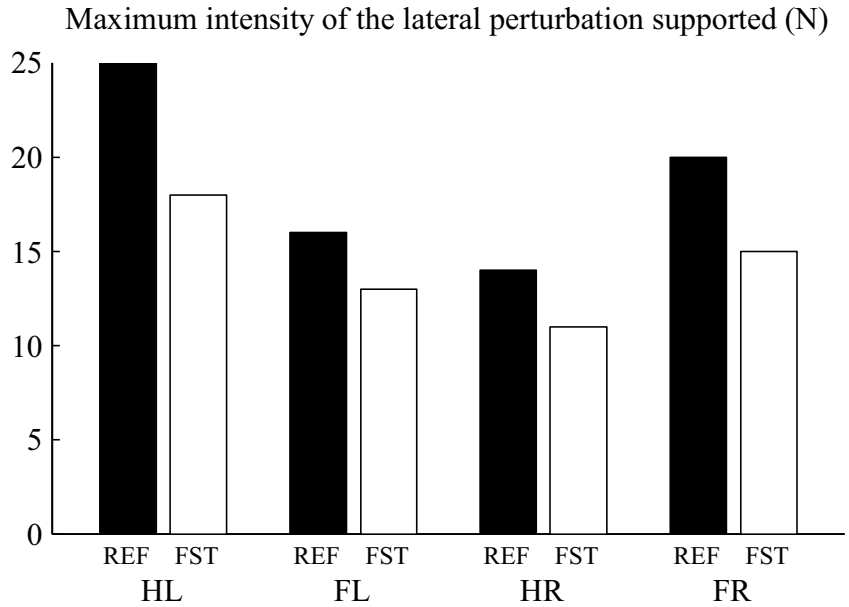

(b) Comparison of the resistance against perturbations of (REF) and (FST) walking patterns

FIGURE 5.11: Influence of the modulations of the cyclic period and the speed on the resistance ability against lateral perturbation

5.5 Performances on uneven terrains

In order to assess in more details the postural stabilization provided by the controller during the locomotion, the performances of the control system were evaluated when coping with two kinds of uneven terrains: elevated steps or slopes (represented in Figure 5.12). In the former case, three situations were considered:

- *hind leg*: the model steps once on an elevated step with its right hind leg
- *foreleg*: the model steps once on an elevated step with its right foreleg
- *lateral step*: the model must walk with both its right legs on a long lateral step

As regards walking on slopes, the situations where the model is walking uphill (*up slope*) or downhill (*down slope*) were investigated.

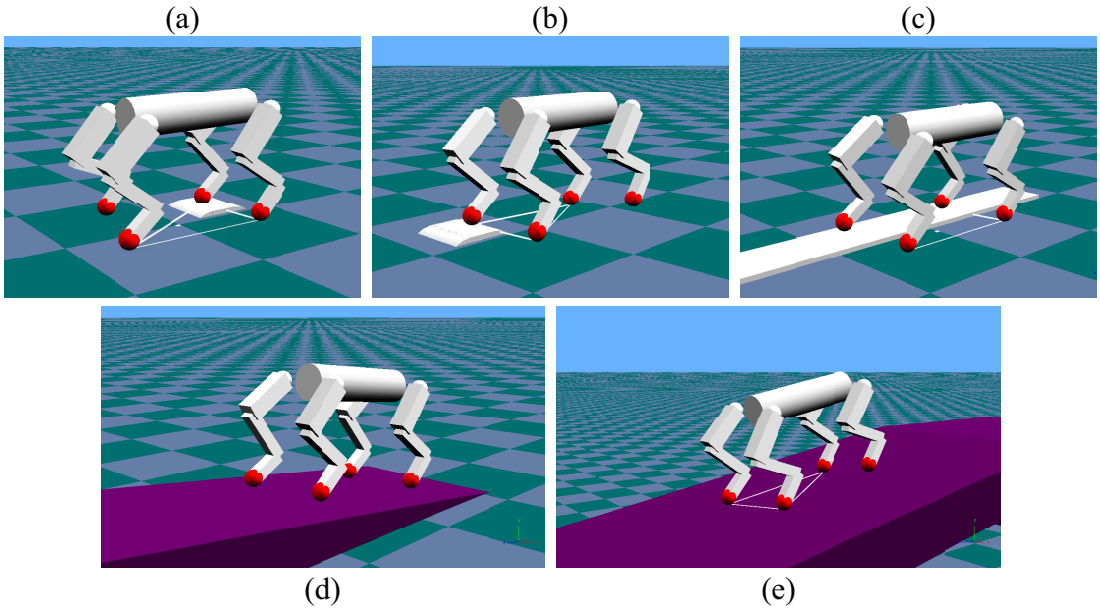

FIGURE 5.12: Types of uneven terrain: (a) hind leg, (b) foreleg, (c) lateral step, (d) up slope, (e) down slope

The performances were evaluated with and without the ascending coordination mechanism, for (REF) and (LNG) walking patterns. The results are summarized in Table 5.2, which gives the maximum height of the step or the maximum inclination of the slope that the model could handle without falling. In the case of the lateral step, the inclination of the lateral slope equivalent to the step was also computed. Globally, the control system is able to handle a certain level of terrain irregularity, both with the reference walking pattern and the walking pattern with a longer cyclic period. As expected, adding the ascending coordination mechanism increases the performances.

TABLE 5.2: Performances on uneven terrain

	(REF)		(LNG)	
Perturbation type	without	with	without	with
Foreleg	16 mm	16 mm	9 mm	10 mm
Hind leg	5 mm	20 mm	12 mm	20 mm
Lateral step	4 mm	14 mm	6 mm	10 mm
(equivalent angle)	1.9 °	6.7 °	2.9 °	4.8 °
Up slope	10 °	10 °	8 °	8 °
Down slope	-6 °	-12 °	-9 °	-10 °

5.5.1 Elevated steps

As regards stepping on elevated steps, walking on the step with the foreleg induced a temporary increase of the rolling motion amplitude so that (REF) performed better than (LNG). On the other hand, walking on the step with the hind leg temporarily decreased the rolling motion amplitude so that performances increased consistently when the ascending coordination mechanism was added.

Dealing with the lateral step caused a prolongated asymmetry in the rolling motion amplitude, leading to a shift of the weight of the body to one side. To compensate, the duty ratios were adjusted by the phase modulations (increased for the left legs and decreased for the right ones). However, when the step was higher than a certain level, the foreleg on left side was overloaded and could not swing anymore. Hence, the performances without the ascending coordination mechanism were relatively poor for both walking patterns and improved greatly when it was added.

5.5.2 Slopes

When walking on an upwards slope, the weight of the body was shifted to the back so that the liftoff of the hind legs was delayed while, for the forelegs, it occurred earlier. Consequently, the gait progressively got closer to a pace as the slope increased. When the slope inclination was greater than a certain value, the liftoff of the forelegs occurred before the one of the hind legs, disrupting the leg coordination and eventually causing the fall of the model.

For downwards slopes, the opposite observations were made, i.e. the liftoff of the forelegs was delayed while the liftoff of the hind legs occurred earlier. As the weight of the body was shifted forward, the load supported by the forelegs during the stance phase increased as the inclination of the down slope increased. When it was higher than a certain value, the transition from stance to swing in the forelegs could not occur anymore without the ascending coordination mechanisms, explaining the gap between the performances with and without it.

5.6 Discussion

5.6.1 Ascending coordination mechanism

Akay et al. (2006)(1) investigated the coordination of fore and hind legs stepping in cats on a transversely-split treadmill. To explain the adaptations of the walking patterns observed when reducing the treadmill speed on which respectively the forelegs or the hind legs were stepping, they proposed that ipsilateral pattern generating networks are asymmetrically coupled via descending inhibitory pathways and an ascending excitatory pathway (see Figure 5.13).

Interestingly, pathway [2] of Figure 5.13 shares similarities with the ascending coordination mechanism introduced in Section 5.3. Both these mechanisms indeed promote the transition to the swing phase in the foreleg when the ipsilateral hind leg is swinging. In Akay et al. study, the role of the this mechanism was investigated from the point of view of leg coordination and its influence on the resistance to lateral perturbations was not investigated. Since sensory signals related to leg loading are known to play an important role in the control of the stance to swing transition in animals (Duysens and Pearson 1980(15) reported for example that the extensor phase is indefinitely prolongated if the force developed by the ankle extensor muscle is over a given threshold), the coordination mechanism might also play a role similar to the one outlined in the experiments reported in this chapter.

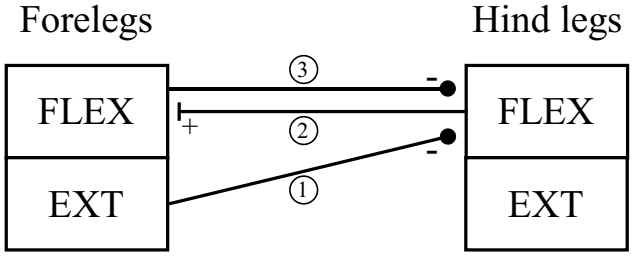

FIGURE 5.13: Proposal for the mechanisms coordinating stepping in the fore and hind legs of walking cats (from Akay et al. (2006)(1)). "*Schematic diagram illustrating an ascending excitatory pathway [2] and a descending inhibitory pathway [3] linking the systems generating flexor bursts in a foreleg and the ipsilateral hind leg, and a pathway inhibiting the system generating the flexor bursts in the hind leg during the extension phase of the foreleg [1].*"

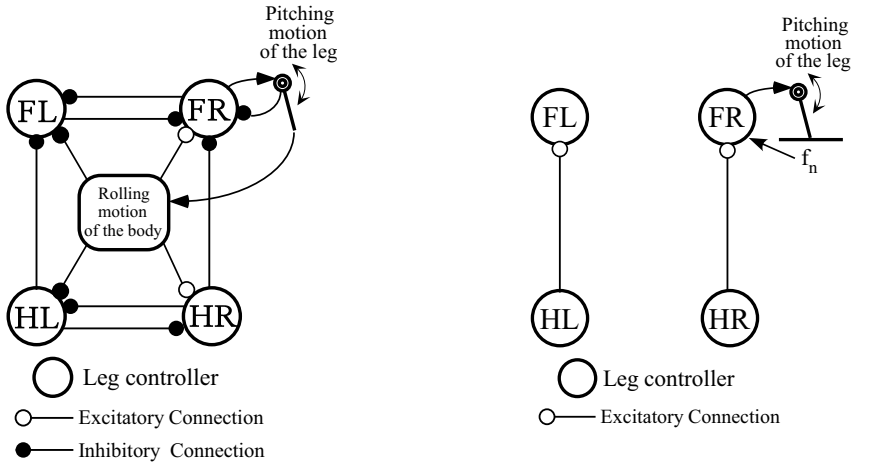

(a) Structure of the controller used in Tekken (modified from Fukuoka et al. (2003)(21))

(b) Structure of the proposed controller

FIGURE 5.14: Comparison between the proposed control system and the one used in Tekken.

5.6.2 Comparison with Tekken

In order to assess the performances of the control system, the comparison with Tekken is used. This choice is justified by the fact that it is rather complicated to compare the performances of different robots because the dimensions of the mechanical model influence the dynamics of the system. However the dimensions of Tekken are rather close to the ones of our model so that it is possible to compare the performances.

As regards the walking cyclic period, walking motions with longer cyclic period could be generated with the proposed control system than the maximum reported in Fukuoka et al. (2003)(21). In animals (Section 3.6.3) as well as in the simulation experiments reported in this thesis (Section 4.6.2), it was found that increasing the walking cyclic period is related with decreasing the walking speed. As explained in Section 1.2.1, at low speed, as Fr is small, postural adjustments become essential to insure the stability during the locomotion. Consequently, it can be advanced that the control system proposed in this thesis, relying on phase modulations based on leg loading information, integrates posture control to a greater extent than the controller used in Tekken. Performances on the types of rough terrain considered are comparable to those of Tekken (10 $^\circ$ of inclination for up and down slopes and 5 $^\circ$ of inclination for lateral slopes).

Regarding the structure of the controller:

- the walk gait could be realized with a simpler architecture than in Tekken (see Figure 5.14). The feedback of the leg loading information (f_n) to the leg controllers at the local level to regulate the phase transitions allows for much more

independence of the leg controllers. In particular, the strong inhibitory connections between contralateral legs are not needed anymore as left-right alternate coordination naturally emerges (Section 4.5). Moreover, feedback of the body rolling motion is no longer required as the stabilization is provided by the phase modulations and the ascending coordination mechanism.

- the trot gait could not be realized using the proposed control system. As presented in Section 4.6.2, increasing the walking speed results in the augmentation of the phase difference from the hind to the foreleg γ, hence the gait gets closer to the trot. However, when it reaches a certain threshold, γ starts to drift toward 0.5, with the gait switching to a trot, then the gait becomes unstable, resulting in the fall. This seems to indicate that the phase modulations only are not able to stabilize a trot gait. On the other hand, in the case of Tekken, this kind of gait could be realized by increasing the walking speed via the setting of a more posterior position as the reference for the hip angle during the stance. As it was observed (like in our experiments) that the amplitude of the body rolling motion decreased with the speed, the influence of the feedback of this sensory information on the CPG output was much reduced. Consequently, it can be concluded that a network of inhibitory connections between the leg controllers, a feature that was implemented in Tekken's control system but is absent in the controller proposed in this thesis, is likely to play a great role for the generation and stabilization of the trot gait.

5.7 Summary

In this chapter, the resistance ability of the walking patterns generated by the control system against perturbations was evaluated. First, the role of the phases modulations based on leg loading information was assessed by using a condition based on the leg controller phase to trigger the transition from stance to swing. This resulted in the incapacity for the controller to properly compensate the asymmetry of the body rolling motion caused by the perturbation. As a consequence, small intensities of lateral perturbation led to the disappearance of the walk gait coordination.

In contrast, when the transition condition based on leg loading information is used, asymmetry in the rolling motion amplitude results in an adjustment of the respective duty ratios of the legs on the right and left sides due to the modulation of the stance phase duration. This generates a recovery force that compensates the asymmetry and restores the posture through phase modulations. When applying a lateral perturbation at various timings during the walking cycle, it appeared that the control system with independent leg controllers was quite resistant to perturbations increasing the rolling motion amplitude, hence accelerating the lateral transfer of leg loading. In that case,

the controller was able to reject the perturbation within a few steps, thanks to the phase modulations. On the other hand, when the applied perturbation resulted in the decrease of the rolling motion amplitude, the lateral transfer of leg loading was slowed down. When the perturbation was over a certain threshold, the load supported by the foreleg did not become smaller than the threshold regulating the stance-to-swing transition, so that the foreleg could not swing. This perturbed the leg coordination, often leading to the fall of the model.

Consequently, an ascending coordination mechanism that promotes the transition to the swing phase in the foreleg when the ipsilateral hind leg is swinging, while reducing the duration of the subsequent foreleg swing phase, was implemented. It improved considerably the resistance ability of the control system against perturbations decreasing the rolling motion amplitude while preserving the good performances obtained in the other cases.

The influence of the walking cyclic period and speed on the stability was investigated and, in both cases, the stability was found to decreases. As the cyclic period increases, the rolling motion amplitude becomes larger so that the model falls more easily on the side when laterally perturbed. As regards the increase of the speed, the longitudinal transfer of leg loading mechanism increasingly interferes with the lateral transfer mechanism in the control of the stance termination of the legs, hence limiting the extent of the duty ratios adjustments that can be achieved.

With the proposed control system, the model could stably walk on terrains of medium degree of irregularity (including steps and slopes), demonstrating the achievement of a certain level of postural control.

Chapter 6

Conclusions

6.1 Conclusions

This thesis considered the use of phase modulations based on leg loading information in a CPG controller to generate stable quadrupedal dynamic walk. Phase modulations are adjustments of the CPG activity resulting from the modulation of the respective durations of the stance and swing phases of the stepping motion. In this thesis, the stress was put on the role of the regulation of the stance to swing transition by the leg loading sensory information. The contribution of this mechanism to rhythmic motion control and posture control during locomotion in the range from low- to medium-speed was investigated using dynamics simulations.

These issues were considered both in the case of two-dimensional stepping, with the motion in the frontal plane prevented, and three-dimensional dynamic walking. Although the implementations of the control systems used in each situation are quite different, both of them are grounded on the same common principles. In agreement with the objectives of this thesis, the transitions between the swing and the stance phases of the leg controller are regulated using leg loading sensory information. This, together with other considerations about adaptability, motivated the choice of a sensor-dependent CPG model.

A biologically-inspired approach was used to generate two-dimensional stepping with musculoskeletal models faithful to the anatomy of the cat. A neural controller able to induce adaptive stepping at various walking speeds with that model was developed in agreement with the common principles. Two-dimensional alternate stepping at constant speed with the fore and the hind legs separately was realized using independent leg controllers. The contribution of the control of the stance-to-swing transition using leg loading information to the emergence and the stabilization of the alternate coordination was explained and verified. Finally, adaptive stepping at various walking speeds with the

hind legs was realized and the adaptations of the stepping patterns that occurred in the simulations were compared with the ones happening in real animals. Similar tendencies were found and an interesting conclusion about the role of leg-loading-information-based regulation of the stance-to-swing transition in animals was drawn accordingly.

Limitations related to the complexity of the neural controller implementation became evident when trying to extend the control system architecture to generate walking patterns in three dimensions. Accordingly, a more traditional approach, combining trajectory generation and local PD control, was substituted to the muscular model and the synergies for the generation of the motor patterns, resulting in a great simplification of the leg controller structure. Using phase modulations based on leg loading information, left-right alternate stepping coordination naturally emerges as a consequence of the entrainment between the stepping of the legs, the body rolling motion and the phase modulations. The vertical coordinate of the AEP position, as well as the PD control gains of the knee and ankle joints, were found to influence the emergent gait. Appropriate setting of these two categories of parameters resulted in the emergence of a walking gait that could be generated with independent leg controllers. Walking patterns could be realized in a broad range of cyclic periods and speeds by adjusting only a few number of the controller parameters.

Next, the stability of the walking patterns was investigated using lateral perturbations. Phase modulations could stabilize the disturbed posture subsequent to the application of a perturbation at all the timings considered, except when the perturbation resulted in a reduction of the modulus of the next extremum of the body roll angle, hence slowing down the lateral transfer of leg loading that occurs during left-right alternate stepping. As a consequence, the foreleg on the loaded side could not swing anymore. An original ascending coordination mechanism was implemented, preventing this situation and contributing to the global stabilizing action of the phase modulations. After the addition of this mechanism, the control system achieved good performances for all the perturbation application timings. Moreover, the model could walk on terrains with a medium level of irregularity both with short (around 0.40 s) and long (around 0.63 s) cyclic periods.

In conclusion, the work presented in this thesis supports the evidence that phase modulations based on leg loading information, and in particular the regulation of the transition from stance to swing using this sensory information, plays a great role in rhythmic motion control and posture control during the locomotion. This mechanism contributes to the emergence and the stabilization of alternate stepping coordination in two-dimensional stepping and left-right alternate stepping in quadrupedal dynamic walk, so that locomotion can be generated even with independent leg controllers in both cases. Regarding quadrupedal dynamic walk, phase modulations adjust the rhythmic motion of the legs to stabilize the rolling motion of the body against various disturbances. To cope with

perturbations slowing down the lateral transfer of leg loading, against which the performances realized by the phase modulations mechanism alone were relatively low, an additional coordination mechanism, promoting stance-to-swing transition in the foreleg when the ipsilateral hind leg is swinging, was implemented. With that additional mechanism, the control system was able to tackle terrain irregularities (such as steps and slopes) while stabilizing the posture, hence demonstrating basic integration of posture and rhythmic motion controls. As using phase modulations based on leg loading information allows to make use of the embodiment for walking (such as the alternate stepping of the legs and rolling motion of the body), this could be realized with a simple and distributed control system.

6.2 Future work

Future efforts will at first be concentrated on the design and the realization of a robotic platform allowing to implement and test the control system developed in simulation in this thesis.

Another interesting issue to consider in future work is the energy efficiency of the walking patterns generated by the control systems developed in this thesis. It is commonly accepted that animals tend to minimize the energy consumption during locomotion. Hence, it would be interesting to investigate this topic in the two-dimensional case, where musculoskeletal models are used, by using a model of the physiological cost associated with the generation of the muscular force. Moreover, the optimization of the energy efficiency is also worth to consider in the three-dimensional case, as that issue will have a great influence on the autonomy of the robot.

Finally, on the basis of the results presented in this study, the contribution to the posture and rhythmic motion controls of additional mechanisms could be investigated. These include for example:

- postural adjustment mechanisms at the motor command generation level, such as the leg stiffness or leg length adjustments during the stance phase, based on leg loading or vestibular sensory information;
- hip joint around the roll axis that would allow to implement the sideway stepping reflex and study the contribution abduction/adduction motions of the hips during the locomotion;
- flexible or articulated spine.

Appendix A

Musculoskeletal Models

A.1 Skeletal systems

The detail of the two skeletal models used in the two-dimensional experiments are represented in Figure A.1, dimensions and the masses of the bodies that compose both of them are listed in Table A.1. In that table, L is the length of the body in the sagittal plane, l_1 the width of the body along x axis and l_2 is the remaining dimension. For cylindrical bodies, R is the radius of the section. The mass m of each body is computed by multiplying the volume by the density which was fixed to 2500 kg/m^3 for all of them, except for the spine (s) and the pelvis (p) of the simplified hind legs model where it was set to 4000 kg/m^3.

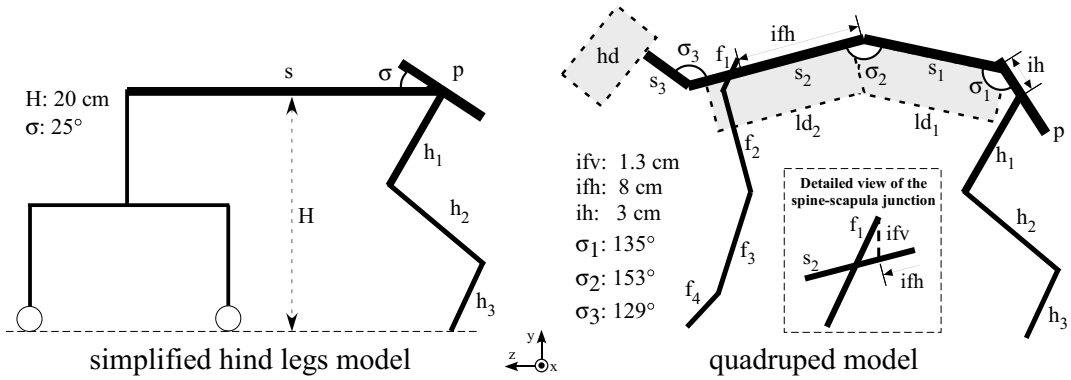

FIGURE A.1: Skeletal models

TABLE A.1: Dimensions and masses of the bodies that compose the skeletal models

Simplified Hind Legs Model

body	L (cm)	l_1 (cm)	l_2 (cm)	m (g)
s	25	4	2	800
p	8	10	4	1280
h_1	9	3	3	202.5
h_2	10	2	2	100
h_3	6	2	2	60

Quadrupedal Model

body	L (cm)	l_1 (cm)	l_2 (cm)	m (g)
s_1	11.5	2	2	115
s_2	14.5	2	2	145
s_3	4.3	2	2	43
p	7	8	2	210
h_1	9	3	3	202.5
h_2	10	2	2	100
h_3	6	2	2	60
f_1	3	2	2	30
f_2	8.5	2	2	85
f_3	8.5	2	2	85
f_4	3.5	2	2	35
body	L (cm)	R (cm)		m (g)
ld_1	11.5	2		361
ld_2	12	2		377
hd	7	2		220

A.2 Muscular systems

A.2.1 Muscle model

The muscle force is calculated using the model of Brown et al. (1996)(8). The muscle fascicles are modeled as active contractile elements (CE) in parallel with passive elastic elements (P). The force generated by the contractile elements, referred by F_{CE}, is the product of two functions: the force-length dependence F_L and the force-velocity dependence F_V. The contribution of F_{CE} to the total force generated by the muscle is scaled by the muscular activation level a_m (output by the motor neurons of the neural controller) and added to the fixed contribution of the passive elastic elements F_P, to give the total force output by the muscle f_m, as in the following equation (for muscle

m):

$$f_m = f_m^{max} \cdot (a_m F_{CE}(x_m, v_m) + F_P(x_m)) \tag{A.1}$$
$$= f_m^{max} \cdot (a_m F_L(x_m) F_V(x_m, v_m) + F_P(x_m)) \tag{A.2}$$

where f_m^{max} is the maximum *isometric force*[1] of muscle m, while x_m and v_m are the length and contraction speed of the muscle, normalized with respect to L_0 (the length where F_L is equal to 1). The contraction speed v_m is defined in such a way that it is positive when the muscle lengthens and negative when the muscle shortens.

The force-length dependence function F_L is given by:

$$F_L(x) = e^{-\left|\frac{x^\beta - 1}{\omega}\right|^\rho} \tag{A.3}$$

while the force-velocity dependence F_V is:

$$F_V(x, v) = \begin{cases} \frac{b_1 - a_1 v}{v + b_1} & \text{if } v \leq 0 \text{ (shortening)} \\ \frac{b_2 - a_2(x) v}{v + b_2} & \text{if } v > 0 \text{ (lengthening)} \end{cases} \tag{A.4}$$

and the force generated by the passive elastic elements F_P:

$$F_P(x) = c_1 \cdot k_1 \cdot ln\left(e^{\frac{x - L_1}{k_1}} + 1\right) + c_2 \cdot (e^{k_2(x - L_2)} - 1) \tag{A.5}$$

The values of the parameters for these equations are summarized in Table A.2.

TABLE A.2: Parameter values for functions F_L, F_V and F_P of the muscle model.

Function	Parameters values		
F_L	ω	β	ρ
	1.26	2.30	1.62
F_V	b_1	a_1	b_2
	-0.69	0.17	0.18
		a_1	
		$-5.34x^2 + 8.41x - 4.70$	
F_P	c_1	k_1	L_1
	70.00	0.05	1.40
	c_2	k_2	L_2
	-0.020	-18.70	0.79

[1]Force output during isometric contraction, i.e. contraction during which the length of the muscle is not allowed to shorten

Using this model, f_m can become negative if the length of the muscle is too small. In reality of course, this does not happen because the muscle and the tendons that connect it to the skeleton are flexible and bend when the tension is too small. To avoid that, f_m is set to 0 when the value given by the muscle model is negative.

Each muscle of the muscular system is individually characterized by an additional set of parameters that allows to fit the general model to the muscle properties. These parameters include f^{max} and L_0 that were mentioned above, as well as the parameters that specify how the muscle is inserted to the skeleton, i.e. how the muscle interacts with the motion of the joint(s) that the muscle actuates. These latter parameters are the ratios of the joint angle rotation versus the variation of the muscle length (referred as r) and the lever arms (referred as l). Each couple (muscle m , joint j) is associated with a specific couple (r_{mj} , l_{mj}).

For the sake of simplicity, Ekeberg and Pearson (2005)(17) defined their model by setting the relative length of all the muscles in a particular configuration called *neutral posture* where all the joints are in their *neutral position* and the muscles have their *neutral length*. $\theta_{j,0}$ and $x_{m,0}$ represents respectively the angle of joint j at its neutral position and the relative length of muscle m when all the joints of the leg are in their neutral positions. Accordingly, at each step of the simulation, the state of each muscle is updated as following:

$$x_m = x_{m,0} + \sum_j s_{mj} r_{mj}^{-1} (\theta_j - \theta_{j,0}) \tag{A.6}$$

$$v_m = \sum_j s_{mj} r_{mj}^{-1} \dot{\theta}_j \tag{A.7}$$

where s_{mj} is a factor depending on the way the muscle is related to the joint:

$$s_{mj} = \begin{cases} 1 & \text{if } \Delta\theta_j > 0 \text{ leads to the } \textit{lengthening} \text{ of muscle } m \\ -1 & \text{if } \Delta\theta_j > 0 \text{ leads to the } \textit{shortening} \text{ of muscle } m \\ 0 & \text{if joint } j \text{ and muscle } m \text{ are } \textit{unrelated} \end{cases} \tag{A.8}$$

The total torque generated at joint j is then computed:

$$\Gamma_j = \sum_i -s_{mj} \cdot l_{mj} \cdot f_m \tag{A.9}$$

A.2.2 Parameters of the fore and hind legs muscular systems

The parameters for the hind legs muscular system are taken from Ekeberg and Pearson (2005)(17), except for the neutral length of PB and the hip neutral angle. The upper part of Figure A.2 gives the definitions of the joint angles. The neutral angles for the

hip, knee and ankle joints are respectively θ_1=60 $^\circ$, θ_2=100 $^\circ$ and θ_3=105 $^\circ$. The other parameters are summarized in Table A.3.

For the forelegs, the lower part of Figure A.2 represents the definitions of the joint angles. The neutral angles for the shoulder, elbow and wrist are respectively θ_1=110 $^\circ$, θ_2=120 $^\circ$ and θ_3=200 $^\circ$, while the fixed angle α between the spine and the scapula is set to 50 $^\circ$. The other muscular system parameters are given in Table A.4.

TABLE A.3: Values of the parameters of the hind legs muscular system

	f^{max} (N)	x_0 (%)	joint (j)	s_{mj}	l (mm)	r (%/ $^\circ$)
IP	333	0.85	hip (1)	1	12	1/2
AB	333	0.85	hip (1)	-1	12	1/2
PB	167	0.85	hip (1)	-1	12	1/2
			knee (2)	1	12	1/2
VL	333	0.85	knee (2)	-1	9	1/2
Gas	200	0.75	knee (2)	1	5	1/4.5
			ankle (3)	-1	15	1/1.5
Sol	167	0.85	ankle (3)	-1	15	1/2
TA	100	0.85	ankle (3)	1	9	1/2

TABLE A.4: Values of the parameters of the forelegs muscular system

	f^{max} (N)	x_0 (%)	joint (j)	s_{mj}	l (mm)	r (%/ $^\circ$)
BC	167	0.90	shoulder (1)	-1	12	1/2.5
LD	333	0.80	shoulder (1)	1	12	1/2.5
B	333	0.85	elbow (2)	1	9	1/2
T	333	0.85	elbow (2)	-1	9	1/2
WF	20	0.85	wrist (3)	-1	9	1/4

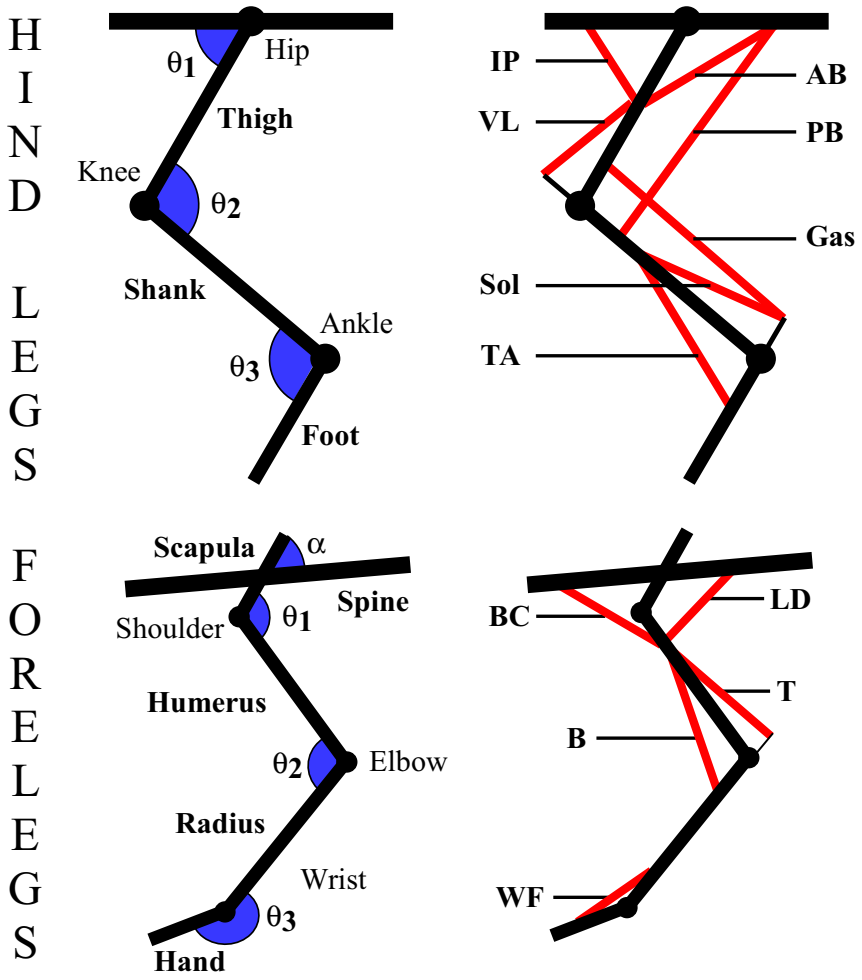

FIGURE A.2: Definition of the joint angles and representation of the muscular systems for the fore and hind legs. In the case of the hind legs, the hip angle is defined on one hand by the thigh segment and, on the other hand, by the spine segment (for the simplified hind legs model) or the line joining the spine-pelvis junction point and the attachment point of the scapula (for the quadrupedal model).

Appendix B

Neural leg controller: implementation details

B.1 Neuronal models

B.1.1 Interneurons (I)

This neuron model is a modified version of the interneuron type used in Wadden and Ekeberg (1998)(62) to design their NPG. It represents a population of functionally similar neurons and its output is the mean firing frequency of the population. It is basically a "leaky integrator" with a saturating transfer function whose output value varies between 0 and 1 (the maximum firing rate). Each neuron is characterized by three parameters: the time constant (τ), the gain (Γ) and the activation threshold (Θ). The main feature of this model is that the excitatory and inhibitory synaptic inputs are handled separately (using the presynaptic inputs from sets Υ_+ and Υ_- respectively):

$$\dot{\xi}_+ = \frac{1}{\tau}\left(\sum_{i\in\Upsilon_+} u_i w_i - \xi_+\right) \tag{B.1}$$

$$\dot{\xi}_- = \frac{1}{\tau}\left(\sum_{i\in\Upsilon_-} u_i w_i - \xi_-\right) \tag{B.2}$$

where w_i is the synaptic weight of the connection i and u_i the output value from the corresponding presynaptic neuron. We added two features to the original model: saturation of the inhibitory synaptic input ($\xi_- \leq 1$) and resetting of ξ_+ to 0 when the neuron is completely inhibited ($\xi_- = 1$). ξ_+ and ξ_- are recombined to generate the output:

$$u = \begin{cases} 1 - \exp\{(\Theta - \xi_+)\Gamma\} - \xi_- & \text{if positive} \\ 0 & \text{otherwise} \end{cases} \tag{B.3}$$

For the interneurons of the PFCM, this was replaced by the following simpler linear model:

$$u_{lin} = \begin{cases} min((\xi_+ - \Theta)\Gamma, 1) - \xi_- & \text{if positive} \\ 0 & \text{otherwise} \end{cases} \quad \text{(B.4)}$$

B.1.2 Sensory neurons (SN)

This neuronal model is used for the transduction of the sensory signals involved in the sensory feedbacks to the NPG and the MOSS. It is similar to the model of interneurons, except for two features. First, the excitatory synaptic input is function of s (the sensory signal) and $\dot{s}$ (its derivative, if available). Second, the output function is simpler (similar to u_{lin} of Equation B.4).

$$\dot{\xi}_+ = \frac{1}{\tau}\left(K_p(s - s_{off}) + K_v\dot{s} - \xi_+\right) \quad \text{(B.5)}$$

$$u_{SN} = \begin{cases} min(\xi_+, 1) - \xi_- & \text{if positive} \\ 0 & \text{otherwise} \end{cases} \quad \text{(B.6)}$$

where s_{off} is an offset value. Currently, four kinds of sensory information s coming from the musculoskeletal model are available to the LC: the force f_m, the length x_m and the contraction speed v_m of each muscle, as well as contact with the ground status for each leg. Two main types of sensory neurons are used in the NPG and MOSS: one using the length and contraction speed of the muscle (i.e $s = x_m$ and $\dot{s} = v_m$) and the other using the force output by the muscle (i.e $s = f_m$). The sensory neuron handling a sensory signal s will be noted SN_s.

B.1.3 Motor neurons (MN)

Motor neurons simply output the sum of the presynaptic inputs (if positive).

$$\xi_+ = \sum_i u_i w_i \quad \text{(B.7)}$$

$$u_{MN} = max(\xi_+, 0) \quad \text{(B.8)}$$

Each muscle m corresponds to one motor neuron MN_m and its output (u_{MN}) is used as the muscular activation level a_m of Equation 3.1.

B.1.4 Variable gain neurons (VG)

Variable gains are building units used to modulate the intensity of the contribution of the sensory feedback pathways to the generation of muscular activation levels. Each of them has two input channels: the first one for the signal ($CH1$) and the second for the

gain intensity ($CH2$). All inputs to the same channel are summed up and the output of the neuron is the product of the two channels:

$$u_{VG} = \sum_{i \in CH1} u_i * \sum_{j \in CH2} u_j \tag{B.9}$$

B.1.5 Tonic input neurons (TI)

These neurons output a constant value.

B.1.6 Initiation and termination units (ITU)

Although this is not strictly speaking a neuronal model but rather an abstract logical unit, the ITU is mentioned in this section as it is one of the building blocks of the neural controller. One ITU is associated with each synergy and is responsible for regulating the activity of this latter through inhibitive connections to all the IM_m and SN_s neurons, so that they cannot activate, except when the output of the ITU is zero. This happens only in two situations:

- the ITU is not active (input from TI is less than 0.5).
- the ITU is active (input from TI greater than 0.5), not inhibited (input from IP is zero) and the initiation condition is fulfilled but not yet the termination condition.

The initiation and termination conditions are either a time condition (a timer is started when inhibition from IP neuron disappears) or a condition on a sensory event (input value coming from a specific SN neuron is greater or not than a certain threshold).

B.2 NPG

B.2.1 Biological groundings of the NPG structure

The design of the NPG structure and the choice of the sensory signals used to trigger the phase transitions are grounded on the following biological facts:

- *After deafferentation, oscillatory patterns of extensor and flexor muscular activity still occur under pharmacological excitation* (Grillner and Zangger 1974(23)): as explained in Section 3.4.2.1, even without sensory feedback, transitions between modules can occur in our model if the synaptic weight of the connections between H and T_1 neurons are high enough to activate T_1, resulting in oscillatory patterns of activity of the flexor and extensor phases.

- *Transition from stance to swing is prevented as long as the hip angle is lower than a given threshold* (Grillner and Rossignol 1978(24)): in the condition stated above, as the intrinsic excitation from H_E to T_{E1} is too weak to evoke the transition, the excitatory input due to the PEP feedback (through PF_E) is really responsible for T_{E1} activation.

- *The extensor phase is indefinitely prolongated if the force developed by the ankle extensor muscle is over a given threshold* (Duysens and Pearson 1980(15)): as long as the leg is loaded, T_{E2} is inhibited by the feedback of leg loading (LL) information (through NF_E), which prevents the transition to the flexor phase.

B.2.2 NPG Parameters

This section provides the values of the NPG parameters used for both the hind and forelegs LC in the experiments reported in Chapter 3. Values of the parameters of the NPG interneurons and sensory neurons are given in Tables B.1 and B.2 respectively. On the other hand, the values of the connection weights between the neurons are listed in Table B.3.

TABLE B.1: Values of the NPG interneurons parameters. Subscripts E and F refer to the extensor and flexor modules respectively. The values of the parameters are slightly modified from Wadden and Ekeberg (1998)(62).

Neuron	Θ	Γ	τ (ms)
$H_{\{E,F\}}$	0.1	1	10
$Q_{\{E,F\}}$	0.5	0.2	10
$T1_F$	1	0.5	50
$T1_E$	1	0.5	100
$T2_{\{E,F\}}$	0.1	1	10
$IP_{\{E,F\}}$	0.1	1	5

TABLE B.2: Values of the NPG sensory neurons parameters of the hind legs LC (top table) and forelegs LC (bottom table). Subscripts E and F refer to the extensor and flexor modules respectively. The threshold for f_{Sol} is the same as in Ekeberg and Pearson (2005)(17), while all the other parameters were deducted by trial and error.

Neuron	s	s_{off}	K_p	K_v	τ (ms)
PF_E	x_{IP}	0.8	5	0	5
NF_E	f_{Sol}	5	1	0	5
PF_F	x_{AB}	0.6	5	0	5
NF_F	x_{AB}	0.9	-20	0	5
Neuron	s	s_{off}	K_p	K_v	τ (ms)
PF_E	x_{BC}	0.7	5	0	5
NF_E	f_T	5	1	0	5
PF_F	x_{LD}	0.7	5	0	5
NF_F	x_{LD}	0.9	-20	0	5

TABLE B.3: Values of the synaptic weights of the connections represented on Figure 3.4. The first column (O) gives the neuron origin of the connection, while the second one (D) is its destination. (i) means that the destination neuron belongs to the same module as the origin neuron, while (c) means that it belongs to the other one. Finally, w is the synaptic weight of the connection. (E) and (F) refer to the extensor and flexor modules respectively.

O	D		w	O	D		w
H	H	(i)	4.0	T_2	H	(i)	-2.0
	Q	(i)	4.0		Q	(i)	-3.0
	T_1	(i)	1.0		H	(c)	3.0
	IP	(i)	-2.0	IP	PF	(i)	-2.0
Q	H	(c)	-5.0	PF	T_1	(i)	1.5 (E)
	T_1	(c)	-5.0				2.0 (F)
	T_2	(c)	-5.0	NF	T_2	(i)	-1.5
T_1	T_2	(i)	5.0				

B.3 MOSS

B.3.1 Synergy implementation

The neural circuit used for the implementation of one synergy can be decomposed in three functional components (as illustrated in Figure B.1):

[A] is responsible for the initiation and termination of the synergy. It is made of one ITU (see Appendix B.1.6). When the corresponding NPG module is inactive, the input from IP neuron inhibits the ITU and, as a consequence, the ITU inhibits the IM_m neurons in [B] and SN_s neurons in [C]. When the NPG module becomes active, IP is inhibited and its inhibitory influence on the ITU is released. When the initiation condition is fulfilled, output from ITU becomes zero until the fulfillment of the termination condition, hence allowing the neurons in [B] and [C] to be active during this interval.

[B] is the part of the synergy that generates the feed-forward component of the muscular activation level patterns. This is given by the activity level of the IM_m neurons. These neurons receive excitatory inputs from two sources: a constant input from the local TI neuron (weighted by the $w_{TI\_IM_m}$) and a variable input depending on the desired propulsive force from the interneurons of the PFCM (weighted by the $w_{IN_j\_IM_m}$) if implemented.

[C] regroups the sensory feedback pathways. Each pathway involves two neurons: a SN_s neuron responsible of the sensory signal transduction and a VG_{s_m} neuron which modulates the intensity of the signal transmitted to the motor neuron MN_m. The VG_{s_m} neurons output represents the feedback component of the muscular activation level patterns. As in the case of [B], the gains of the VG_{s_m} are set by the constant input from the local TI neuron (weighted by the $w_{TI\_VG_{s\_m}}$) and the variable input from the interneurons of the PFCM (weighted by the $w_{IN_j\_VG_{s\_m}}$) if implemented. As an illustration, the detailed structure of this part in the case of the stance synergy for the hind legs is presented in Figure B.2.

On Figure B.1, all the connections between TI neuron and the IM_m and VG_{s_m} neurons are represented, while, in reality, only a limited number of them has a synaptic weight different from zero (this applies for the connections coming from the PFCM as well). The IM_m neurons and VG_{s_m} neurons (for all s) of all the synergies are connected to the corresponding motor neuron MN_m of muscle m which sums all the contributions and output the muscular activation levels a_m(see Figure 3.3). Even if this implementation of a synergy is extremely basic (the feed-forward muscles activation levels are constant and all the muscles involved in a synergy are activated and deactivated simultaneously), this was sufficient for our purposes.

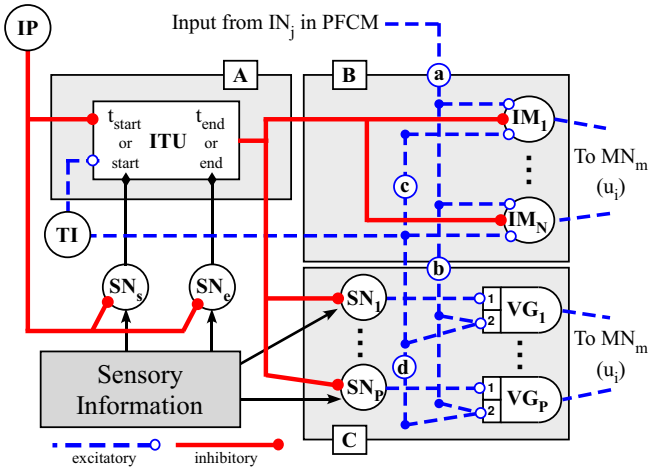

FIGURE B.1: Synergy structure. [A]: Initiation and termination part. [B]: Feed-forward part. [C]: Feedback part. The connections (a), (b), (c) and (d) are respectively the connections from the PFCM to the IM_m neurons (weighted by the $w_{IN_j\_IM_m}$), from the PFCM to the VG_{s_m} neurons (weighted by the $w_{IN_j\_VG_{s\_m}}$), from TI to the IM_m neurons (weighted by the $w_{TI\_IM_m}$) and from TI to the VG_{s_m} neurons (weighted by the $w_{TI\_VG_{s\_m}}$). Although all the connections are represented on this figure, in general only a limited number of them has a synaptic weight that is not zero (see Tables B.7, B.8 and B.10 for example).

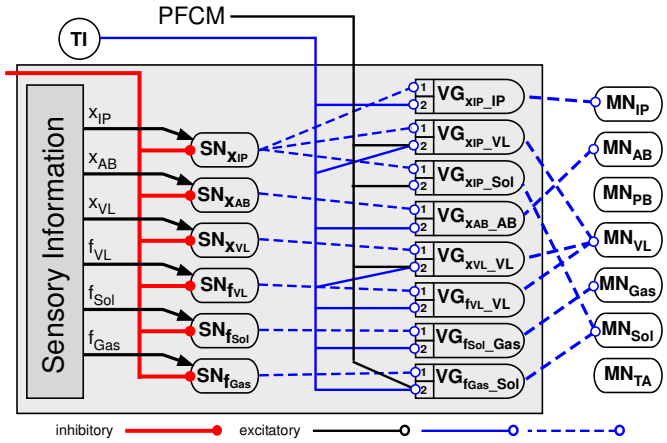

FIGURE B.2: Detailed view of the structure of the sensory feedback pathways (part [C] in Figure B.1) implemented in the stance synergy for the hind legs. These are detailed in Table B.6. Different pathways can share the same sensory neuron ($SN_{x_{IP}}$ for example).

B.3.2 Muscles activated during each synergy

B.3.2.1 Liftoff

For the hind legs, only PB is activated to induce flexion of the knee joint. On the other hand, for the forelegs, activation of B must be accompanied by a simultaneous activation

of LD because an additional extension of the shoulder is needed to allow the elbow to bend with having the hand touching the ground.

B.3.2.2 Swing

For the hind legs, IP is activated to induce hip flexion, as well as TA in order to allow for bigger toes clearance by flexing the ankle. The motion of the knee during the swing (the flexion initiated during the liftoff and its later extension) is essentially passive. However, in order to slow down the extension of the knee at the end of the swing, PB needs to be activated (if the activation is too low, the movement of the leg results in a kick motion and, consequently, the knee is too much extended at touchdown). This is the role of the sensory feedback pathway $x_{PB} \rightarrow PB$. As the leg approaches the AEP, the activation of TA has to be decreased to prepare for landing. This is done by the pathway $x_{PB} \rightarrow TA$.

Similarly, for the forelegs, BC is activated to induce shoulder flexion, while activation of B is bending the elbow. As the leg is getting close to the AEP, activation of LD (pathway $x_{LD} \rightarrow LD$) contributes to slow down the extension of the shoulder and stabilize it through coactivation with its antagonist BC(pathway $x_{LD} \rightarrow BC$, in addition to the FF activation). The elbow is progressively extended by reducing B activation (pathway $x_{LD} \rightarrow B$) while increasing the one of T (pathway $x_{LD} \rightarrow T$). Finally, WF is activated as well around the end of the swing to stabilize the ankle and and keep it in an flexed position.

B.3.2.3 Touchdown

Various muscles are activated to set and stabilize the position of each joint during the touchdown synergy.

For the hind legs, this includes the activation of IP in order to prevent the leg to have a too backward landing position and TA to set the landing position of the ankle. Gas is also activated as TA antagonist to stabilize the ankle joint position, but also to limit the extension motion of the knee, induced by the gravity. It is helped in this later task by the feedback-induced activation of PB (pathway $x_{PB} \rightarrow PB$).

For the forelegs, all the muscles are activated in a feed-forward way, except LD which is activated by the sensory feedback pathway from x_{LD}.

B.3.2.4 Stance

During the stance synergy, all the extensors are activated in a feed-forward way (AB, VL, Gas and Sol for the hind legs and LD and T for the forelegs) and/or by one or

more of the sensory feedback pathways implemented in that synergy. At the end of the stance, hip and shoulder flexor muscles are progressively activated to prevent the body to fall forward too fast (hence helping to regulate the speed) and, for the hind legs, to allow for efficient forward trust by the muscles of the knee and ankle joints (pathways $x_{IP} \rightarrow IP$ and from $x_{BC} \rightarrow BC$). For the forelegs, this is accompanied by the simultaneous decrease of activation of the shoulder extensor (pathway $x_{BC} \rightarrow LD$). Remaining feedback pathways of the stance synergy can be subdivided in three functional groups.

• *AB stretch feedback* (hind legs only): In the muscular activation patterns found in the literature, the activation level of AB is usually set constant during the stance and increased to increase the speed. However, using this approach, the speed could not be decreased under a certain lower limit (around 0.4-0.5 m/s) because, in that case, AB does not provide enough torque to overcome the braking torque induced by gravity just following the touchdown. As a consequence, the leg is stuck and the body falls backwards. This can be overcome if an additional muscular activation is provided at the beginning of the stance to compensate the gravity. Therefore, a sensory feedback pathway relying on AB length and contraction speed was introduces, which provides an additional activation of AB at the beginning of the stance (pathway $x_{AB} \rightarrow AB$). Dependence upon muscle contraction speed implies that the contribution of this feedback progressively vanishes as the walking speed increases, so that the traditional constant activation profile is obtained at higher speed.

• *Load compensation feedbacks* (both hind and forelegs): The feedbacks of the second group help to support the body weight and contribute to stabilize the posture. For the hind legs, this includes three muscle force feedback pathways ($f_{VL} \rightarrow VL$, $f_{Sol} \rightarrow Gas$ and $f_{Gas} \rightarrow Sol$) and one stretch feedback pathway ($x_{VL} \rightarrow VL$ only). For the forelegs, only one pathway of such type is implemented ($f_T \rightarrow T$). The combination of force and stretch feedbacks to the extensors was shown to strongly increase the stiffness of the leg relative to external load and thus stabilize the body height (Prochazka et al. 2002(46)).

• *Feedbacks supporting the propulsion* (both hind and forelegs) The last group of feedbacks helps the forward propulsion of the body. For the hind legs, they involve the progressively increasing activation of the knee and ankle extensors when the leg approaches the PEP (pathways $x_{IP} \rightarrow VL$ and $x_{IP} \rightarrow Sol$ respectively). Similarly, for the forelegs, activation of the elbow extensor T is increased by a pathway from x_{BC}.

B.3.3 MOSS parameters

B.3.3.1 Activation conditions

The conditions of initiation and termination of the synergies are given in Table B.4.

TABLE B.4: Synergy initiation and termination conditions. "t" and "s" refer respectively to a condition based on timing or on a sensory event. "td event" means touchdown event, i.e. when the foot touches the ground. This event is detected by the the contact sensor at the tip of the foot. (H) and (F) refer respectively to the hind and forelegs.

	Flexor Phase				Extensor Phase			
	Liftoff		Swing		Touchdown		Stance	
Initiation	t	0 ms	t	10 ms (H) 60 ms (F)	t	0 ms	s	td event
Termination	t	50 ms (H) 65 ms (F)	t	∞	s	td event	t	∞

B.3.3.2 Muscular activations

This section provides the values of the MOSS parameters for a locomotion speed of $v \simeq 0.6\ ms^{-1}$. The synaptic weights of the connections from the TI neuron to the IM neurons in each synergy, i.e. the feed-forward component, used for the experiments described in Section 3.5 are given in Table B.5. On the other hand, the implemented sensory feedback pathways are listed with the values of their parameters in Table B.6.

TABLE B.5: Synaptic weights of the connections from the TI neuron to the IM neurons in each synergy (LO: liftoff, SW: swing, TD: touchdown and ST: stance) for the hind legs (up) and forelegs (down). "·" means that the synaptic weight is zero, i.e. that there is actually no connection between the TI neuron and the IM of this muscle in that synergy.

Syn.	IP	AB	PB	VL	Gas	Sol	TA
LO	·	·	0.2	·	·	·	0.1
SW	0.5	·	·	·	·	·	0.5
TD	0.05	·	·	0.05	0.1	·	0.5
ST	·	0.2	·	0.1	0.05	0.1	·

Syn.	BC	LD	B	T	WF
LO	·	0.15	1.4	·	·
SW	0.3	·	0.25	·	·
TD	0.4	·	0.02	0.3	0.2
ST	·	0.4	·	0.3	·

TABLE B.6: Parameters of the sensory feedback pathways and their associated gains for the hind legs (up) and the forelegs (down). The second column gives the synergy in which the pathway is implemented. Column three to column six are the sensory input and the value of the parameters of the SN neuron (see Equation B.5). Column seven (m) gives the muscle whose motor neuron receives the output of the VG neuron. Finally, the last column (w) is the synaptic weight of the connection from the TI neuron to the VG neuron of the pathway.

N°	Syn.	s	s_{off}	K_p	K_v	m	w
h1	SW	x_{PB}	0	0	0.2	PB	0.04
h2	SW	x_{PB}	0.9	-3	0	TA	0.2
h3	TD	x_{PB}	0	0	0.2	PB	0.04
h4	ST	x_{AB}	0.8	3	0.5	AB	1.0
h5	ST	f_{VL}	0	0.007	0	VL	0.25
h6	ST	f_{Sol}	0	0.01	0	Gas	0.25
h7	ST	f_{Gas}	0	0.01	0	Sol	0.25
h8	ST	x_{VL}	0.8	4	0	VL	0.1
h9	ST	x_{IP}	0.8	2	0	VL	0.6
h10	ST	x_{IP}	0.8	2	0	Sol	0.6
h11	ST	x_{IP}	0.8	2	0	IP	0.2

N°	Syn.	s	s_{off}	K_p	K_v	m	w
f1	SW	x_{LD}	0.75	1	0	BC	0.3
f2	SW	x_{LD}	0.75	1	0	B	-1.5
f3	SW	x_{LD}	0.75	1	0	T	1.5
f4	SW	x_{LD}	0.75	1	0	WF	1.0
f5	SW	x_{LD}	0.85	5	0.2	LD	0.06
f6	TD	x_{LD}	0.85	5	0.2	LD	0.06
f7	ST	x_{BC}	0.8	1.5	0	LD	-4.5
f8	ST	x_{BC}	0.8	1.5	0	BC	1.5
f9	ST	x_{BC}	0.8	1.5	0	T	0.5
f10	ST	f_T	0	0.003	0	T	0.47

B.4 PFCM

Using the simplified hind legs model, sets of values of the excitatory inputs to the IM_m and VG_{s_m} neurons of each synergy at the MOSS level resulting in the steady walking of the model were found, and this for various speeds of locomotion. In a second time, for the parameters having the greatest influence on locomotion speed (see Section 3.4.5), the function of the input value according to the speed was divided into two components: a constant component (the value of the input at the lowest simulated walking speed) and a variable component.

The constant component is provided by the TI neuron of each synergy. The output of TI was set to one and the synaptic weights of the connections to the IM and VG neurons (respectively $w_{TI\_IM_m}$ and $w_{TI\_VG_{s\_m}}$) were adjusted to match the desired value of the inputs. These are presented in Table B.7 (for the $w_{TI\_IM_m}$) and in Table B.8 (for the $w_{TI\_VG_{s\_m}}$).

TABLE B.7: Synaptic weights $w_{TI\_IM_m}$ of the connections from the TI neuron to the IM neurons in each synergy (LO: liftoff, SW: swing, TD: touchdown and ST: stance). "·" means that the synaptic weight is zero, i.e. that there is actually no connection between TI and the IM of this muscle in that synergy.

	IP	AB	PB	VL	Gas	Sol	TA
Liftoff	·	·	0.05	·	·	·	·
Swing	0.2	·	·	·	·	·	0.05
Touchdown	0.05	·	·	·	0.1	·	0.05
Stance	·	·	·	0.02	·	0.2	·

TABLE B.8: Synaptic weights $w_{TI\_VG_{s\_m}}$ of the connections from the TI neuron to the VG neurons of the sensory feedback pathways. The pathways are referred by the numbers given in Table B.6 and only the synaptic weights w are listed as all the other parameters have the same values. "·" means that the synaptic weight of the connection is zero.

pathway n°	h1	h2	h3	h4	h5	h6	h7	h8	h9	h10	h11
w	0.065	0.2	0.065	1.0	0.3	0.3	0.3	0.1	0.3	·	0.3

On the other hand, the variable component of the inputs is provided by the connections coming from the interneurons in the PFCM and modulated by the synaptic weights $w_{IN_j\text{-}IM_m}$ and $w_{IN_j\text{-}VG_{s\_m}}$. The outputs of the interneurons of the PFCM are themselves function of the control input Ψ coming from an upper neural system. For the sake of simplicity, the PFCM was implemented as a single layer of interneurons with linear output. Due to the limited number of variable inputs, three interneurons were enough to generate adequate values of the inputs. The parameters of the interneurons are given

in Table B.9 while the synaptic weights of their connections to the IM_m and VG_{s_m} neurons in the MOSS are given in Table B.10.

TABLE B.9: Parameters of Equations B.1, B.2 and B.4 for the PFCM interneurons.

	Θ	Γ	τ (ms)
IN_1	0	1	5
IN_2	0.1	1	5
IN_3	0.2	1	5

TABLE B.10: Synaptic weights $w_{IN_j\_IM_m}$ and $w_{IN_j\_VG_{s\_m}}$ of the connections from the PFCM interneurons IN_j to the IM and VG neurons in the MOSS. The connections that are not listed in this table have a null synaptic weight, i.e. there is no connection.

Origin (PFCM)	Destination (MOSS)		weight
	Synergy	Neuron	
IN_2	LO	IM_{PB}	1
IN_2	SW	IM_{IP}	0.4
IN_1	ST	IM_{AB}	1
IN_1	ST	IM_{VL}	0.4
IN_1	SW	$VG_{x_{PB}\_PB}$	0.3
IN_1	TD	$VG_{x_{PB}\_PB}$	0.3
IN_3	ST	$VG_{f_{VL}\_VL}$	0.3
IN_3	ST	$VG_{f_{Gas}\_Sol}$	0.3
IN_2	ST	$VG_{x_{IP}\_VL}$	2.5
IN_2	ST	$VG_{x_{IP}\_Sol}$	1

Appendix C

Trajectory generation

C.1 Swing phase trajectory

The trajectory $\boldsymbol{r}_{sw}(\phi)$ must satisfy the following boundary conditions:

$$\begin{array}{rclcrcl} \boldsymbol{r}_{sw}(0) & = & \boldsymbol{r}_{LO} & & \boldsymbol{r}_{sw}(\hat{\phi}_{AEP}) & = & \hat{\boldsymbol{r}}_{AEP} \\ \boldsymbol{v}_{sw}(0) & = & \boldsymbol{v}_{LO} & & \boldsymbol{v}_{sw}(\hat{\phi}_{AEP}) & = & \hat{\boldsymbol{v}}_{AEP} \end{array} \tag{C.1}$$

where $\boldsymbol{r}$ and $\boldsymbol{v}$ are respectively the position and speed (derivative with respect to time) vectors. Reference speed at AEP $\hat{\boldsymbol{v}}_{AEP}$ is set to $\mathbf{0}$ in order to allow for a smooth landing. The speed profile has to be continuous at LO to prevent a sudden undesirable generation of torque that could destabilize the model. This done by taking as an initial condition the desired value of the speed, as well as the position, of the foot when the transition from stance to swing is triggered. Finally, the trajectory must insure a sufficient toes clearance (h_{tc}).

A cycloid trajectory is used to generate the basic stepping-forward motion and is superposed with two other functions in order to satisfy the boundary conditions:

- the x component of a cycloid trajectory to account for the height difference between the LO and the AEP positions $\hat{r}_{AEP,y} - r_{LO,y}$
- a decreasing linear function to account for the initial speeds. The rate of vanishing of the influence of the initial speeds is set using the parameters a_1.

If t_{LO} is the time at LO, t the current time, ϕ the current phase, ω the angular frequency and using the following definitions:

$$\begin{aligned}
\tau &= \phi/\hat{\phi}_{AEP} && \text{(C.2)}\\
\dot{\tau} &= \omega/\hat{\phi}_{AEP} && \text{(C.3)}\\
\Delta x &= \hat{r}_{AEP,x} - r_{LO,x} && \text{(C.4)}\\
\Delta y &= \hat{r}_{AEP,y} - r_{LO,y} && \text{(C.5)}\\
\phi_1 &= a_1 \cdot \hat{\phi}_{AEP} && \text{(C.6)}\\
c_x(\xi) &= (\xi - \frac{1}{2\pi} sin(2\pi\xi)) && \text{(C.7)}\\
c_y(\xi) &= (1 - cos(2\pi\xi)) && \text{(C.8)}
\end{aligned}$$

the x components of the position and speed of $\boldsymbol{r}_{sw}$ are computed the following way:

$$\begin{aligned}
\dot{p}_x &= max(\frac{\phi_1 - \phi}{\phi_1} \cdot v_{LO,x}, 0) && \text{(C.9)}\\
p_x &= \int_{t_{LO}}^{t} \dot{p}_x(\xi)\,\mathrm{d}\xi && \text{(C.10)}\\
q_x &= \Delta x - p && \text{(C.11)}\\
r_{sw,x} &= r_{LO,x} + q_x \cdot c_x(\tau) + p_x && \text{(C.12)}\\
v_{sw,x} &= q_x \cdot \dot{\tau} \cdot c_y(\tau) + \dot{p}_x(1 - c_x(\tau)) && \text{(C.13)}
\end{aligned}$$

and the y components as:

$$\begin{aligned}
\dot{p}_y &= max(\frac{\phi_1 - \phi}{\phi_1} \cdot v_{LO,y}, 0) && \text{(C.14)}\\
p_y &= \int_{t_{LO}}^{t} \dot{p}_y(\xi)\,\mathrm{d}\xi && \text{(C.15)}\\
q_y &= \Delta y - p_y && \text{(C.16)}\\
r_{sw,y} &= r_{LO,y} - \frac{h_{tc}}{2} \cdot c_y(\tau) + q_y \cdot c_x(\tau) + p_y && \text{(C.17)}\\
v_{sw,y} &= -\pi \cdot h_{tc} \cdot \dot{\tau} \cdot sin(2\pi\tau) + q_y \cdot \dot{\tau} \cdot c_y(\tau) + \dot{p}_y(1 - c_x(\tau)) && \text{(C.18)}
\end{aligned}$$

with $a_1 = 0.25$ and h_{tc}= 2 cm.

C.2 Stance phase trajectory

Using the definitions:

$$\begin{aligned}
\tilde{\phi} &= \phi - \hat{\phi}_{AEP} && \text{(C.19)}\\
\tilde{\phi}_{st} &= 2\pi - \hat{\phi}_{AEP} && \text{(C.20)}\\
& && \text{(C.21)}
\end{aligned}$$

the trajectory $\boldsymbol{r}_{st}(\tilde{\phi})$ must satisfy the following boundary conditions:

$$\begin{array}{rclcrcl} \boldsymbol{r}_{st}(0) & = & \boldsymbol{r}_{TD} & & \boldsymbol{r}_{st}(\tilde{\phi}_{st}) & = & \hat{\boldsymbol{r}}_{PEP} \\ \boldsymbol{v}_{st}(0) & = & \boldsymbol{v}_{TD} & & \boldsymbol{v}_{st}(\tilde{\phi}_{st}) & = & \hat{\boldsymbol{v}}_{PEP} \end{array} \tag{C.22}$$

where $\boldsymbol{r}$ and $\boldsymbol{v}$ are respectively the position and speed (derivative with respect to time) vectors. $\boldsymbol{r}_{TD}$ is measured when touchdown occurs and the initial speed $\boldsymbol{v}_{TD}$ is set to $\mathbf{0}$. As mentioned in Section 4.4.2.2, $\hat{\boldsymbol{r}}_{PEP}$ and $\hat{\boldsymbol{v}}_{PEP}$ are given by:

$$\begin{array}{rclcrcl} \hat{r}_{PEP,x} & = & r_{TD,x} - \hat{L}_{str} & & \hat{v}_{PEP,x} & = & -\frac{\hat{L}_{str}(1-\hat{\beta})}{\hat{\beta}\hat{T}_{sw}} \\ \hat{r}_{PEP,y} & = & \hat{H} & & \hat{v}_{PEP,y} & = & 0 \end{array} \tag{C.23}$$

The x and y components of $\boldsymbol{\nu}$, the derivative of $\boldsymbol{r}_{st}$ with respect to the phase, are represented in Figure C.1, using the following definitions:

$$\tilde{\phi}_{td} = a_{td} \cdot \tilde{\phi}_{st} \tag{C.24}$$

$$\tilde{\phi}_{m} = a_{m} \cdot \tilde{\phi}_{n} \tag{C.25}$$

$$\tilde{\phi}_{d} = a_{d} \cdot \tilde{\phi}_{n} \tag{C.26}$$

$$\tag{C.27}$$

where $\tilde{\phi}_n$ is such that $r_{st,x}(\tilde{\phi}_n) = 0$. If $b_x = \hat{L}_{str}/\tilde{\phi}_{st}$, $\tilde{\phi}_n$ is given by:

$$\tilde{\phi}_n = \begin{cases} \frac{2\ r_{TD,x}\ +\ b_x\ \tilde{\phi}_{td}}{2\ b_x} & \text{if } 2\ r_{TD,x} > b_x\ \tilde{\phi}_{td} \\ \sqrt{\frac{2\ \tilde{\phi}_{td}\ r_{TD,x}}{b_x}} & \text{if not} \end{cases} \tag{C.28}$$

Accordingly, if t_{TD} is the time at TD, t the current time, and ω the angular frequency, the x and y components of the trajectory are given by:

$$\nu_x(\tilde{\phi}) = \begin{cases} -\frac{\tilde{\phi}\ b_x}{\tilde{\phi}_{td}} & \text{if } 0 < \tilde{\phi} < \tilde{\phi}_{td} \\ -b_x & \text{if } \tilde{\phi}_{td} \leq \tilde{\phi} \end{cases} \tag{C.29}$$

$$r_{st,x}(t) = r_{TD,x} + \int_{t_{TD}}^{t} \nu_x(\tilde{\phi})\omega \, \mathrm{d}\xi \tag{C.30}$$

and:

$$\Delta y = \hat{r}_{PEP,y} - r_{TD,y} \tag{C.31}$$

$$b_y = \frac{\Delta y}{\tilde{\phi}_n(a_d(1-k) - \frac{a_m}{2}) + k\tilde{\phi}_{st}} \tag{C.32}$$

$$\nu_y(\tilde{\phi}) = \begin{cases} \frac{\tilde{\phi}\ b_y}{\tilde{\phi}_m} & \text{if } 0 < \tilde{\phi} < \tilde{\phi}_m \\ b_y & \text{if } \tilde{\phi}_m \leq \tilde{\phi} < \tilde{\phi}_d \\ b_y \cdot exp(log(\kappa) \cdot \frac{\tilde{\phi}-\tilde{\phi}_d}{\tilde{\phi}_{st}-\tilde{\phi}_d}) & \text{if } \tilde{\phi}_d \leq \tilde{\phi} < \tilde{\phi}_{st} \\ 0 & \text{if } \tilde{\phi}_{st} \leq \tilde{\phi} \end{cases} \tag{C.33}$$

$$r_{st,y}(t) = r_{TD,y} + \int_{t_{TD}}^{t} \nu_y(\tilde{\phi})\omega \, \mathrm{d}\xi \tag{C.34}$$

with $\{a_{td}, a_m, a_d, \kappa, k\} = \{0.1, 0.2, 0.7, 0.01, 0.215\}$.

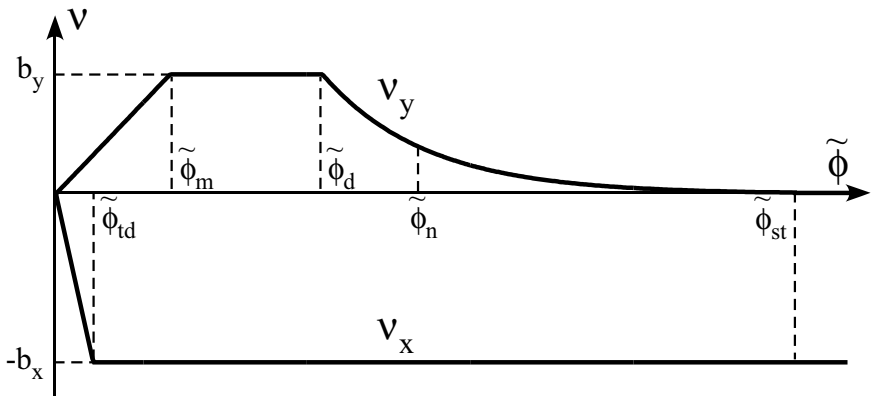

FIGURE C.1: ν_x and ν_y functions.

C.3 Inverse kinematic model

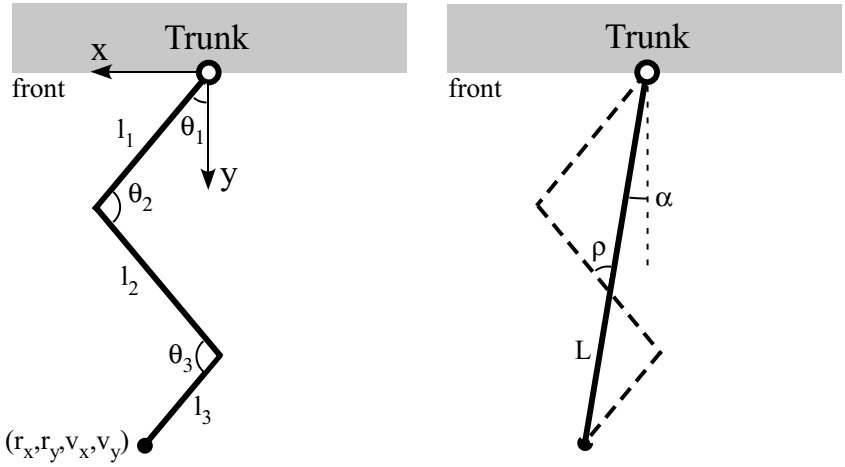

FIGURE C.2: Parameters of the inverse kinematics model

If α, L and ρ are defined as in Figure C.2, the joints angles (θ_j) and angular speeds ($\dot{\theta}_j$) are computed the following way (as the leg is tri-segmented, the constraint that the knee and ankle joints angles are identical, i.e. $\theta_2 = \theta_3$, is used):

$$\alpha = atan(r_x/r_y) \tag{C.35}$$

$$L = \sqrt{r_x^2 + r_y^2} \tag{C.36}$$

$$\theta_2 = \theta_3 = acos\left(\frac{(l_1^2 + l_2^2 + l_3^2 + 2l_1l_3) - L^2}{2l_2(l_1 + l_3)}\right) \tag{C.37}$$

$$\rho = atan\left(\frac{(l_1 + l_3)sin\theta_2}{l_2 - (l_1 + l_3)cos\theta_2}\right) \tag{C.38}$$

$$\theta_1 = \pi + \alpha - \theta_2 - \rho \tag{C.39}$$

$$\dot{\alpha} = \frac{v_x r_y - v_y r_x}{r_x^2 + r_y^2} \tag{C.40}$$

$$\dot{L} = \frac{v_x r_x - v_y r_y}{\sqrt{r_x^2 + r_y^2}} \tag{C.41}$$

$$\dot{\theta}_2 = \dot{\theta}_3 = \frac{L\dot{L}}{l_2(l_1 + l_3)sin\theta_2} \tag{C.42}$$

$$\dot{\rho} = \frac{(l_1 + l_3)(l_2cos\theta_2 - (l_1 + l_3))\dot{\theta}_2}{l_2^2 + (l_1 + l_3)^2 - 2l_2(l_1 + l_3)cos\theta_2} \tag{C.43}$$

$$\dot{\theta}_1 = \dot{\alpha} - \dot{\theta}_2 - \dot{\rho} \tag{C.44}$$

where $\boldsymbol{r}$ and $\boldsymbol{v}$ are respectively the position and speed of the foot (provided by the trajectory generation).

Appendix D

Quadrupedal walk: initial conditions and transient phase

The transient phase, which lasts from the beginning of the simulation (where the model is standing, at rest) and until the moment where the model reaches the steady state, is represented in Figures D.1 and D.2 for the walking pattern of Figure 4.9 (with the parameter values given in Table 4.3).

At the beginning of the simulation, for all the leg controllers, the initial position and speed of the foot are set as follows:

$$\begin{array}{lllllll} r_x & = & 0 & & r_y & = & 0.18\ m \\ v_x & = & 0 & & v_y & = & 0 \end{array} \tag{D.1}$$

Both right leg controllers (HR and FR) start in the swing phase, while both left leg controllers (HL and FL) starts in the stance phase (as represented in Figure D.1). The initial values of the leg controller phases ϕ are set as follows:

$$\phi^{*R} = 0 \qquad \text{and} \quad \phi^{*L} = \pi \tag{D.2}$$

Forcing the right legs to swing induces rolling motion of the body (as shown in Figure D.2), due to the inverted pendulum motion around the left feet. However, as $\theta_{roll} = 0$ at the beginning of the simulation, the duration of the swing phase of the first step must be reduced to prevent the generation of excessive rolling motion, which would cause the model to fall on its right side. Hence, ω^{*R}_{mod} is initially set to $\hat{\omega}$, so that the swing phase duration of the first step is reduced to half of its nominal value.

Within a few walking periods, phase differences characteristic of the walk gait emerges. The body rolling motion amplitude as well as the cyclic periods stabilize and the steady state is reached after around 1.6 s.

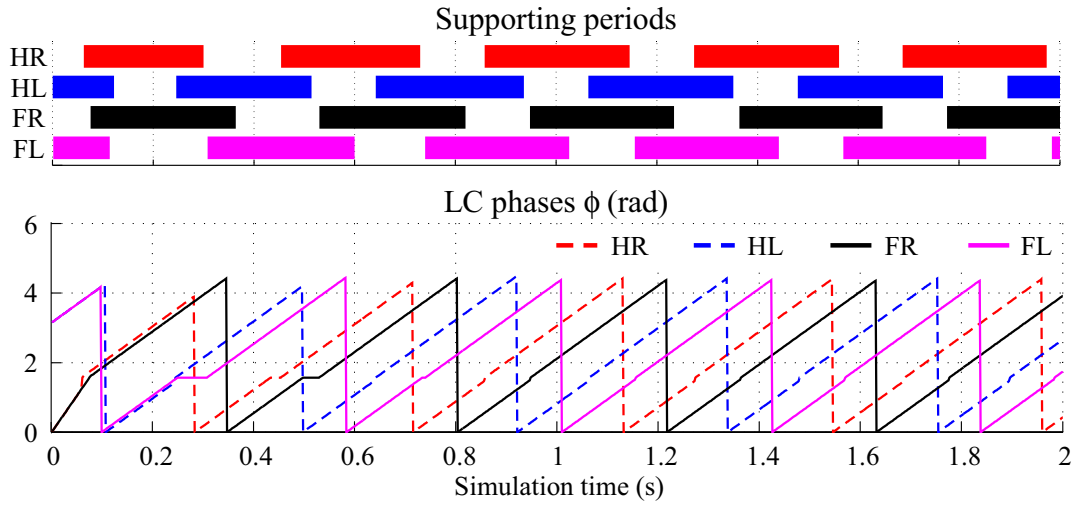

FIGURE D.1: Transient phase: supporting periods and leg controller phases.

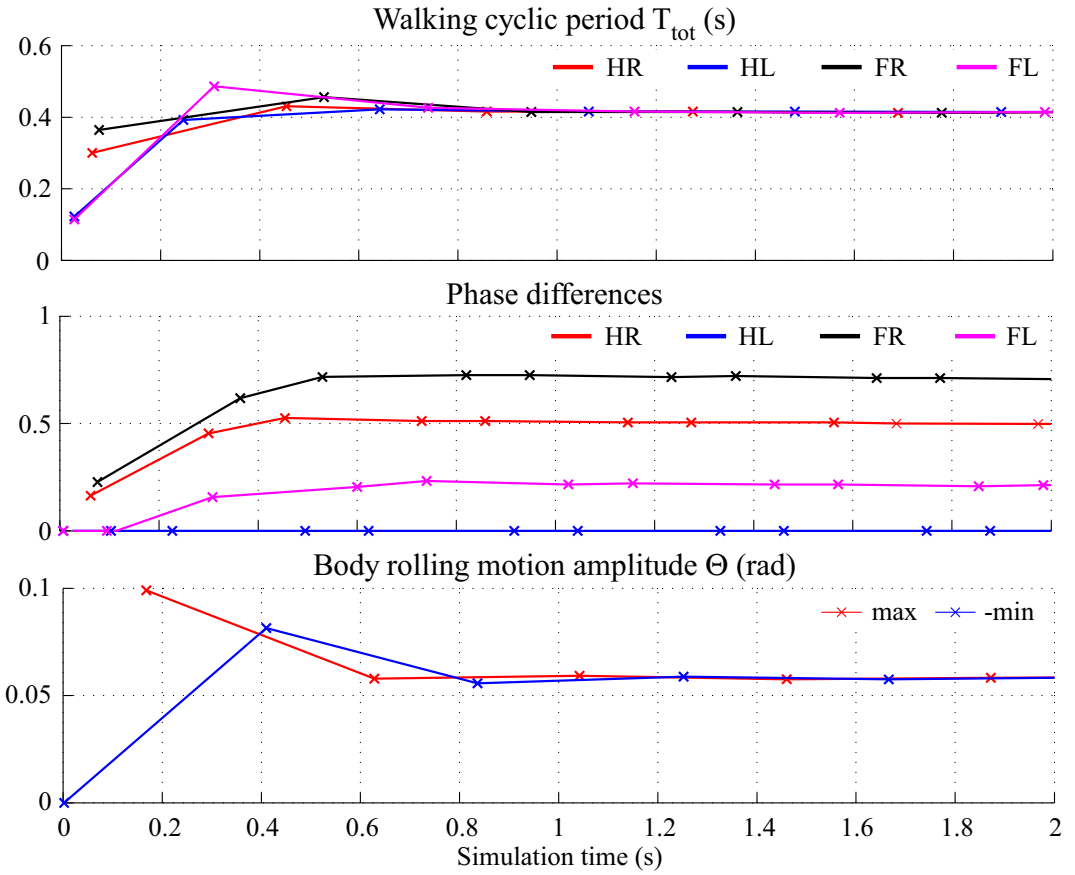

FIGURE D.2: Transient phase: cyclic periods, phase differences and body rolling motion amplitude.

Appendix E

Simulation environment

All the simulations were carried out using Webots(63), a commercial mobile robot simulation software developed by Cyberbotics Ltd.

E.1 Control levels

Webots implements two levels of control:

- the *controller level*, executed every multiple of the controller time step h_c which must be greater or equal to 1 ms
- the *physics plugin level*, executed every step of the dynamics simulation, with no limitation on the duration of the time step (h_p).

As numerical instabilities occurred when using a time step of 1 ms to compute the forces with the musculoskeletal models, only the neural controller was implemented at the controller level and the computations of the muscular forces and joint torques were achieved at the physics plugin level, using a smaller time step. h_c and h_p were set respectively to 2 ms and 0.1 ms.

For the experiments of Chapters 4 and 5, a similar repartition was used: the trajectories were generated at the controller level but the computation of the joint torques was realized at the physics plugin level, with respetively $h_c = 2$ ms and $h_p = 0.5$ ms.

E.2 Ground reaction forces

In Webots, the computation of the constraining forces associated to predefined constraints or collisions involves two parameters: the Error Reduction Parameter (ERP)

and the Constraint Force Mixing (CFM). The stiffness (k_p) and damping (k_d) of the equivalent spring-damper model can be computed as:

$$k_p = \mathrm{ERP}/(h_p \cdot \mathrm{CFM}) \tag{E.1}$$

$$k_d = (1 - \mathrm{ERP})/\mathrm{CFM} \tag{E.2}$$

For the experiments with the musculoskeletal models, the default values for ERP and CFM were used (equivalent to $k_p = 2.0e^8 N.m^{-1}$ and $k_d = 8.0e^4 N.s.m^{-1}$). In the case of the experiments with the simplified simulation model, ERP and CFM were set to achieve $k_p = 3.0e^4 N.m^{-1}$ and $k_d = 2.0e^3 N.s.m^{-1}$ (similar to the values used by Taga 1995(54) for example).

Bibliography

[1] Akay, T., Mc Vea, D.A., Tachibana, A. & Pearson, K.G. (2006). Coordination of fore and hind leg stepping in cats on a transversely-split treadmill. *Exp. Brain Res.*, 175, 211-222.

[2] Alexander, R.M. (1984). The gaits of bipedal and quadrupedal animals. *Int. J. of Robotics Research*, 6(3), 49-59.

[3] Alexander, R.M. (2003). *Principles of Animal Locomotion*. Princeton University Press.

[4] Aoi, S. & Tsuchiya, K. (2005). Locomotion control of a biped robot using nonlinear oscillators. *Autonomous Robots*, 19(3), 219-232.

[5] Aoi, S. & Tsuchiya, K. (2006). Stability analysis of a simple walking model driven by an oscillator with a phase reset using sensory feedback. *IEEE Trans. Robotics*, 22(2), 391-397.

[6] Biewener, A.A. (2003). *Animal Locomotion*. Oxford Animal Biology Series, Oxford University Press.

[7] Boczek-Funcke, A., Kuhtz-Buschbeck, J.P. & Illert, M. (1996). Kinematic analysis of the cat shoulder girdle during treadmill locomotion: an x-ray study. *European Journal of Neuroscience*, 8, 261-272.

[8] Brown, I., Scott, S. & Loeb, G. (1996). Mechanics of feline soleus: II Design and validation of a mathematical model. *Journal of Muscle Research and Cell Motility*, 17, 221-233.

[9] Buehler, M., Battaglia, R., Cocosco, A., Hawker, G., Sarkis, J. & Yamazaki, K. (1998). Scout: a simple quadruped that walks, climbs and runs. In *Proc. of the 1998 IEEE International Conference on Robotics and Automation*, 1707-1712.

[10] Burrows, M. (1996). The control of walking in orthoptera. I: Leg movements in normal walking. *J. Exp. Biol.*, 58, 45-58.

[11] Cohen, A.H. & Boothe, D.L. (1999). Sensorimotor interactions during locomotion: principles derived from biological systems. *Autonomous Robots*, 7(3), 239-245.

[12] Cruse, H. (1990). What mechanism coordinate leg movement in walking arthropods? *Trends in Neurosciences*, 12, 15-21.

[13] Cruse, H. (2002). The functional sense of central oscillations in walking. *Biological Cybernetics*, 86, 271-280.

[14] Deliagina, T. & Orlovsky, G. (2002). Comparative neurobiology of postural control. *Current Opinion in Neurobiology*, 12, 652-657.

[15] Duysens, J. & Pearson, K.G. (1980). Inhibition of flexor burst generation by loading ankle extensor muscles in walking cats. *Brain Research*, 187, 321-32.

[16] Ekeberg, O. (1993). A combined neuronal and mechanical model of fish swimming. *Biological Cybernetics*, 69, 363-374.

[17] Ekeberg, O. & Pearson, K. (2005). Computer simulation of stepping in the hind legs of the cat: an examination of mechanisms regulating the stance-to-swing transition. *Journal of Neurophysiology*, 94(6), 4256-68.

[18] English, A. W. (1978). An electromyographic analysis of forelimb muscles during overground stepping in the cat. *Journal of Experimental Biology*, 76, 105-122.

[19] English, A. W. (1978). Functional analysis of the shoulder girdle of cats during locomotion. *Journal of Morphology*, 156, 279-292.

[20] Espenschied, K.S., Quinn, R.D., Beer, R.D. & Chiel, H.J. (1996). Biologically based distributed control and local reflexes improve rough terrain locomotion in a hexapod robot. *Robotics and Autonomous Systems*, 18, 59-64.

[21] Fukuoka, Y., Kimura, H. & Cohen, A. H. (2003). Adaptive dynamic walking of a quadruped robot on irregular terrain based on biological concepts. *The International Journal of Robotics Research*, 22(3-4), 187-202.

[22] Full, R. J. & Koditschek, D. E. (1999). Templates and anchors: neuromechanical hypotheses of legged locomotion on land. *J. Exp. Biol.*, 202, 3325-3332.

[23] Grillner, S. & Zangger, P. (1974). Locomotor movements generated by the deafferented spinal cord. *Acta Physiologica Scandinavia*, 91, 38A-39A.

[24] Grillner, S. & Rossignol, S. (1978). On the initiation of the swing phase of locomotion in chronic spinal cats. *Brain Research*, 146, 269-77.

[25] Grillner, S. (1981). Control of locomotion in bipeds, tetrapods and fish. *Handbook of Physiology II*, American Physiology Society, Bethesda, MD, 1179-1236.

[26] Halbertsma, J.M. (1983). The stride cycle of the cat: the modelling of locomotion by computerized analysis of automatic recordings. *Acta Physiologica Scandinavia*, Suppl., 521, 1-75.

[27] Hirai, K., Hirose, M., Haikawa, Y. & Takenaka, T. (1998). The Development of Honda Humanoid Robot. In *Proc. of the 1998 IEEE International Conference on Robotics and Automation*, 1321-1326.

[28] Ijspeert, A.J. (2001). A connectionist central pattern generator for the aquatic and terrestrial gaits of a simulated salamander. *Biological Cybernetics*, 84(5), 331-348.

[29] Ijspeert, A.J., Crespi, A., Ryczko, D., & Cabelguen, J.M. (2007). From swimming to walking with a salamander robot driven by a spinal cord model. *Science*, 315(5817), 1416-1420.

[30] Ilg, W., Albiez, J., Jedele, H., Berns, K. & Dillmann, R. (1999). Adaptive periodic movement control for the four legged walking machine BISAM. In *Proc. of the 1999 IEEE International Conference on Robotics and Automation*, 2354-2359.

[31] Kimura, H., Shimoyama, I. & Miura, H. (1990). Dynamics in the dynamic walk of a quadruped robot. *Advanced Robotics*, 4(3), 283-301.

[32] Kimura, S., Yano, M. & Shimizu, H. (1993). A self-organized model of walking patterns in insects. *Biological Cybernetics*, 69, 183-193.

[33] Kimura, S., Yano, M. & Shimizu, H. (1994). A self-organized model of walking patterns in insects - II. The loading effect and leg amputation *Biological Cybernetics*, 70, 505-512.

[34] Kimura, H., Akiyama, S. & Sakurama, K. (1999). Realization of dynamic walking and running of the quadruped using neural oscillator. *Autonmous Robots*, 7(3), 247-258.

[35] Kimura, H., Fukuoka, Y. & Cohen, A. H. (2007). Adaptive dynamic walking of a quadruped robot on natural ground based on biological concepts. *The International Journal of Robotics Research*, 26(5), 475-490.

[36] Kuhtz-Buschbeck, J.P., Boczek-Funcke, A., Illert, M. & Weinhardt, C. (1994). X-Ray study of the cat hindlimb during treadmill locomotion. *European Journal of Neuroscience*, 6, 1187-1198.

[37] Lewis, M.A., Etienne-Cummings, R., Hartmann, M.J., Xu, Z.R. & Cohen, A.H. (2003). An in silico central pattern generator: silicon oscillator, coupling, entrainment, and physical computation. *Biological Cybernetics*, 88, 137-151.

[38] Matsuoka, K. (1987). Mechanisms of frequency and pattern control in the neural rhythm generators. *Biological Cybernetics*, 56, 345-353 (1987)

[39] Miura, H. & Shimoyama, I. (1984). Dynamical walk of biped locomotion. *Int. J. Robotics Research*, 3(2), 60-74.

[40] Miyakoshi, S., Taga, G., Kuniyoshi, Y. & Nagakubo, A. (1998). Three dimensional bipedal stepping motion using neural oscillators - Towards humanoid motion in the real world. In *Proc. of the IROS 1998*, 84-89.

[41] Ogihara, N., Aoi, S., Sugimoto, Y., Nakatsukasa, M. & Tsuchiya, K. (2006). Exploration of locomotory mechanism in the Japanese monkey based on an anatomically-based musculoskeletal model. *Tech. Report of IEICE*, 106(330), 33-36.

[42] Ono, K., Furuichi, T. & Takahasi, R. (2004). Self-excited walking of a biped mechanism with feet. *Int. J. of Robotics Research*, 23(1), 55-68.

[43] Orlovsky, G.N., Deliagina, T.G. & Grillner, S. (1999). *Neural Control of Locomotion, From Mollusc to Man*. Oxford University Press.

[44] Pearson, K.G. & Franklin, R. (1984). Characteristics of leg movements and patterns of coordination in locusts walking on rough terrain. *Int. J. of Robotics Research*, 1(3), 101-112.

[45] Poulakakis, I., Smith, J.A. & Buehler, M. (2006). On the dynamics of bounding and extensions towards the half-bound and the gallop gaits. In *H. Kimura et al., Adaptive Motion of Animals and Machines*, Springer, 77-86.

[46] Prochazka, A., Gritsenko, V. & Yakovenko, S. (2002). Sensory control of locomotion : reflexes versus higher-level control. *Sensorimotor control*, Kluwer Academic/-Plenum Publishers.

[47] Raibert, M. (1985). *Legged Robots That Balance*. MIT Press, Boston.

[48] Righetti, L. & Ijspeert, A. (2008). Pattern generators with sensory feedback for the control of quadruped locomotion. In *Proc. of the 2008 IEEE International Conference on Robotics and Automation*.

[49] Rossignol, S. (1996). Neural control of stereoscopic leg movements. In *L.B. Rowell and J.T. Sheperd, Handbook of physiology - exercise regulation and integration of multiple systems*, 173-216, Oxford University Press, Baltimore.

[50] Saranli, U., Buehler, M. & Koditscheck, D.E. (2001). RHex: a simple and highly mobile hexapod robot. *International Journal of Robotics Research*, 20(7), 616-631.

[51] Shik, M.L., Orlovsky, G.N. & Severin, F.V. (1966). Organization of locomotor synergy. *Biophysics*, 11, 879-886.

[52] Smith, J.L., Buford, J.A. & Zernicke, R.F. (1988). Constraints during backward walking in the quadruped. In *Posture and gait: development, adaptation and modulation* (eds. B. Amblard, A. Berthoz and F. Clarac), 391-400, Elsevier, Amsterdam.

[53] Taga, G., Yamaguchi, Y. & Shimizu, H. (1991). Self-organized control of bipedal locomotion by neural oscillators. *Biological Cybernetics*, 65, 147-159.

[54] Taga, G. (1995). A model of the neuro-musculo-skeletal system for human locomotion I. Emergence of basic gait. *Biological Cybernetics*, 73, 97-111.

[55] Taga, G. (1995). A model of the neuro-musculo-skeletal system for human locomotion II. - real-time adaptability under various constraints. *Biological Cybernetics*, 73, 113-121.

[56] Takanishi, A., Takeya, T., Karaki, H. & Kato, I. (1990). A control method for dynamic biped walking under unknown external force. In *Proc. of the IROS 1990*, 795-801.

[57] Ting, L.H. and McKay, J.L. (2007). Neuromechanics of muscle synergies for posture and movement. *Current Opinion in Neurobiology*, 17, 622-628.

[58] Tomita, M. (1967). A study on the movement pattern of four limbs in walking. *J. Anthrop. Soc. Nippon*, 75, 120-146, 171-194.

[59] Tomita, N. & Yano, M. (2003). A model of learning free bipedal walking in indefinite environment - constraints self-emergence/self-satisfaction paradigm. In *Proc. of SICE Annual Conference*, Fukuin, Japan, 3176-3181.

[60] Tsujita, K., Tsuchiya, K. & Onat, A. (2001). Adaptive Gait Pattern Control of a Quadruped Locomotion Robot. In *Proc. of the IROS2001*, Maui, Hawaii, USA.

[61] Vukobratović M. & Borovac, B. (2004). Zero-Moment Point - Thirty Five Years of its Life. *International Journal of Humanoid Robotics*, 1(1), 157-173.

[62] Wadden, T. & Ekeberg, O. (1998). A neuro-mechanical model of legged locomotion: single leg control. *Biological Cybernetics*, 79, 161-173.

[63] Webots: http://www.cyberbotics.com

[64] Yakovenko, S., Gritsenko, V. & Prochazka, A. (2004). Contribution of stretch reflexes to locomotor control: a modeling study. *Biological Cybernetics*, 90, 146-155.

[65] Yoneda, K., Iiyama, H. & Hirose, S. (1994). Sky-hook suspension control of a quadruped walking vehicle. In *Proc. of the 1994 IEEE International Conference on Robotics and Automation*, 999-1004.

Acknowledgements

I thank my supervisor Hiroshi Kimura for helping me discovering and growing the creativity and enthusiasm that I did not know I had. Throughout three years, it has been his vision that carried me forward to this day. I thank Prof. Kunikatsu Takase for invaluable advice and care. I also thank Prof. Tanaka, Prof. Morita, Prof. Koike and Prof. Tano for kind examination and invaluable advice.

This work would not have been possible without the help of many individuals. I thank Prof. Pearson for our few but unique conversations and for kindly sharing with me his expertise regarding animal locomotion, as well as Prof. Ekeberg for his advices related to the simulation of musculoskeletal models. I owe many thanks to all the members of the CPG meeting group (Prof. F. Mori, Prof. J. Nishii, Prof. K. Tsujita, Prof. I. Nishikawa, Prof. H. Nishimaru, Dr. N. Ogihara, Dr. S. Aoi, Dr. Y. Sugimoto) for their advices and guidance. I also thank all the past and present members in Takase and Kimura Laboratories, especially Dr. Jia, Dr. Chugo, Toshiki Masuda and Yuji Otoda, for the privilege to work with such colleagues.

Outside the laboratory, many people directly or indirectly contributed to the completion of this dissertation. I would like to thank all my friends and family for their support and encouragements in times of doubt. In particular, this thesis is dedicated to my loving girlfriend, Susanne Zwick, and my parents, Anouk Carette and Philippe Maufroy, whose love supported me through long years of struggle and gave me the energy and motivation to continue. Their contributions are beyond words.

Author Biography

Christophe Maufroy was born in Etterbeek, Belgium, on October 17, 1981. He received respectively the degrees of *Ingénieur Civil Mécanicien* and *Ingénieur des Arts et Manufactures*, both equivalent to a M.E. degree, from the Université Libre de Bruxelles, Brussels, Belgium, and the Ecole Centrale Paris, Paris, France in September 2004. He has been with the Graduate School of Information Systems, University of Electro-Communications, since April 2006, working toward the Ph.D. degree. His research interest is related to the comprehension of how, in animals, simple and local control strategies result in the emergence of adaptive locomotion through the interactions between the control system, the body and the environment and how the principles underlying such emergent behaviors can be applied to robots. Christophe Maufroy is a student member of the Robotics Society of Japan (RSJ).

List of Publications Related to the Thesis

Journal papers

1. C. Maufroy, H. Kimura and K. Takase, Towards a general neural controller for quadrupedal locomotion, Neural Networks, Vol. 21(4), pp 667-681, 2008 (related to Chapter 3)

International conference papers

1. C. Maufroy, H. Kimura and K. Takase, Stable Dynamic Walking of a Quadruped via Phase Modulations against Small Disturbances, IEEE International Conference on Robotics and Automation 2009 (accepted) (related to Chapter 4 and 5)
2. C. Maufroy, H. Kimura and K. Takase, Towards a general neural controller for 3D quadrupedal locomotion, Proc. of the SICE Annual Conference 2008, Tokyo, Japan, pp. 2495-2500, 2008 (related to Chapter 3)
3. C. Maufroy, H. Kimura and K. Takase, Biologically Inspired Neural Controller for Quadruped, Proc. of IEEE International Conference on Robotics and Biomimetics, Sanya, China, pp.1212-1217, 2007 (related to Chapter 3)
4. C. Maufroy and H. Kimura, Towards a General Neural Controller for Quadrupedal Locomotion, Proceedings of the 2nd International Symposium on Mobiligence, Awaji, Japan, pp. 117-120, 2007 (related to Chapter 3)